

AD _____

Award Number: DAMD17-99-1-9200

TITLE: Peripheral Benzodiazepine Receptor (PBR) in Human Breast Cancer

PRINCIPAL INVESTIGATOR: Vassilios Papadopoulos, Ph.d.

CONTRACTING ORGANIZATION: Georgetown University Medical Center
Washington, D.C. 20057

REPORT DATE: April 2003

TYPE OF REPORT: Final

PREPARED FOR: U.S. Army Medical Research and Materiel Command
Fort Detrick, Maryland 21702-5012

DISTRIBUTION STATEMENT: Approved for Public Release;
Distribution Unlimited

The views, opinions and/or findings contained in this report are those of the author(s) and should not be construed as an official Department of the Army position, policy or decision unless so designated by other documentation.

20040317 013

REPORT DOCUMENTATION PAGEForm Approved
OMB No. 074-0188

Public reporting burden for this collection of information is estimated to average 1 hour per response, including the time for reviewing instructions, searching existing data sources, gathering and maintaining the data needed, and completing and reviewing this collection of information. Send comments regarding this burden estimate or any other aspect of this collection of information, including suggestions for reducing this burden to Washington Headquarters Services, Directorate for Information Operations and Reports, 1215 Jefferson Davis Highway, Suite 1204, Arlington, VA 22202-4302, and to the Office of Management and Budget, Paperwork Reduction Project (0704-0188), Washington, DC 20503

1. AGENCY USE ONLY (Leave blank)		2. REPORT DATE April 2003	3. REPORT TYPE AND DATES COVERED Final (1 Apr 2000 - 31 Mar 2003)	
4. TITLE AND SUBTITLE Peripheral Benzodiazepine Receptor (PBR) in Human Breast Cancer			5. FUNDING NUMBERS DAMD17-99-1-9200	
6. AUTHOR(S) Vassilios Papadopoulos, Ph.D.				
7. PERFORMING ORGANIZATION NAME(S) AND ADDRESS(ES) Georgetown University Medical Center Washington, D.C. 20057 E-Mail: papadopv@georgetown.edu			8. PERFORMING ORGANIZATION REPORT NUMBER	
9. SPONSORING / MONITORING AGENCY NAME(S) AND ADDRESS(ES) U.S. Army Medical Research and Materiel Command Fort Detrick, Maryland 21702-5012			10. SPONSORING / MONITORING AGENCY REPORT NUMBER	
11. SUPPLEMENTARY NOTES Original contains color plates: ALL DTIC reproductions will be in black and white				
12a. DISTRIBUTION / AVAILABILITY STATEMENT Approved for Public Release; Distribution Unlimited				12b. DISTRIBUTION CODE
13. ABSTRACT (Maximum 200 Words) The peripheral-type benzodiazepine receptor (PBR) is an 18 kDa high affinity cholesterol and drug binding protein, part of the aggressive human breast cancer cell phenotype <i>in vitro</i> . We report herein that in human biopsies elevated PBR expression is limited to certain cancers, such as those of breast, colon-rectum and prostate tissues, where elevated PBR expression is associated with tumor progression. In search of the function of PBR in human breast cancer we found that (i) the ability of the aggressive cells to form tumors <i>in vivo</i> may depend on the amount of PBR present in the cells; (ii) the increase in PBR expression in aggressive cancers may be due to gene amplification; (iii) PBR protein expression is directly involved in regulating cell proliferation in human breast cancer cells, probably by decreasing the levels of the cyclin-dependent protein kinase inhibitor p21 ^{WAF/CIP1} , a protein known to be involved in tumor suppression, thus influencing cell cycle; and (iv) the epithelial origin of human breast cancer cells plays a crucial role in defining the function of PBR in cell proliferation.				
14. SUBJECT TERMS Breast Cancer				15. NUMBER OF PAGES 136
				16. PRICE CODE
17. SECURITY CLASSIFICATION OF REPORT Unclassified	18. SECURITY CLASSIFICATION OF THIS PAGE Unclassified	19. SECURITY CLASSIFICATION OF ABSTRACT Unclassified		20. LIMITATION OF ABSTRACT Unlimited

NSN 7540-01280-5500

Standard Form 298 (Rev. 2-89)
Prescribed by ANSI Std. Z39-18
298-102

Table of Contents

Cover.....	1
SF 298.....	2
Table of Contents.....	3
Introduction.....	4
Body.....	4
Key Research Accomplishments.....	6
Reportable Outcomes.....	7
Conclusions.....	8
References.....	8
Appendices.....	8

INTRODUCTION

In this IDEA Award we proposed to test the hypothesis that the peripheral-type benzodiazepine receptor (PBR), an 18 kDa high affinity cholesterol and drug binding protein may be used as a marker for the detection and diagnosis of breast tumors and that the regulation of PBR expression/function may eventually help in understanding the mechanisms involved in the progression of breast cancer and developing new tools for the treatment of the disease. Based on our initial preliminary studies on human breast cancer cells (1) we proposed two aims: (i) examine the expression and subcellular localization of PBR in a panel of human tumor breast biopsies and normal breast tissue biopsies and (ii) determine the function of PBR in human breast tumor cell lines. In this progress report we present preliminary data from the screening of the human biopsies and evidence on the role of PBR in human breast tumor cell growth.

BODY

In the approved statement of work we proposed two tasks:

1. Analyze the expression and subcellular localization of PBR in human tumor breast biopsies.
2. Determine the function of PBR in human breast tumor cell lines.

1. Expression of PBR in human tumors: relationship to breast, colorectal and prostate tumor progression

High levels of PBR are part of the aggressive human breast cancer cell phenotype *in vitro* (Hardwick et al., Cancer Research, 1999, 59:831-842). We examined PBR levels and distribution in normal tissue and tumors from multiple cancer types by immunohistochemistry. Among normal breast tissues, fibroadenomas, primary and metastatic adenocarcinomas, there is a progressive increase in PBR levels parallel to the invasive and metastatic ability of the tumor ($p < 0.0001$). In colorectal and prostate carcinomas, PBR levels were also higher in tumor than in the corresponding non-tumoral tissues and benign lesions ($p < 0.0001$). In contrast, PBR was highly concentrated in normal adrenal cortical cells and hepatocytes, whereas in adrenocortical tumors and hepatomas PBR levels were decreased. Moreover, malignant skin tumors showed decreased PBR expression compared with normal skin. These results indicate that elevated PBR expression is not a common feature of aggressive tumors, but rather may be limited to certain cancers, such as those of breast, colon-rectum and prostate tissues, where elevated PBR expression is associated with tumor progression. Thus, we propose that PBR overexpression could serve as a novel prognostic indicator of an aggressive phenotype in breast, colorectal and prostate cancers.

A manuscript describing in detail these findings was recently published in the *Journal of Receptor and Signal Transduction Research* (Appendix 1).

Further studies in evaluating the subcellular distribution of the receptor and its relationship to the aggressive phenotype of the tissues failed to demonstrate a clear relationship.

2a. PBR levels correlate with the ability of human breast cancer MDA-MB-231 cell line to grow in SCID mice

MDA-MB-231 (MDA-231) human breast cancer cells have a high proliferation rate, lack the estrogen receptor, express the intermediate filament vimentin, the hyaluronan receptor CD44, and are able to form tumors in nude mice. The MDA-231 cell line has been used in our laboratory to examine the role of the

peripheral-type benzodiazepine receptor (PBR) in the progression of cancer. During these studies two populations of MDA-231 cells were subcloned based on the levels of PBR. The subclones proliferated at approximately the same rate, lacked the estrogen receptor, expressed vimentin and CD44, and had the same *in vitro* chemoinvasive and chemotactic potential. Both restriction fragment length polymorphism and comparative genomic hybridization analyses of genomic DNA from these cells indicated that both subclones are of the same genetic lineage. However, only the subclone with high PBR levels was able to form tumors when injected in SCID mice. These data suggest that the ability of MDA-231 cells to form tumors *in vivo* may depend on the amount of PBR present in the cells.

A manuscript describing in detail these findings was published in the *International Journal of Cancer* (Appendix 2).

2b. PBR gene amplification in MDA-MB-231 aggressive breast cancer cells

Our previous studies using human breast cancer cell lines, and present studies using animal models and human tissue biopsies have suggested a close correlation between the expression of PBR and the progression of breast cancer. Although we previously reported a dramatic increase in PBR mRNA levels parallel to the aggressive phenotype of the breast cancer cells (Hardwick et al., *Cancer Research*, 1999, 59:831-842), we examined the possibility that gene amplification may also be one of the reasons of increased PBR protein levels in aggressive breast tumor cells and tissue biopsies. We investigated the genetic status of the PBR gene in two human breast cancer cell lines: MDA-MB-231 cells, which are an aggressive breast cancer cell line that contains high levels of PBR, and MCF-7 cells, which are a non-aggressive cell line that contains low levels of PBR. Both DNA (Southern) blot and fluorescence *in situ* hybridization (FISH) analyses indicated that the PBR gene is amplified in MDA-MB-231 relative to MCF-7 cells. These unexpected data suggest that PBR gene amplification may be an important indicator of breast cancer progression.

A manuscript describing in detail these findings was published in *Cancer Genetics and Cytogenetics* (Appendix 3).

2c. *In vivo* and *in vitro* peripheral-type benzodiazepine receptor polymerization: functional significance in drug ligand and cholesterol binding

As noted above PBR is an 18 kDa protein. Antisera for distinct PBR areas identified immunoreactive proteins of 18, 40, 56 kDa and occasionally 72, 90 and 110 kDa in testicular Leydig and human breast cancer cells. These sizes may correspond to PBR polymers and correlated to the levels of reactive oxygen species. UV photoirradiation generates ROS species, which increased the size of intramembraneous particles of recombinant PBR reconstituted into proteoliposomes consistent with polymer formation, determined both by SDS-Page and by freeze-fracture electron microscopy. Spectroscopic analysis revealed the formation of dityrosines as the covalent cross-linker between PBR monomers. Moreover, photoirradiation increased PK 11195 drug ligand binding and reduced cholesterol-binding capacity of proteoliposomes. Further addition of PK 11195 drug ligand to polymers increased the rate of cholesterol binding. These data indicate that reactive oxygen species induce *in vivo* and *in vitro* the formation of covalent PBR polymers. We propose that the PBR polymer might be the functional unit responsible for ligand-activated cholesterol binding and that PBR polymerization is a dynamic process modulating the function of this receptor in cholesterol transport and other cell-specific PBR-mediated functions.

A manuscript describing in detail these findings was published in *Biochemistry* (Appendix 4). Please note that DOD funds were used only for the studies dealing with the human breast cancer cells. The studies on Leydig cells were funded by a NIH grant.

2d. PBR overexpression and knockdown in human breast cancer cells indicate a role in tumor cell proliferation mediated by activation of p21^{WAF1/CIP1} expression.

As noted above PBR has been shown to be expressed at high levels in various forms of cancer, and its expression is positively correlated with aggressive metastatic behavior in human breast cancer cells. The effects of PBR drug ligands on cell proliferation and apoptosis have been described, but the role of the PBR protein in these processes has not yet been examined. Therefore, we have used transfection of the tetracycline-repressible MCF-7 cell line (MCF-7 Tet-Off) with human PBR cDNA, transfection of MDA-MB-231 cells with small interfering RNAs (siRNAs) targeting human PBR, radioligand binding assays and real-time quantitative PCR to examine the role of PBR protein in cell proliferation. The human breast cancer cell line MCF-7 is normally non-aggressive and expresses extremely low PBR levels (Hardwick et al., Cancer Research, 1999, 59:831-842). Induction of PBR expression in MCF-7 Tet-Off cells increased PBR ligand binding and cell proliferation. Multiple siRNAs complementary to PBR (PBR-siRNAs) enabled us to evaluate the role of PBR in cell proliferation in PBR-enriched, aggressive MDA-MB-231 human breast cancer cells. Transfection of MDA-MB-231 cells with PBR-siRNAs targeting different sites of PBR mRNA led to different levels of mRNA and protein knockdown. The decreased PBR expression was associated with decreased cell proliferation, and with increased levels of the cyclin-dependent protein kinase inhibitor p21^{WAF1/CIP1} which is known to be involved in tumor-suppression. Collectively, these results indicate that PBR protein expression is directly involved in regulating cell proliferation in human breast cancer cells, probably by influencing a mechanism involved in cell cycle control.

A manuscript describing in detail these findings is under revision in *Molecular Carcinogenesis* (Appendix 5).

2e. PBR and PBR drug ligands in fibroblast and fibrosarcoma cell proliferation: Role of ERK, c-jun and ligand-activated PBR-independent pathways

During these studies a number of reports appeared showing that specific PBR ligands were able to regulate cell proliferation, although their action is controversial and probably cell-type specific. In addition, the studies presented above in human breast cancer cells, which are of epithelial origin, raised the obvious question whether the effects seen and mechanisms identified are specific to human breast cancer cells. Thus we designed a study to examine the expression of PBR in cells of mesenchymal origin, i.e. human fibroblast and fibrosarcoma cells, as well as its role in the regulation of their proliferation. Both mesenchymal cell types express high levels of PBR, localized exclusively in mitochondria. The PBR-specific drug ligands, the isoquinoline carboxamide PK 11195 and the benzodiazepine Ro5-4864, at relative high concentrations (10^{-4} M), exert a strong inhibitory effect on cell proliferation by arresting the cells at the G0/G1 phase of the cell cycle, in a calcium-independent manner, while no apoptotic cell death was observed. In normal fibroblasts, this inhibition was correlated with a decrease in the activation of ERK and c-Jun. PBR knockdown by RNA inhibition did not affect the proliferation of either cell type and did not influence the inhibitory effect of PK 11195 and Ro5-4864 on cell growth. Our data suggest that in fibroblasts and fibrosarcoma cells PBR drug ligands inhibit cell proliferation in a PBR-independent manner. These results are in contrast to data reported on epithelial human breast cancer cells, suggesting that the origin of the cell type, epithelial or mesenchymal, is crucial in defining the role of PBR in cell proliferation.

A manuscript describing in detail these findings was submitted for publication (Appendix 6).

KEY RESEARCH ACCOMPLISHMENTS

We could summarize the following observations as the key research accomplishments of this funding period:

- Elevated PBR expression is not a common feature of aggressive tumors, but rather may be limited to certain cancers, such as those of breast, colon-rectum and prostate tissues, where elevated PBR expression is associated with tumor progression. Thus, we propose that PBR overexpression could serve as a novel prognostic indicator of an aggressive phenotype in breast, colorectal and prostate cancers.
- The ability of the aggressive, hormone-independent, MDA-MB-231 cells to form tumors *in vivo* may depend on the amount of PBR present in the cells.
- It appears that the increase in PBR expression in more aggressive cancers is the result of both gene amplification and increased gene transcription/translation.
- PBR in aggressive breast cancer cells is expressed as a polymer and preferentially as a dimer.
- PBR protein expression is directly involved in regulating cell proliferation in human breast cancer cells, probably by influencing a mechanism involved in cell cycle control.
- Knocking down PBR expression in aggressive human breast cancer cells is associated with decreased cell proliferation, and with increased levels of the cyclin-dependent protein kinase inhibitor p21^{WAF1/CIP1} which is known to be involved in tumor-suppression.
- The origin of the cell type, epithelial (such as human breast cancer cells) or mesenchymal (such as fibroblasts), is crucial in defining the role of PBR and the effect of PBR drug ligands in cell proliferation.

REPORTABLE OUTCOMES

- Han Z, Slack SR, Li W, Papadopoulos V (2003) Expression of peripheral benzodiazepine receptor (PBR) in human tumors: relationship to breast, colon and prostate tumor progression. *Journal of Receptor Research and Signal Transduction*, 23:225-238.
- Hardwick M, Rone J, Han Z, Haddad B, Papadopoulos V (2001) Peripheral-type benzodiazepine receptor levels correlate with the ability of human breast cancer MDA-MB-231 cell line ability to grow in SCID mice. *International Journal of Cancer*, 94:322-327.
- Hardwick M, Rone J, Barlow K, Haddad B, Papadopoulos V (2002) Peripheral-type benzodiazepine receptor (PBR) gene amplification in MDA-231 aggressive breast cancer cells. *Cancer Genetics & Cytogenetics*, 139:48-51.
- Han Z, Slack RS, Papadopoulos V (2002) Peripheral benzodiazepine receptor levels correlate with breast and other tumor progression and metastasis. Era of Hope 2002 Department of Defense Breast Cancer Research Program Meeting., Florida, USA.
- Delavoie F, Li H, Hardwick M, Robert J-C, Giatzakis C, Péranzi G, Yao Z-X, Maccario J, Lacapère JJ, Papadopoulos V. (2003) *In vivo* and *in vitro* peripheral-type benzodiazepine receptor polymerization: functional significance in drug ligand and cholesterol binding. *Biochemistry*, 42:4506-4519.
- Li W, Hardwick M, Papadopoulos V. Peripheral-type benzodiazepine receptor (PBR) overexpression and knockdown in human breast cancer cells indicate a role in tumor cell proliferation mediated by activation of p21^{WAF1/CIP1} expression. *Molecular Carcinogenesis*, under revision.

- Kletsas D, Li W, Han Z, Papadopoulos V. Peripheral-type benzodiazepine receptor (PBR) and PBR drug ligands in fibroblast and fibrosarcoma cell proliferation: Role of ERK, c-jun and ligand-activated PBR-independent pathways. Submitted for publication.

CONCLUSIONS

Funding of this project allowed as to investigate the expression and function of PBR in human breast cancer. The reported studies indicate that aggressive, metastatic breast tumors contain higher levels of PBR compared to normal breast tissue and this protein could be used as a prognostic/diagnostic marker of the disease. We also demonstrated that PBR is intimately involved in the regulation of cell cycle and cell proliferation and is part of the molecular changes responsible for tumor growth in vivo.

REFERENCES

Not applicable.

APPENDICES

1. Han Z, Slack SR, Li W, Papadopoulos V (2003) Expression of peripheral benzodiazepine receptor (PBR) in human tumors: relationship to breast, colon and prostate tumor progression. *Journal of Receptor Research and Signal Transduction*, 23:225-238.
2. Hardwick M, Rone J, Han Z, Haddad B, Papadopoulos V (2001) Peripheral-type benzodiazepine receptor levels correlate with the ability of human breast cancer MDA-MB-231 cell line ability to grow in SCID mice. *International Journal of Cancer*, 94:322-327.
3. Hardwick M, Rone J, Barlow K, Haddad B, Papadopoulos V (2002) Peripheral-type benzodiazepine receptor (PBR) gene amplification in MDA-231 aggressive breast cancer cells. *Cancer Genetics & Cytogenetics*, 139:48-51.
4. Delavoie F, Li H, Hardwick M, Robert J-C, Giatzakis C, Péranzi G, Yao Z-X, Maccario J, Lacapère JJ, Papadopoulos V. (2003) *In vivo* and *in vitro* peripheral-type benzodiazepine receptor polymerization: functional significance in drug ligand and cholesterol binding. *Biochemistry*, 42:4506-4519.
5. Li W, Hardwick M, Papadopoulos V. Peripheral-type benzodiazepine receptor (PBR) overexpression and knockdown in human breast cancer cells indicate a role in tumor cell proliferation mediated by activation of p21^{WAF1/CIP1} expression. *Molecular Carcinogenesis*, under revision.
6. Kletsas D, Li W, Han Z, Papadopoulos V. Peripheral-type benzodiazepine receptor (PBR) and PBR drug ligands in fibroblast and fibrosarcoma cell proliferation: Role of ERK, c-jun and ligand-activated PBR-independent pathways. Submitted for publication.

Expression of Peripheral Benzodiazepine Receptor (PBR) in Human Tumors Relationship to Breast, Colorectal, and Prostate Tumor Progression[#]

Zejiu Han,^{1,2} Rebecca S. Slack,⁵ Wenping Li^{1,2} and Vassilios Papadopoulos^{1,2,3,4,5,*}

¹Division of Hormone Research, ²Department of Cell Biology, ³Department of Pharmacology, ⁴Department of Neurosciences, and ⁵Lombardi Cancer Center, Georgetown University Medical Center, Washington, District of Columbia, USA

ABSTRACT

High levels of peripheral-type benzodiazepine receptor (PBR), the alternative-binding site for diazepam, are part of the aggressive human breast cancer cell phenotype in vitro. We examined PBR levels and distribution in normal tissue and tumors from multiple cancer types by immunohistochemistry. Among normal breast tissues, fibroadenomas, primary and metastatic adenocarcinomas, there is a progressive increase in PBR levels parallel to the invasive and metastatic ability of the tumor ($p < 0.0001$). In colorectal and prostate carcinomas, PBR levels were also higher in tumor than in the corresponding non-tumoral tissues and benign lesions ($p < 0.0001$). In contrast, PBR was highly concentrated in normal adrenal cortical cells and hepatocytes, whereas in adrenocortical tumors and hepatomas PBR levels were decreased. Moreover, malignant skin tumors showed decreased PBR expression compared with normal skin. These results indicate that elevated PBR expression is not a common feature of aggressive tumors, but rather

[#]Supported by the U.S. Army Medical Research Material Command under DAMD17-99-1-9200 award.

*Correspondence: Vassilios Papadopoulos, Division of Hormone Research, Department of Cell Biology, Georgetown University Medical Center, 3900 Reservoir Road, NW, Washington, DC 20057, USA; Fax: 202-687-7855; E-mail: papadopv@georgetown.edu.

may be limited to certain cancers, such as those of breast, colon-rectum and prostate tissues, where elevated PBR expression is associated with tumor progression. Thus, we propose that PBR overexpression could serve as a novel prognostic indicator of an aggressive phenotype in breast, colorectal and prostate cancers.

Key Words: Benzodiazepines; Cancer; Metastasis; Cholesterol.

Abbreviations: PBR, peripheral-type benzodiazepine receptor; GBM, glioblastoma multiforme; BPH, benign prostate hypertrophy.

INTRODUCTION

Two classes of benzodiazepine receptors have been identified, the central-type benzodiazepine receptor located on the neuronal plasma membrane, part of the GABA_A/benzodiazepine receptor complex (1) and the peripheral-type benzodiazepine receptor (PBR)³ (2). Peripheral-type benzodiazepine receptor was identified in peripheral tissues because of its ability to bind the benzodiazepine diazepam (ValiumTM) (2). The pharmacological and molecular properties of these two receptors are distinct (2). Peripheral-type benzodiazepine receptor is an 18 kDa receptor protein which in steroid-synthesizing tissues, such as gonads, adrenal, placenta and brain, is extremely abundant. PBR primarily resides in the outer mitochondrial membrane where it regulates the transport of cholesterol to the mitochondrial inner membrane, the rate-determining step in steroidogenesis (2). Recent studies demonstrated that PBR is a high affinity cholesterol binding protein (3,4). Peripheral-type benzodiazepine receptor is also present in non-steroidogenic organs including kidney, lung, heart, liver, and skin (2). In addition, it has been shown that PBR is involved in mitochondrial respiration (5), regulation of cell proliferation (6), and apoptosis (7).

Peripheral-type benzodiazepine receptor ligand binding, protein and mRNA levels were found to increase in a manner parallel to the increased aggressive phenotype of a battery of human breast tumor cells (8,9). Peripheral-type benzodiazepine receptor in aggressive MDA-MB-231 cells and human breast metastatic tumor biopsies is localized primarily in and around the nucleus, in contrast to the largely cytoplasmic localization seen in less aggressive MCF7 cells and in normal breast tissue (8). Moreover, the ability of MDA-MB-231 cells to form tumors in vivo depends on the amount of PBR present in the cells (10). In addition, drug-induced reduction of PBR levels in MDA-MB-231 cells was accompanied by reduced expression of several genes with close ties to either cell proliferation, differentiation, or apoptosis and correlated with reduced cell proliferation in vitro and tumor growth in nude mice (11).

Although there is evidence that PBR ligand binding capacity is higher in human tumors, such as glioma, liver, colon, ovarian, and endometrial carcinoma, than in the corresponding normal tissue (6,8,12-15), there is no indication that this increased PBR expression correlates with metastasis and no data are available on the expression of PBR in human breast, prostate, lung, skin, adrenal, and testis tumors. In this report, we examined the expression of PBR in primary and metastatic human malignant tumor biopsies compared with corresponding normal tissue, benign lesions, and vicinal non-tumoral tissues. In addition, the correlation between PBR expression and tumor metastasis was evaluated. Our results show that elevated PBR expression is associated with breast, colorectal and prostate tumor progression.

Q1

MATERIALS AND METHODS

Human Biopsies

Human biopsies were obtained from Lombardi Cancer Center Tissue Resource at Georgetown University Medical Center, the Harvard Brain Tissue Resource Center (Belmont, MA) or ResGen (Huntsville, AL). Pathologists verified histological diagnosis and grading (Tables 1 and 2). Protocols for the use of human tissue were approved by the Georgetown University Internal Review Board. Samples for immunohistochemistry were fixed in 10% formalin and embedded with paraffin. Sections (5 μ m) were cut and placed on glass slides. Frozen biopsy samples (-80°C) were used for total RNA extraction.

T1, T2

Immunohistochemistry

All sections were deparaffinized and immunostaining was performed using an affinity-purified anti-peptide rabbit polyclonal anti-PBR antiserum raised against the conserved amino acid sequence 9–27 at a concentration of 1:400 (2 $\mu\text{g}/\text{mL}$) as described (8). After overnight incubation at 4°C , the immunoreactivity was detected using horseradish peroxidase-conjugated anti-rabbit IgG (1:500) (Transduction Laboratories, San Diego, CA). Because PBR is highly expressed in adrenal tissue, immunoreactivity of rat and human adrenal tissue was used for positive control. For the negative control, the primary antibody was preabsorbed with 10 $\mu\text{g}/\text{mL}$ of the PBR peptide used to generate the antiserum. Counterstaining was carried out with Mayer's hematoxylin (Sigma Diagnostics, St. Louis, MO). Immunoreactivity was evaluated by two investigators (Han, Z and Papadopoulos, V) as described (16) with minor modifications. Cytoplasmic and nuclear labeling were evaluated using a semiquantitative method taking into account the staining intensity and the number of stained cells in different random fields. The immunostaining was scored by the percentage of positive cells vs. the total same type cells as –(no staining or $<10\%$), +(mild, $10\%–30\%$), ++(moderate, $30\%–50\%$), +++(strong, $50\%–70\%$), and ++++(intense, $>70\%$).

Quantitative Real-Time PCR

Frozen biopsy tissues and tumors were homogenized in Trizol reagent (Invitrogen, Carlsbad, CA) according to the manufacturer's specifications, then total RNA was submitted to On-Column DNase I digestion with RNase-free DNase in order to remove genomic DNA contamination, and subsequently purified using the QIAGEN RNeasy Total RNA isolation kit (QIAGEN, Valencia, CA). Real-time quantity PCR was performed in ABI PRISM 7700 Sequence Detector (Applied Biosystems, Foster City, CA) as previously described (17). Briefly, total RNA was reverse transcribed into cDNA. The resulting cDNAs were then processed for amplification of PBR using specific forward and reverse primers: $5'\text{-TCTTCTTTGGTGCCCGACA-3'}$ and $5'\text{-CCAGCAGGAGATCCACCAAG-3'}$. Each sample was run in triplicate. Direct detection of the PCR products was achieved by measuring the increase in fluorescence caused by the binding of SYBR[®] Green I Dye to double-stranded (ds) DNA. The comparative C_T method was used to analyze the data. The amount of PBR mRNA expression was normalized to the endogenous reference (18S rRNA).

Table 1. Comparison of PBR expression in human breast, colon-rectum and prostate biopsies.

Tissue	Histopathological type (case)	Mean age (y)	Gender (M/F)	Differentiation	PBR						p-value ^a
					-	+	++	+++	++++	+	
					N (%)	N (%)	N (%)	N (%)	N (%)	N (%)	
Breast	Non-tumoral tissue (8)	39.9			—	3 (38)	5 (62)	—	—	—	<0.0001
	Fibroadenoma, adenosis (22)	40.0			—	9 (41)	13 (59)	—	—	—	
	W/o metastasis (9)	59.8		W(2), M(3), P(4)	—	3 (33)	4 (45)	2 (22)	—	—	
	infiltrating ductal carcinoma (8)										
	infiltrating lobular carcinoma (1)										
Colon-rectum	With metastasis (23)	54.4		W(2), M(4), P(12), U(5)	—	—	9 (39)	14 (61)	—	—	<0.0001
	infiltrating ductal carcinoma (20)										
	infiltrating lobular carcinoma (3)										
Prostate	Non-tumoral tissue (6)	75.6	4/2		—	6 (100)	—	—	—	—	<0.0001
	Adenoma (10)	64.6	8/2		1 (10)	2 (20)	6 (60)	1 (10)	—	—	
	Adenocarcinoma w/o metastasis (12)	64.4	5/7	W(3), M(8), P(1)	—	1 (8)	8 (67)	2 (17)	1 (8)	—	
	Adenocarcinoma with metastasis (21)	67.0	8/13	W(2), M(15), P(4)	—	2 (10)	5 (24)	4 (19)	10 (47)	—	
	Normal tissue (6)	60.8			—	2 (33)	4 (67)	—	—	—	
	BPH (15)	71.2			—	10 (67)	5 (33)	—	—	—	
	Adenocarcinoma (16)	61.4		W(1), M(11), P(4)	—	—	2 (13)	8 (50)	6 (37)	—	

^aThe p-value was calculated using the Jonkheere-Terpstra test.

Notes: Immunohistochemistry was carried out by overnight incubation with rabbit anti-PBR antiserum (1:400) followed by HRP-conjugated anti-rabbit IgG (1:500) for 1 hour. The immunostaining was scored by the percentage of positive cells vs. the total same type cells as - (no staining or <10%), + (mild, 10-30%), ++ (moderate, 30-50%), +++ (strong, 50-70%), and ++++ (intense, >70%). W, M, P, and U represent well, moderately, poorly and unknown differentiation.

Table 2. Comparison of PBR expression in human biopsies.

Tissue	Histopathological type (case)	Mean age (y)	Gender (M/F)	Differentiation	PBR					p-value*
					-	+	++	+++	++++	
					N (%)	N (%)	N (%)	N (%)	N (%)	
Ovary	Normal tissue (7)	56, 2 unknown			2 (28)	5 (72)	—	—	—	0.06
	Adenocarcinoma (20)	55.2		W(3), M(1), P(8), U(8)	3 (15)	8 (40)	5 (25)	3 (15)	1 (5)	
Lung	Non-tumoral tissue (10)	61.0	6/4		—	10 (100)	—	—	—	0.02
	Adenocarcinoma (8)	62.7	3/5	M(1), P(5), U(2)	—	4 (50)	4 (50)	—	—	
Brain	Non-tumoral tissue (3)	70.6	2/1		—	3 (100)	—	—	—	0.25
	GBM (11), anaplastic Astrocytoma (1)	60.5	7/5		—	6 (50)	3 (25)	1 (8)	2 (17)	
Skin	Normal tissue (6)	49.6	2/4		—	4 (66)	1 (17)	1 (17)	—	0.002
	Basal cell carcinoma (7)	60.2	4/3		—	1 (14)	6 (86)	—	—	
	Squamous cell carcinoma (10)	64.6	6/4	W(2), M(3), P(2), U(3)	—	9 (90)	1 (10)	—	—	
	Melanoma (7)	53.0	3/4		1 (4)	6 (86)	—	—	—	
Adrenal	Normal tissue (5)	52.5, 1 unknown	2/2, 1 unknown		—	—	1 (20)	3 (60)	1 (20)	0.05
	Cortical adenoma (3), Cortical adenoma (1)	52.5	2/2	low grade	—	—	3 (100)	—	—	
Liver	Normal tissue (12)	60, 1 unknown	7/4, 1 unknown		—	1 (8)	3 (25)	7 (59)	1 (8)	0.44
	Hepatocellular carcinoma (1)	60.5	9/4	W(4), P(2), U(7)	3 (22)	1 (8)	4 (31)	1 (8)	4 (31)	
Testis	Normal tissue (5)	33, 2 unknown			—	1 (20)	1 (20)	2 (40)	1 (20)	0.25
	Seminoma (8)	33.1			2 (25)	2 (25)	1 (13)	3 (37)	—	

*The p-value was calculated using the Jonckheere-Terpstra test.

Notes: Immunohistochemistry and scoring were carried out as described under *Materials and Methods* and in the Notes of Table 1. W, M, P, and U represent well, moderately, poorly, and unknown differentiation.

Statistical Analysis

A pattern of increasing or decreasing PBR expression over increasing severity of histopathological types was tested within each organ using the exact Jonckheere-Terpstra test (18) as implemented in StatXact (19). This analysis for ordered categorical data measures the evidence against a null hypothesis that all histopathological types within a single organ have the same staining intensity levels in the same proportions. The organs are breast, colon-rectum, prostate, brain, lung, ovary, skin, adrenal, liver, and testis cancers. The notation is as follows. τ_1 represents the normal samples, and τ_2 through τ_n represent each histopathological subtype by increasing severity where n is the number of histopathological subtypes. The two-sided alternative hypothesis is that either $\tau_1 \leq \tau_2 \leq \dots \leq \tau_n$ or $\tau_1 \geq \tau_2 \geq \dots \geq \tau_n$. A significant p -value indicates that there is a tendency for either increasing or decreasing PBR expression associated with increasing severity of histopathological types. With 10 organs being tested, a Bonferroni adjustment was used to control for multiple tests. Peripheral-type benzodiazepine receptor expression was considered to be significantly associated with histopathological severity if the p -value was less than 0.005 (0.05/10 organs).

Comparison of quantitative realtime PCR analysis of colon, breast carcinomas vs. their normal tissues was performed using unpaired t test (Prism, GraphPad, Inc., San Diego, CA).

RESULTS AND DISCUSSION

The immunoreactivity of purified anti-PBR antibody was verified by immunohistochemistry of rich in PBR rat and human adrenal tissues [Fig. 1(A and B)]. Preabsorption of the antibody with PBR peptide blocked this activity [Fig. 1(C and D)]. Immunoblot of rich in PBR mitochondria of MA-10 mouse Leydig cells and isolated recombinant PBR protein identified the corresponding 18-kDa protein (3,20). In addition, this antiserum recognized the 36-kDa PBR dimer present in human breast cancer cells (20).

We examined the expression of PBR in 10 types of human malignant tumor biopsies compared with corresponding non-tumoral tissues and benign lesions. Peripheral-type benzodiazepine receptor is constitutively present, at various expression levels, in all tissues examined Fig. 2 (Tables 1 and 2). Peripheral-type benzodiazepine receptor was primarily seen in the epithelium of breast, colon, prostate, ovary, skin, and lung. Moreover, PBR was also present in adrenal cortical cells, hepatocytes, brain glial cells and Leydig and germ cells of testis. Both nuclear and cytoplasmic pattern of staining were observed, which is consistent with the pattern of PBR sublocalization in breast cancer cell lines and biopsies observed in our previous study (8). It is suggested that nuclear PBR is responsible for regulating movement of cholesterol into the nuclear membrane and that this regulation is related to its modulation of MDA-231 cell proliferation (8). However, it is still open to debate what role cholesterol may play in the nucleus and cell proliferation and how PBR regulates cell proliferation.

Breast PBR expression levels [Fig. 2(A1-A4); Table 1] increased noticeably with increasing severity of breast lesion histopathology ($p < 0.0001$). Non-tumoral, fibroadenoma, and adenosis cases were very similar with about 40% of cases with weak expression (+) and about 60% with moderate expression (++). Primary adenocarcinoma

F1

F2

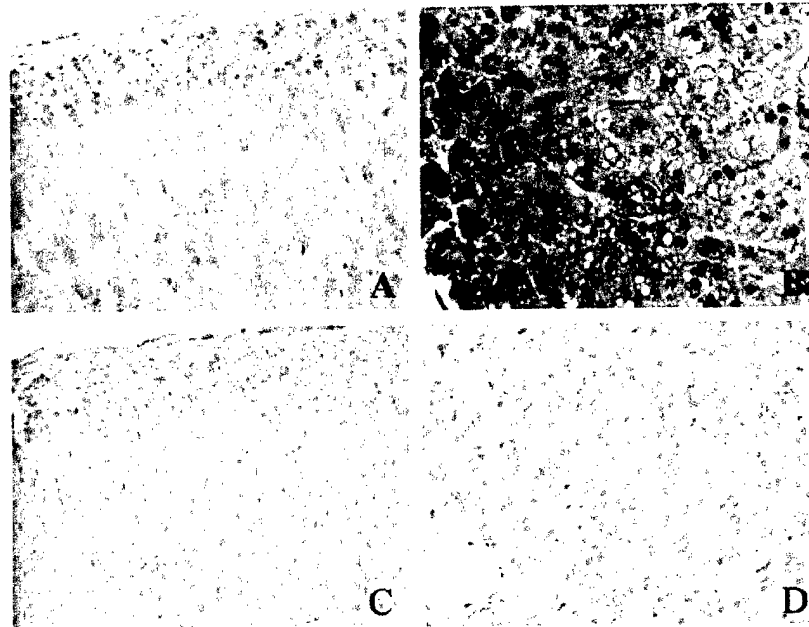
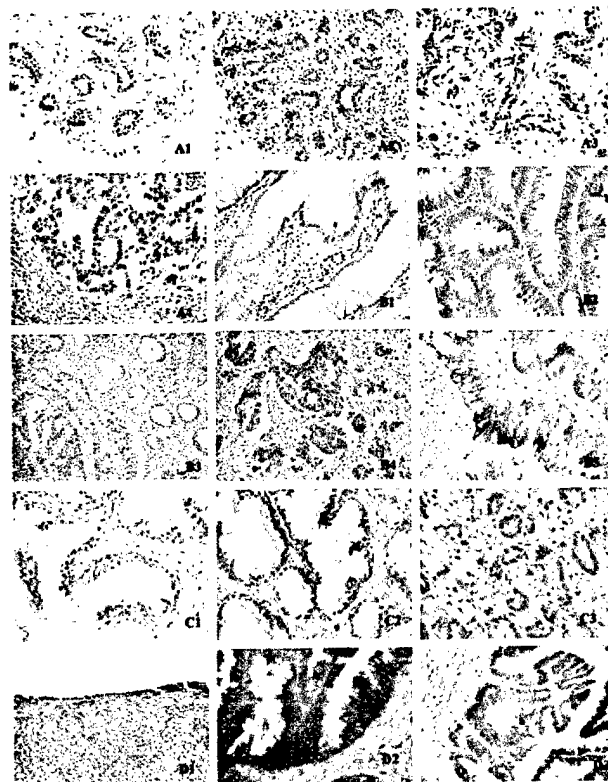
WEB
COLOR

Figure 1. Immunohistochemistry controls. The immunoactivity of the anti-PBR antiserum (2 µg/mL) used was verified by the positive staining of rich in PBR rat (A) and human (B) adrenal tissues. Antiserum preabsorbed with the PBR peptide (10 µg/mL) used to generate the antiserum, failed to recognize the antigen in these sections (C and D).

samples contained 3 (33%) cases with weak (+), and 4 (45%) with moderate expression (++) and 2 (22%) with strong staining (+++). The metastatic cases had only 9 (39%) with moderate staining and 14 (61%) with strong staining. These data show that higher levels of PBR expression are present in aggressive breast tumor cells. Non-tumoral tissue, fibroadenoma and adenosis tissues gave nearly identical results, with increasing expression in primary adenocarcinoma and even more in metastatic adenocarcinoma. These data are in agreement with in vitro studies on human breast cancer cell lines showing that PBR protein and drug ligand binding capacity were increased in aggressive breast cancer cells relative to non-aggressive cells (8,9). Moreover, these results also agree with data showing that the ability of aggressive breast tumor cells to form tumors in vivo might depend on the amount of PBR present in the cells (10). Although in most cells PBR is primarily located in the mitochondria, a perinuclear/nuclear localization has been described in aggressive breast cancer and glioma cell lines (8,21). In the present study, both nuclear and cytoplasmic stainings were observed. In agreement with these protein data and the in vitro cell data (8), breast tumors showed increased PBR mRNA levels compared with normal breast tissue ($p < 0.05$) (Fig. 3).

Peripheral-type benzodiazepine receptor expression in aggressive colorectal carcinomas [Fig. 2(B1-B5); Table 1] is significantly different from non-tumoral tissue and benign

F3



WEB
COLOR

Figure 2. Peripheral-type benzodiazepine receptor expression in human biopsies. Peripheral-type benzodiazepine receptor immunohistochemistry was carried out as described under *Materials and Methods*. Peripheral-type benzodiazepine receptor was highly expressed in primary breast infiltrating intraductal carcinoma (A3) and the same type of carcinoma with lymph node metastasis (A4) compared with non-tumoral breast tissue (A1) and fibroadenoma (A2). The expression of PBR was increased in colorectal adenocarcinoma (B3, B4, and B5) relative to non-tumoral tissue (B1) and adenoma (B2). Peripheral-type benzodiazepine receptor expression was found increased in prostate adenocarcinoma (C3) relative to BPH (C2) and non-tumoral prostate tissue adjacent to BPH (C1). Normal ovary epithelium (D1) showed very weak staining but mucinous cystadenocarcinoma (D2) and serous adenocarcinoma of the ovary (D3) manifested increase of PBR expression. Lung adenocarcinoma cells (E2) expressed much more PBR than non-tumoral lung tissue (E1). Peripheral-type benzodiazepine receptor was highly expressed in the cytoplasm of normal adrenal cortical cells (F1) and the nuclei of low-grade adrenal cortical carcinoma tumor cells (F2). Hepatocellular carcinoma (G2) showed decreased PBR expression compared with its vicinal non-neoplastic hepatocytes and normal hepatocytes (G1). Normal epidermis (H1), basal cell carcinoma (H2), squamous cell carcinoma (H3) and melanoma (H4) all showed positive staining. Peripheral-type benzodiazepine receptor was seen in the germ cells and Leydig cells of normal testis (I1) and seminoma tumor cells (I2). Peripheral-type benzodiazepine receptor positive glial cells were rare in normal brain tissue (J1) whereas the population of positive tumor cells was markedly increased in anaplastic astrocytoma (J2) and GBM (J3).

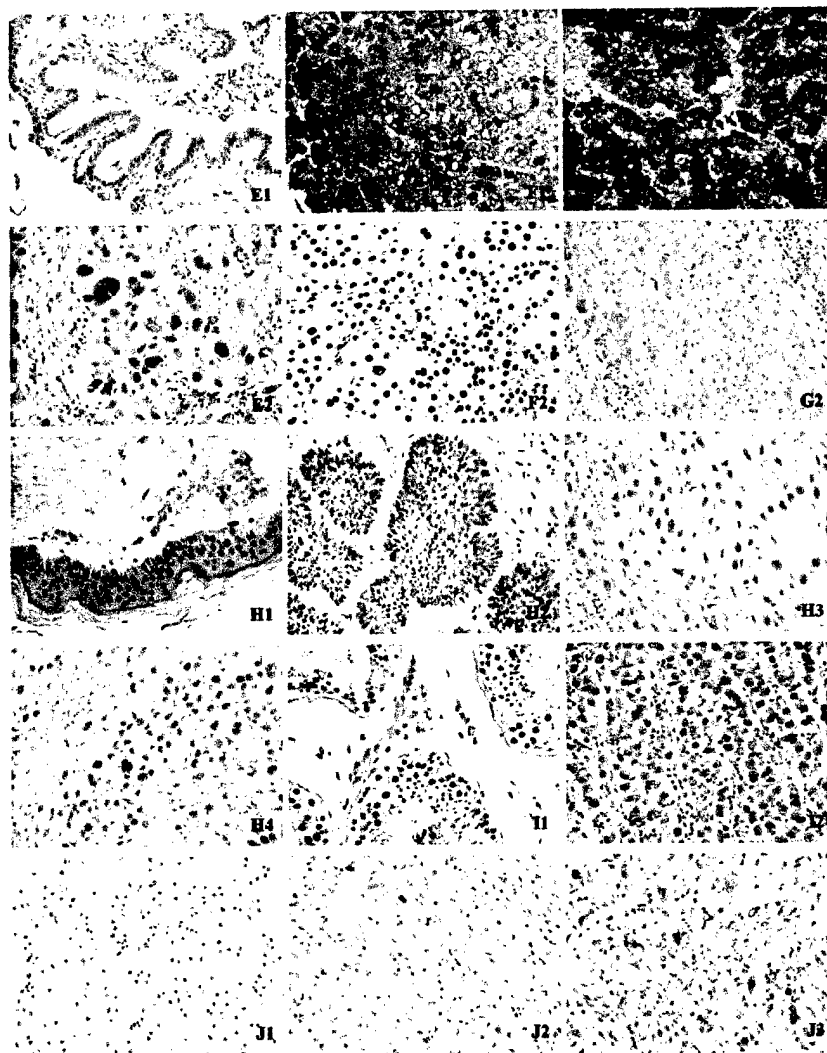


Figure 2. Continued.

lesions ($p < 0.0001$) and similar to that observed in breast cancer. All of the non-tumoral colorectal tissues presented only weak (+) PBR staining. Adenoma and primary adenocarcinoma samples showed 60% and 67% moderate (++) expression, respectively. Ten (47%) of the metastatic adenocarcinoma samples were intensely stained (++++), with only 2 (10%) with weak expression. These data are in agreement with earlier studies reporting increased PBR drug ligand binding sites in colon adenocarcinomas as compared

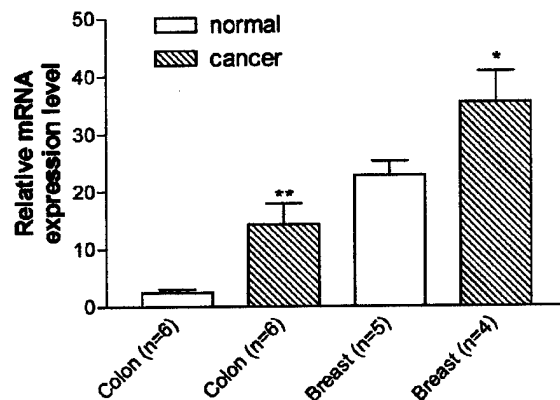


Figure 3. Peripheral-type benzodiazepine receptor mRNA levels in human breast and colon tumors. Peripheral-type benzodiazepine receptor mRNA levels were determined by quantitative real-time PCR carried out as described under *Materials and Methods*. The amount of PBR mRNA expression was normalized to the endogenous reference (18S rRNA). PBR mRNA levels are increased in both breast and colon tumors compared with their corresponding normal tissues. *p* values were determined using the unpaired *t* test. Results are means \pm SEM. Key: ***p* < 0.01; **p* < 0.05.

to normal human colon (22). At the mRNA level (Fig. 3), colon carcinoma showed significant increase of mRNA expression compared to normal colon tissue ($p < 0.01$). This result is consistent with the observation of prognostic significance of PBR overexpression in stage III colorectal cancer (23).

Peripheral-type benzodiazepine receptor immunoreactivity was seen in all the prostatic tissues [Fig. 2(C1–C3); Table 1] examined, but differed significantly between normal samples, BPH samples and adenocarcinomas ($p < 0.0001$). BPH cases [Fig. 2(C2)] exhibited mostly weak (+) staining (67%) with some moderate staining (++). Adenocarcinoma cases [Fig. 2(C3)] had moderate (++), 2 cases (13%), strong (+++), 8 cases (50%), and intense (++++) , 6 cases (37%), staining. These results indicate a strong correlation between PBR levels and prostate histopathology. Thus, PBR may be considered as one parameter along with prostatic specific antigen and prostate-specific acid phosphatase (24) in the diagnosis of prostatic adenocarcinoma. It has been reported that PBR drug ligand binding is present in both mitochondrial and microsomal fractions of Dunning G prostatic adenocarcinomas from orchiectomized rats compared to tumors from sham operated controls. Treatment with testosterone repressed PBR drug ligand binding in both fractions to control values, suggesting a role of testosterone on the PBR density in these hormone-sensitive prostatic tumors (25).

To the best of our knowledge, there has been no report about the correlation between normal lung and lung tumor PBR levels. All 10 normal lung tissues [Fig. 2(E1); Table 2] showed weak expression (+), while half (4 cases) of the adenocarcinomas had weak (+) and half moderate staining (++) [Fig. 2(E2)]. This difference is significant ($p = 0.02$) and

471 although it suggests that PBR might be involved in the progression of lung cancer, further
472 investigation is required.

473 Brain tissue samples measured for PBR expression show a small trend indicating
474 increased expression among GBM and anaplastic astrocytomas [Fig. 2(J1-J3); Table 2]. All
475 three of the non-tumoral tissue samples showed weak PBR expression, while 9 (75%) of the
476 GBM and anaplastic astrocytoma samples had no staining (-), with 1 (8%) and 2 (17%)
477 cases with weak (+) and moderate (++) expression, respectively. Immunoreactive PBR was
478 found in the nuclei of the neurons and cytoplasm of glial cells with weak strength in normal
479 brain, whereas its expression increases in the group of GBM and anaplastic astrocytoma.
480 These results suggest that PBR is expressed constitutively at low level until the onset of the
481 tumor. It has been suggested that PBR expression is associated with the malignancy grade of
482 astrocytoma and affect the life expectancy of tumor-bearing patients (6).

483 There were notable differences between the normal ovarian tissue and ovarian
484 carcinomas ($p = 0.06$), normal ovarian tissue had no staining (28%) and mild staining
485 (72%) only [Fig. 2(D1); Table 2]. The majority of tumor samples express PBR with 40%
486 weak staining, 25% moderate staining and 20% strong or intense staining, [Fig. 2(D2 and
487 D3)]. As the fourth leading cause of death in women, epithelial ovarian carcinoma is
488 usually diagnosed in advanced stages. However, it has been reported that a robust increase
489 in the number of PBR binding sites in ovarian carcinoma occurs when compared with
490 benign ovarian tumors and normal tissues (14). Thus, further investigation with more
491 samples is needed to elicit the possible correlation of PBR expression with the progression
492 of ovarian neoplasm.

493 Even though it is known that hormones regulate PBR levels, the molecular mecha-
494 nisms involved in the regulation of PBR during tumor progression remain unknown. In
495 contrast to the increased PBR levels found in epithelial tumors from breast, colon-rectum,
496 prostate, lung, and ovary tumors, the opposite results were found in the tumors of skin,
497 adrenal, liver, and testis.

498 Normal skin tissue and less aggressive tumors have significantly ($p = 0.002$) higher
499 levels of staining compared to more advanced or malignant tissues [Fig. 2(H1-H4);
500 Table 2]. Normal tissue showed PBR immunostaining ranging from weak (+, 66%), to
501 moderate (++, 17%) and strong (+++, 17%) intensity, in agreement with a recent report
502 (26), while basal cell carcinoma samples [Fig. 2(H2)] had mostly (86%) moderate (++)
503 staining and the rest had weak (+) expression. Squamous cell carcinoma PBR immuno-
504 staining [Fig. 2(H3)] was mostly weak (+, 90%). Melanoma cases [Fig. 2(H4)] also
505 presented mostly (86%) weak (+) staining. These data indicate that PBR is expressed at
506 higher levels in the normal skin epidermal cells whereas its expression level decreased in
507 the corresponding tumors. It has been suggested that PBR may participate in an
508 antioxidant pathway in normal skin epidermal cells (26).

509 Table 2 presents information about the levels of PBR expression present in adrenal
510 [Fig. 2(F1)], liver [Fig. 2(G1)] and testis [Fig. 2(I1)] tissues and their respective
511 malignancies [Fig. 2(F2, G2 and I2)]. The trend observed suggests that PBR is expressed
512 at high levels in normal adrenal cortical cells, hepatocytes and Leydig cells as well as germ
513 cells (although in reduced levels) of testis, whereas its presence decreased in their
514 corresponding tumors. However, there were not enough samples to evaluate convincingly
515 the statistical significance of these data. The present findings with liver tumors do not
516 support the observation showing upregulation of PBR expression in human hepatocellular
517 carcinoma (12).

In conclusion, among breast, colorectal and prostate carcinomas, PBR expression dramatically increases compared to their non-malignant counterparts. Metastatic breast and colorectal adenocarcinomas manifest increased PBR expression relative to their primary malignancies. Brain, lung and ovarian tumors show a small trend in which malignant tumors express more PBR than the corresponding non-tumoral tissues. We also observed that PBR is present in high levels in the cytoplasm of normal adrenocortical cells and hepatocytes, whereas PBR levels are lower in cortical adenoma, adenocarcinoma and hepatocellular carcinomas where it primarily localizes in the nuclei. Peripheral-type benzodiazepine receptor levels are higher in the epidermal cells of normal skin than in skin basal cell carcinomas, squamous cell carcinomas and melanomas. Testis seminomas show varied levels of PBR expression while the Leydig cells and germ cells contain PBR at very high and moderate levels, respectively. Despite the limited number of certain samples, these data provide a basis to study the predictive value of PBR expression in assessing the progression of the disease and the efficacy of various treatments. In addition, recent data showed the induction of apoptosis and cell death in various cancer cell lines by pharmacological concentrations of high affinity PBR drug ligands (8,27-29). Taken together, these results support further efforts on the evaluation of PBR as a predictive means of breast, colorectal, and prostatic tumor progression and the use of these drugs as anti-tumor agents in clinical trials.

ACKNOWLEDGMENTS

We are grateful to the Lombardi Cancer Center Tumor Bank and Biostatistics Core for the tissue biopsies, pathology reports and their support, to the Harvard Brain Tissue Resource Center (supported in part by PHS grant number MH/NS 31862) and Drs. S.W. Byers and M. Culty for critically reviewing the manuscript.

REFERENCES

1. Costa E, Guidotti A, Mao CC, Suria A. New concepts of the mechanism of action of benzodiazepines. *Life Sci* 1975; 17:167-186.
2. Papadopoulos V. Peripheral-type benzodiazepine/diazepam binding inhibitor receptor: biological role in steroidogenic cell function. *Endocr Rev* 1993; 14:222-240.
3. Li H, Yao Z, Degenhardt B, Teper G, Papadopoulos V. Cholesterol binding at the cholesterol recognition/interaction amino acid consensus (CRAC) of the peripheral-type benzodiazepine receptor and inhibition of steroidogenesis by an HIV TAT-CRAC peptide. *Proc Natl Acad Sci* 2001; 98:1267-1272.
4. Lacapère JJ, Delavoie F, Li H, Péranski G, Maccario J, Papadopoulos V, Vidic B. Structural and functional study of reconstituted peripheral benzodiazepine receptor (PBR). *Biochem Biophys Res Comm* 2001; 284:536-641.
5. Hirsch JD, Beyer CF, Malkowitz L, Beer B, Blume AJ. Mitochondrial benzodiazepine receptors mediate inhibition of mitochondrial respiratory control. *Mol Pharmacol* 1989; 35:157-163.
6. Miettinen H, Kononen J, Haapasalo H, Helén P, Sallinen P, Harjuntausta T, Helin H, Alho H. Expression of peripheral-type benzodiazepine receptor and diazepam binding

- 565 inhibitor in human astrocytomas: relationship to cell proliferation. *Cancer Res* 1995;
566 55:2691-2695.
- 567 7. Papadopoulos V, Dharmarajan AM, Li H, Culty M, Lemay M, Sridaran R. Mitochondrial
568 peripheral-type benzodiazepine receptor expression: correlation with the GnRH-agonist
569 induced apoptosis in the corpus luteum. *Biochem Pharmacol* 1999; 58:1389-1393.
- 570 8. Hardwick M, Fertikh D, Culty M, Li H, Vidic B, Papadopoulos V. Peripheral-type
571 benzodiazepine receptor (PBR) in human breast cancer: correlation of breast
572 cancer cell aggressive phenotype with PBR expression, nuclear localization, and PBR-
573 mediated cell proliferation and nuclear transport of cholesterol. *Cancer Res* 1999; 59:
574 832-842.
- 575 9. Beinlich A, Strohmeier R, Kaufmann M, Kuhl H. Relation of cell proliferation to
576 expression of peripheral benzodiazepine receptors in human breast cancer cell lines.
577 *Biochem Pharmacol* 2000; 60:397-402.
- 578 10. Hardwick M, Rone J, Han Z, Haddad B, Papadopoulos V. Peripheral-type benzodia-
579 zepine receptor levels correlate with the ability of human breast cancer MDA-MB-231
580 cell line to grow in SCID mice. *Int J Cancer* 2001; 94:322-327.
- 581 11. Papadopoulos V, Kapsis A, Li H, Amri A, Hardwick M, Culty M, Kasprzyk PG,
582 Carlson M, Moreau JP, Drieu K. Drug-induced inhibition of the peripheral-type
583 benzodiazepine receptor expression and cell proliferation in human breast cancer
584 cells. *Anti Cancer Res* 2000; 20:2835-2848.
- 585 12. Venturini I, Alho H, Podkletnova I, Corsi L, Rybnikova E, Pellicci R, Baraldi M,
586 Pelto-Huikko M, Helén P, Zeneroli ML. Increased expression of peripheral benzo-
587 diazepine receptors and diazepam binding inhibitor in human tumors sited in the liver.
588 *Life Sci* 1999; 65:2223-2231.
- 589 13. Katz Y, Eitan A, Amiri Z, Gavish M. Dramatic increase in peripheral benzodiazepine
590 binding sites in human colonic adenocarcinoma as compared to normal colon. *Eur J*
591 *Pharma* 1988; 148:483-484.
- 592 14. Katz Y, Ben-Baruch G, Kloog Y, Menczer J, Gavish M. Increased density of
593 peripheral benzodiazepine-binding sites in ovarian carcinomas as compared with
594 benign ovarian tumors and normal ovaries. *Clinical Sci* 1990; 78:155-158.
- 595 15. Batra S, Iosif CS. Peripheral benzodiazepine receptor in human endometrium and
596 endometrial carcinoma. *Anti Cancer Res* 2000; 20:463-466.
- 597 16. Simony-Lafontaine J, Esslimani M, Bribes E, Gourgou S, Lequeux N, Lavail R,
598 Grenier J, Kramar A, Casellas P. Immunocytochemical assessment of sigma-1 receptor
599 and human sterol isomerase in breast cancer and their relationship with a series of
600 prognostic factors. *Br J Cancer* 2000; 82:1958-1966.
- 601 17. Li W, Pretner E, Shen L, Drieu K, Papadopoulos V. Common gene targets of *Ginkgo*
602 *biloba* extract (EGb 761) in human tumor cells: relation to cell growth. *Cell Mol Biol*
603 2002; 48:655-662.
- 604 18. Hollander M, Wolfe DA. *Nonparametric Statistical Methods*. New York: John Wiley
605 & Sons, 1973.
- 606 19. Mehta C, Patel N. *StatXact4 for Windows*. Cambridge, MA: Cytel Software Corp,
607 2000.
- 608 20. Delavoie F, Li H, Hardwick M, Robert JC, Giatzakis C, Peranzi G, Yao Z, Maccario J,
609 Lacapere JJ, Papadopoulos V. In vivo and in vitro peripheral-type benzodiazepine
610 receptor polymerization: functional significance in drug ligand and cholesterol
611 binding. *Biochemistry* 2003; 42:4506-4519.

- 612 21. Brown RC, Degenhardt B, Kotoula M, Papadopoulos V. Location-dependent role of
613 the human glioma cell peripheral-type benzodiazepine receptor in proliferation and
614 steroid biosynthesis. *Cancer Lett* 2000; 156:125-132.
- 615 22. Ishii K, Kano T, Akutagawa M, Makino M, Tanaka T, Ando J. Effects of flurazepam
616 and diazepam in isolated guinea-pig taenia coli and longitudinal muscle. *Eur J*
617 *Pharma* 1982; 83:329-333.
- 618 23. Maaser K, Grabowski P, Sutter AP, Höpfner M, Foss H, Stein H, Berger G, Gavish M,
619 Zeitz M, Scherübl H. Overexpression of the peripheral benzodiazepine receptor is a
620 relevant prognostic factor in stage III colorectal cancer. *Clin Cancer Res* 2002;
621 8:3205-3209.
- 622 24. Epstein JI, Wojno KJ. The prostate and seminal vesicles. In: Sternberg SS,
623 Antonioli DA, Carter D, Mills SE, Oberman HA, eds. *Diagnostic Surgical Pathology*.
624 Vol. 2. 3rd ed. Philadelphia, PA: Lippincott Williams & Wilkins, 1999:1900-1901.
- 625 25. Alenfall J, Batra S. Modulation of peripheral benzodiazepine receptor density by
626 testosterone in Dunning G prostatic adenocarcinoma. *Life Sci* 1995; 56:1897-1902.
- 627 26. Stoebner PE, Carayon P, Penarier G, Frechin N, Barneon G, Casellas P, Cano JP,
628 Meynadier J, Meunier L. The expression of peripheral benzodiazepine receptors in
629 human skin: the relationship with epidermal cell differentiation. *Br J Dermatol* 1999;
630 140:1010-1016.
- 631 27. Camins A, Diez-Fernandez C, Pujadas E, Camarasa J, Escubedo E. A new aspect of
632 the antiproliferative action of peripheral-type benzodiazepine receptor ligands. *Eur J*
633 *Pharm* 1995; 272:289-292.
- 634 28. Hirsch T, Decaudin D, Susin SA, Marchetti P, Larochette N, Resche-Rigon M,
635 Kroemer G. PK11195, a ligand of the mitochondrial benzodiazepine receptor,
636 facilitates the induction of apoptosis and reverses Bcl-2-mediated cytoprotection.
637 *Exp Cell Res* 1998; 241:426-434.
- 638 29. Maaser K, Höpfner M, Jansen A, Weisinger G, Gavish M, Kozikowski AP,
639 Weizman A, Carayon P, Reicken EO, Zeitz M, Scherübl H. Specific ligands of the
640 peripheral benzodiazepine receptor induce apoptosis and cell cycle arrest in human
641 colorectal cancer cells. *Br J Cancer* 2001; 85:1771-1780.

PERIPHERAL-TYPE BENZODIAZEPINE RECEPTOR LEVELS CORRELATE WITH THE ABILITY OF HUMAN BREAST CANCER MDA-MB-231 CELL LINE TO GROW IN SCID MICE

Matthew HARDWICK¹, Janice RONE^{2–4}, Zeqiu HAN¹, Bassem HADDAD^{2–4} and Vassilios PAPADOPOULOS^{1,4,5*}

¹Division of Hormone Research, Department of Cell Biology, Georgetown University Medical Center, Washington, DC, USA

²Department of Oncology, Georgetown University Medical Center, Washington, DC, USA

³Department of Obstetrics and Gynecology, Georgetown University Medical Center, Washington, DC, USA

⁴Lombardi Cancer Center, Georgetown University Medical Center, Washington, DC, USA

⁵Department of Pharmacology, Georgetown University Medical Center, Washington, DC, USA

MDA-MB-231 (MDA-231) human breast cancer cells have a high proliferation rate, lack the estrogen receptor, express the intermediate filament vimentin, the hyaluronan receptor CD44, and are able to form tumors in nude mice. The MDA-231 cell line has been used in our laboratory to examine the role of the peripheral-type benzodiazepine receptor (PBR) in the progression of cancer. During these studies 2 populations of MDA-231 cells were subcloned based on the levels of PBR. The subclones proliferated at approximately the same rate, lacked the estrogen receptor, expressed vimentin and CD44, and had the same *in vitro* chemoinvasive and chemotactic potential. Both restriction fragment length polymorphism and comparative genomic hybridization analyses of genomic DNA from these cells indicated that both subclones are of the same genetic lineage. Only the subclone with high PBR levels, however, was able to form tumors when injected in SCID mice. These data suggest that the ability of MDA-231 cells to form tumors *in vivo* may depend on the amount of PBR present in the cells.

© 2001 Wiley-Liss, Inc.

Key words: PBR; benzodiazepine; breast cancer; MDA-231

Aberrant cell proliferation and increased invasive and metastatic behavior are hallmarks of the advancement of breast cancer. In an effort to elucidate the mechanisms responsible for the progression of breast cancer, several laboratories have extensively characterized a battery of human breast cancer cell lines for several breast cancer markers such as the estrogen receptor (ER), the fibroblast cytoskeletal protein vimentin, the hyaluronan receptor, CD44, as well as their chemotactic and chemoinvasive potential.^{1–3} Although several studies have utilized these cell lines to determine the mechanism(s) responsible for the transition from non-aggressive to aggressive breast cancer, these mechanisms remain elusive. Work in our laboratory and others suggests that 1 potential candidate may be the peripheral-type benzodiazepine receptor (PBR). Recently we have shown that PBR expression is markedly increased in aggressive breast cancer cell lines, such as the MDA-231 cell line, relative to non-aggressive breast cancer cell lines as well as in aggressive metastatic human breast tumor biopsies compared with normal breast tissues.⁴ Moreover, ligands specific for PBR regulated the proliferation rate of the aggressive MDA-231 breast cancer cell line.⁴ PBR is an 18kDa transmembrane protein known to play a crucial role during steroidogenesis.^{5,6} Increased expression of PBR has been found in numerous tumor types and PBR has been shown to regulate the differentiation state and proliferation rates of several cancer cell lines.^{7–20} Over the past several years our laboratory has examined the role of PBR in breast cancer using the MDA-231 cell line. While examining MDA-231 cells from various origins we observed variations in their PBR levels. From the MDA-231 cell line that we previously used to investigate the role of PBR,⁴ subclones were isolated based on their PBR levels of expression. To determine if these differing PBR levels had any effect on the MDA-231 aggressive phenotype, we tested the anchorage-dependent and -independent proliferation of the subclones, as well as the expression of ER, vimentin, and

CD44. We also tested their *in vitro* chemotactic and chemoinvasive potential and their ability to grow in SCID mice.

MATERIAL AND METHODS

Cell culture

The MDA-231 cell line, obtained from the Lombardi Cancer Center, Georgetown University Medical Center, was grown as previously described.⁴ In some experiments cells were passaged twice in antibiotic-free DMEM, 10% FBS. Cells were then grown to confluency and maintained in without change of media for 5 days. All cultures were grown to 10 passages and either used or discarded. The media was then harvested and submitted to the Lombardi Cancer Center Tissue Core Facility for mycoplasma screening.

[³H]PK 11195 binding studies

Cells were grown to confluency in DMEM, 10% FBS. All cells were harvested from culture dishes and assayed for protein concentration by the Bradford method²¹ using the Bio-Rad Protein Assay kit (Bio-Rad Laboratories, Hercules, CA) and [³H]PK 11195 binding studies on 20 µg of protein from cell suspensions were performed as previously described.⁴ Scatchard plots were analyzed by the LIGAND program.²²

Crystal violet cell proliferation

Cells were grown to confluency, trypsinized, plated on 96-well plates at a concentration of 2,000 cells/well and maintained in DMEM, 10% FBS. Media was changed every 2 days. At the specified time points cells were stained Crystal Violet solution as described previously.¹⁷

Estrogen receptor enzyme immunoassay (ER-EIA)

Cells were harvested from confluent cultures by trypsinization and washed once with PBS. Cells were then washed once in phosphate buffer (5 mM sodium phosphate, pH 7.4, 10 mM thioglycerol, and 10% glycerol). Nuclear extracts from each cell line were prepared as previously described.²³ One hundred micrograms of each nuclear extract was incubated with 1 ER bead for 18 hr and processed according to the Abbott ER-EIA Monoclonal

Grant sponsor: National Institute of Health; Grant number: CA-80763; Grant sponsor: U.S. Department of Defense; Grant number: DAMD17-99-1-9200.

*Correspondence to: Division of Hormone Research, Department of Cell Biology, Georgetown University Medical Center, 3900 Reservoir Road, Washington, DC 20007, USA. Fax: +202-687-7855.
E-mail: papadopv@georgetown.edu

Received 29 January 2001; Revised 17 April 2001; Accepted 21 May 2001

Published online 3 August 2001; DOI 10.1002/ijc.1472

Protocol (1997). For each wash, beads were washed 10 times in distilled H₂O on a Brandel 24-well Harvester (Brandel, Gaithersburg, MD) in 12 × 75 mm borosilicate glass tubes.

Immunocytochemistry

Eight-chamber glass slides (Fisher Scientific, Pittsburgh, PA) were coated with poly-L lysine (Sigma Chemicals, St. Louis, MO) for several hr. Ten thousand cells per well for each cell line were loaded onto the slides and were incubated overnight at 37°C, 6% CO₂. The cells were fixed in 10% formaldehyde for 10 min at room temperature. After washing well with distilled H₂O, anti-PBR²⁴ diluted 1:400 in PBS supplemented with 10% FBS, anti-vimentin (Boehringer-Mannheim, Indianapolis, IN), diluted 1:3 in PBS supplemented with 10% FBS or anti-CD44 (Calbiochem, San Diego, CA) diluted 1:100 in PBS supplemented with 10% FBS, was added each well and incubated overnight at 4°C. After rinsing the slides well in PBS, horseradish peroxidase (HRP) conjugated goat anti-mouse secondary antibody (BD Biosciences Transduction Laboratory, Lexington, KY), diluted 1:1,000 in PBS supplemented with 10% FBS, was added to each well and incubated for 1 hr at RT. Visualization of HRP activity with 3-amino-9-ethyl carbazole (AEC) and counterstaining with hematoxylin was performed as previously described.⁴

Chemotactic and chemoinvasion assays

For chemotaxis assays, cells were grown to confluency, trypsinized, and plated on 8 µm 24-well inserts (Becton Dickinson Labware, Bedford, MA) at a concentration of 3×10^5 cells/insert in DMEM, 0.1% FBS. The inserts were then placed in 24-well companion plates (Becton Dickinson Labware) containing 800 µl DMEM, 10% Tet-approved FBS (Clontech, San Diego, CA) and incubated at 37°C, 6% CO₂ for 48 hr. Before beginning the chemoinvasion assay, 8 µm 24-well inserts (Becton Dickinson Labware) were coated with 200 µg/cm² matrigel (Becton Dickinson Labware) and left to dry overnight. Several hr before the beginning of the assay, the matrigel was rehydrated with DMEM, 0.1% FBS. All cells were grown to confluency, trypsinized, and plated on matrigel-coated 8 µm 24-well inserts at a concentration of 3×10^5 cells/insert in DMEM, 0.1% FBS. The inserts were then placed in 24-well companion plates (Becton Dickinson Labware) containing 800 µl DMEM, 10% FBS and incubated at 37°C, 6% CO₂ for 48 hr.

At the end of each incubation, cells were removed from the inside chamber by use of suction followed by a cotton swab. The membranes were then incubated for 10 min with Crystal Violet (0.5% Crystal Violet, 25% methanol) at room temperature. Excess Crystal Violet was removed by washing the membranes 6 times with room temperature tap H₂O. All staining of the inside of the membranes was removed with a cotton swab. Membranes were then dried overnight. The stain was solubilized from membranes and absorbance was read at 570 nm as previously described.¹⁷

Tumor growth in SCID mice

Cells were grown to confluency, trypsinized, counted and resuspended in sterile PBS at a concentration of 5×10^5 cells/100 µl. One hundred micrograms of the cell suspensions were then injected into the mammary fat pad of 8 SCID mice for each cell

line. Tumor growth was measured weekly for 1 month. Protocols were approved by the Georgetown University Animal Care and Use Committee.

Restriction fragment length polymorphism (RFLP)

To examine the genetic identity of the MDA-231 PL and PH cells, frozen cell pellets were sent to Cellmark Diagnostics, Inc. (Germantown, MD). Genomic DNA (DNAGEN) was prepared, digested with HinfI enzyme, electrophoresed, blotted onto nylon membranes and hybridized with the indicated probes. Probe-DNA complexes were visualized by chemiluminescence (2000 Standard Operating Procedures, 100-25, Cellmark Diagnostics, Inc.).

Comparative genomic hybridization (CGH)

CGH was performed according to standard procedures.²⁵ Normal control DNA was prepared from peripheral blood lymphocytes of a cytogenetically normal male and tumor DNA was extracted from the 2 cell lines, MDA-231 PH and PL. Nick translation was performed to label tumor DNA with bio-16-dUTP (Boehringer-Mannheim, Germany) and control DNA with digoxigenin-11-dUTP (Boehringer-Mannheim). Each of the labeled genomes (500 ng) were hybridized in the presence of excess Cot-1 DNA (50 µg) (GIBCO-BRL, Gaithersburg, MD) to metaphase chromosomes prepared from a karyotypically normal donor. The biotin-labeled tumor genome was visualized with avidin conjugated to fluorescein isothiocyanate (FITC) (Vector Laboratories Inc., Burlingame, CA) and the digoxigenin-labeled control DNA was detected with a mouse anti-digoxin antibody (Sigma Aldrich) followed by detection with a goat anti-mouse antibody conjugated to tetra-methyl-rhodamine isothiocyanate (TRITC) (Sigma Aldrich). Chromosomes were counterstained with 4',6-diamidino-2-phenylindole (DAPI) and embedded in anti-fading agent to reduce photobleaching.

Gray scale images of the FITC-labeled tumor DNA, the TRITC labeled control DNA and the DAPI counterstain from at least 8 metaphases from each hybridization were acquired with a cooled charge-coupled device CCD camera (CH250, Photometrics, Tucson, AZ) connected to a Leica DMRBE microscope equipped with fluorochrome specific optical filters TR1, TR2, TR3 (Chroma Technology, Brattleboro, VT). Quantitative evaluation of the hybridization was done using commercially available software (Applied Imaging, Pittsburgh, PA). Average ratio profiles were computed as the mean value of at least 8 ratio images to identify chromosomal copy number changes in all cases.

RESULTS

We previously described the MDA-231 cell line as having a maximal PBR ligand binding (B_{max}) of 8.7 pmol/mg of protein.⁴ From this MDA-231 cell line we isolated sub-populations based on PBR levels. Scatchard analysis of the saturation isotherms generated using 2 of the isolated MDA-231 subclones indicated that these cells had divergent PBR ligand binding (Table I). Three of the new isolated cell lines had a B_{max} of 2.9 pmol/mg protein (Fig. 1a; Table I). Although all of the experiments reported herein were performed with all 3 cell lines, because the results obtained were similar only representative data from 1 of the cell lines are shown.

TABLE I—COMPARISON OF MDA-231 SUBCLONES FOR EXPRESSION OF VARIOUS MARKERS OF BREAST TUMOR AGGRESSION¹

Cells	PK 11195 binding		ER	Vimentin	CD44	Chemoinvasion	Chemotaxis
	KD (nM)	B _{max} (pmol/mg prot)					
MDA-231 PH	7.5 ± 0.9	6.4 ± 1.0	—	+	+	+++++	+++++
MDA-231 PL	1.8 ± 1.0	2.9 ± 1.0	—	+	+	+++++	+++++

¹PK 11195 binding values for the MDA-231 PH and PL cell lines were obtained from the Scatchard analyses presented in Figure 1. KD, dissociation constant; B_{max}, maximal PK 11195 binding. Quantification of estrogen receptor (ER) expression was determined using the ER-Enzyme Immuno-Assay (ER-EIA). —, the absence of ER expression. Vimentin and CD44 expression were determined by immunocytochemistry. +, visible detection of protein expression. Chemotaxis and chemoinvasion were determined as described in Material and Methods. +++++, values are 80–100% of MDA-231 PH values.

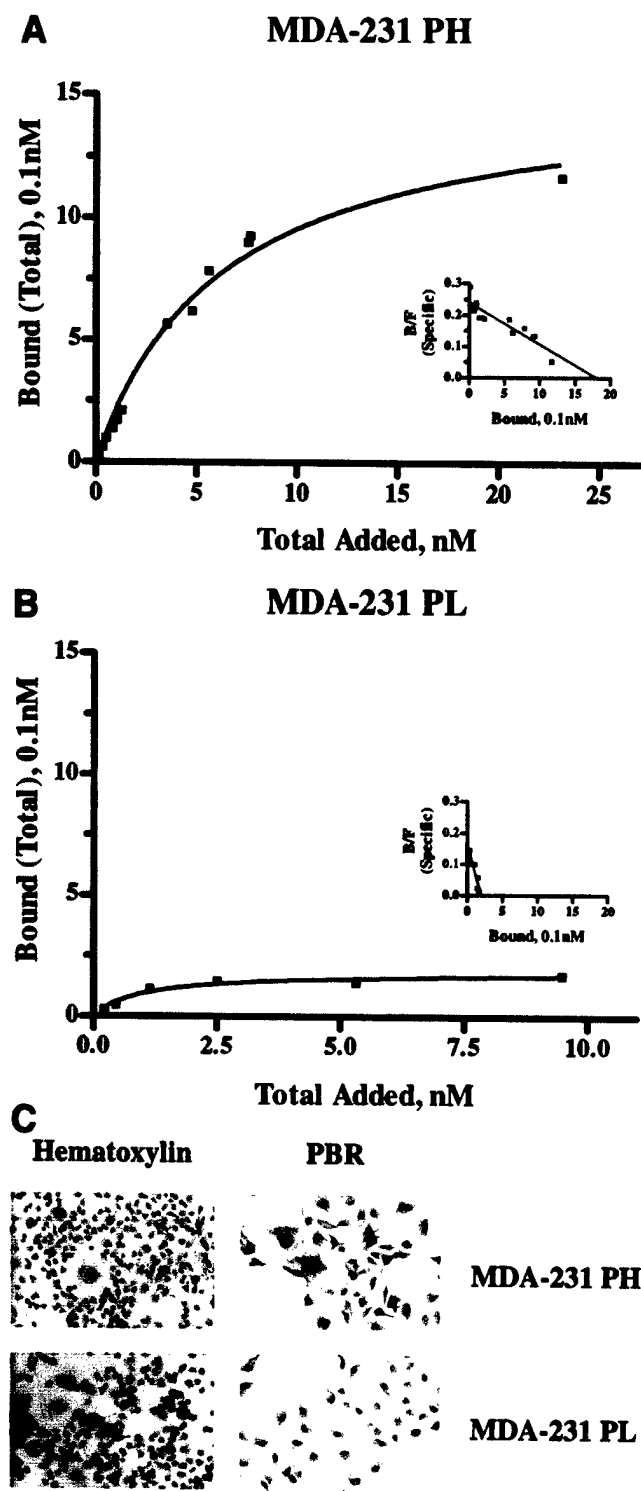


FIGURE 1 – PBR ligand binding characteristics and PBR immunoreactivity in the MDA-231 PH and MDA-231 PL cell lines. (a) PK 11195 ligand binding was measured in the presence of 20 μ g of cellular protein and the indicated concentrations of [3 H]PK 11195. Representative saturation isotherms and Scatchard plots are shown. (b) MDA-231 PH and MDA-231 PL were plated on slides, fixed, and stained either with hematoxylin or incubated with anti-PBR antiserum. Pictures were taken at 10 \times and 40 \times magnification for hematoxylin and PBR, respectively.

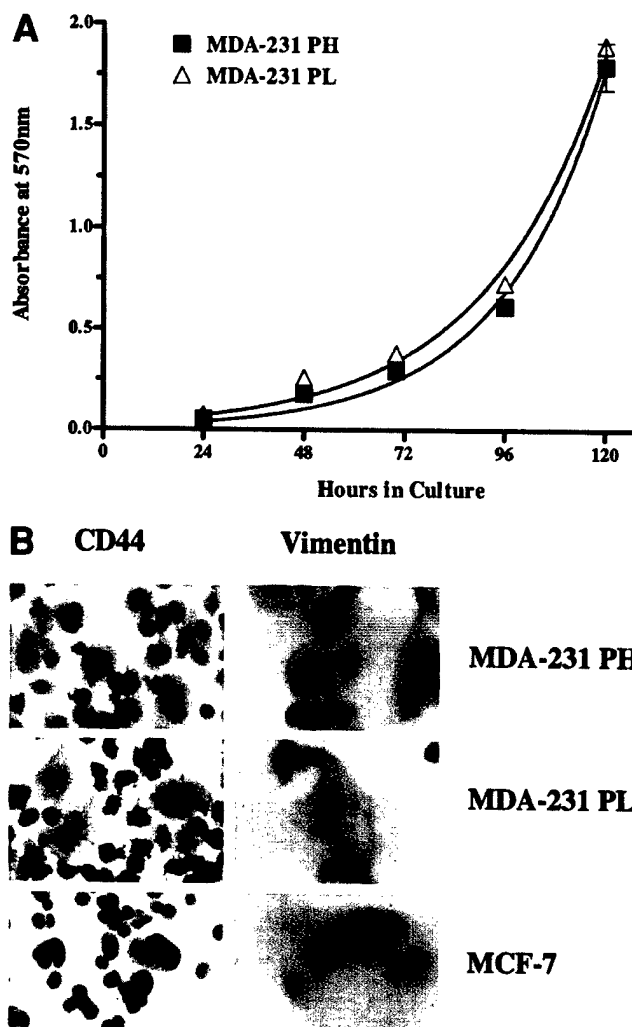


FIGURE 2 – MDA-231 PH and MDA-231 PL cell proliferation rates and expression of CD44 and vimentin. (a) MDA-231 PH and MDA-231 PL Cell proliferation rates. Cells were plated at a density of 2,000 cells per well on 96-well plates and followed for 6 days. Every 24 hr, cells were stained with Crystal Violet. Absorbance was read at 570 nm. Results shown are representative of 3–4 independent experiments. (b) MDA-231 PH and MDA-231 PL were plated on slides, fixed, and incubated with anti-vimentin or anti-CD44 antisera. Original magnification $\times 40$.

These cells are referred to MDA-231 PBR Low (MDA-231 PL). Other subclones of MDA-231 cells had a B_{max} equal or higher than 6.4 pmol/mg protein, similar to our original published results (Fig. 1a; Table I). Although all of the experiments reported herein were performed with 3 clones, because the results obtained were similar only representative data from 1 of the cell lines are shown. This cell line is called MDA-231 PBR High (MDA-231 PH). The MDA-231 PL cell line also differed from the MDA-231 PH cell line in the PK 11195 dissociation constant (K_D ; Fig. 1a; Table I). It should be noted that PBR ligand binding was performed multiple times over the course of several passages (approximately 10) and similar results were obtained. Differences in PBR expression seen with radioligand binding assays were confirmed with immunocytochemistry using the recently developed anti-PBR peptide affinity-purified antiserum (Fig. 1b).²⁴ Despite differences in B_{max} and K_D , the cells for all of the sub-populations appear morphologically similar (Fig. 1b).

Under normal culture conditions, both sub-populations appeared to grow at the same rate. To insure that this was the case, however,

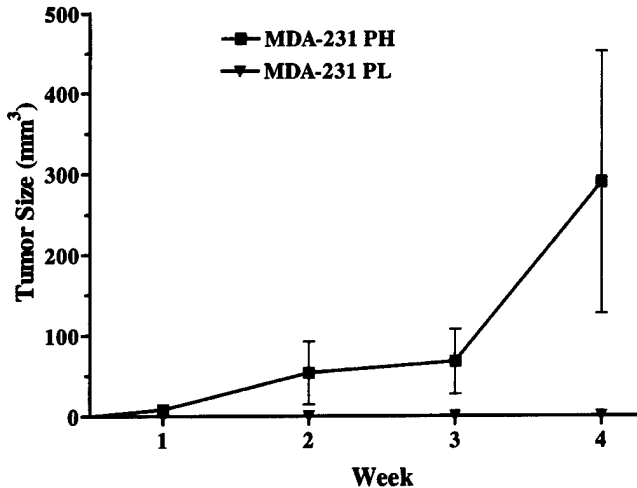


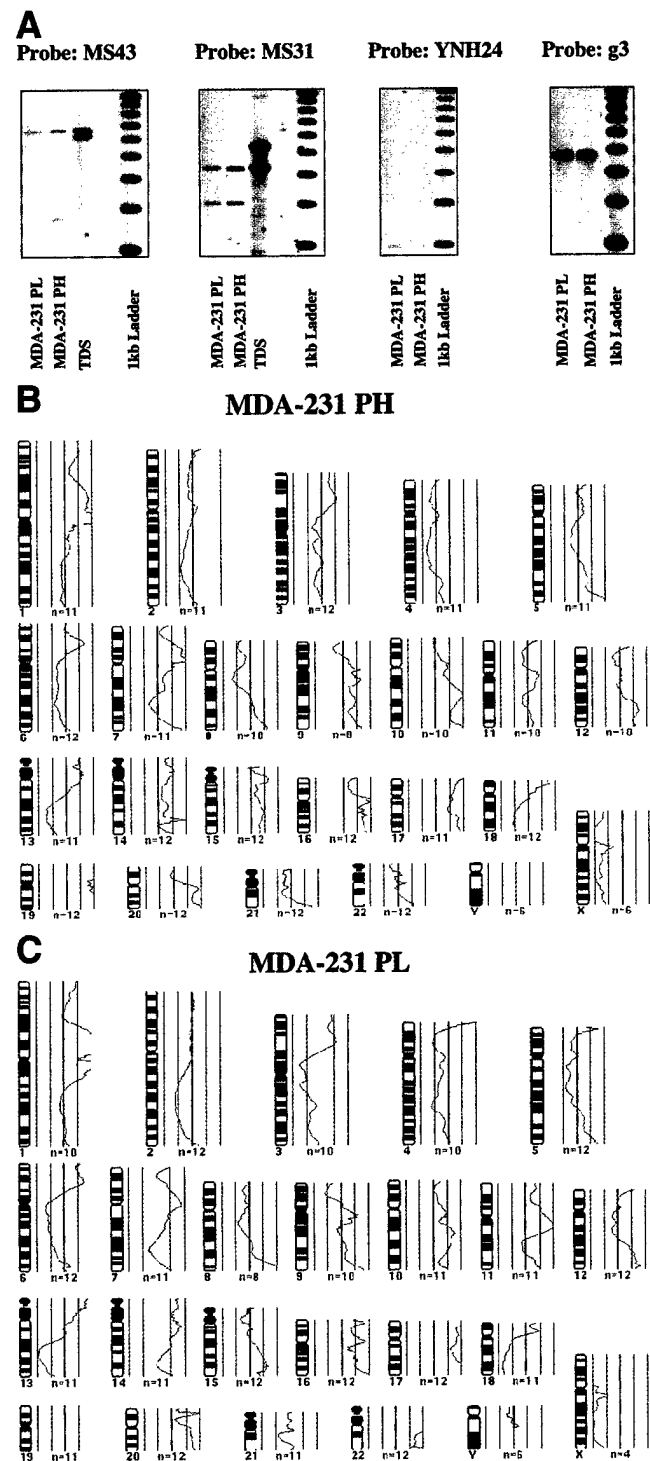
FIGURE 3 – MDA-231 PH and MDA-231 PL tumor growth in SCID mice. Cells were grown to confluency, trypsinized, counted and resuspended at a concentration of 5×10^5 cells/100 μ l in sterile PBS. One hundred μ l of cell suspensions was injected into each of 8 mice per cell line. Tumor growth was followed for 1 month with caliper measurements at the indicated times. Both cell lines tested negative for mycoplasma contamination (data not shown).

we followed the growth of each population over several days and quantified the number of cells with Crystal Violet (Fig. 2a). Over 5 consecutive days there was no appreciable difference between the MDA-231 PH and MDA-231 PL proliferation curves.

Our main hypothesis with regards to PBR in cancer is that increased expression of PBR confers a more aggressive phenotype in cancer cells. Therefore, decreased expression of PBR should indicate a differentiation toward a less-aggressive phenotype. As indicated above, the MDA-231 and several other breast cancer cell lines are well characterized for several breast cancer markers, as well as their chemotactic and chemoinvasive potential.¹⁻³ The MDA-231 cell line, as well as other late stage or highly-aggressive breast cancer cell lines, lack ER expression, express vimentin and CD44, and are highly chemotactic and chemoinvasive.¹⁻³ Conversely, early stage or non-aggressive breast cancer cell lines are ER positive, vimentin negative, express trace CD44 levels, and possess very little chemotactic or chemoinvasive potential.¹⁻³ We found no difference in the expression of ER (Table I), vimentin (Fig. 2b), or CD44 (Fig. 2b) between the MDA-231 sub-populations. Likewise, no significant differences in the chemotactic or chemoinvasive potential were found between MDA-231 PH and MDA-231 PL cells (Table I).

FIGURE 4 – RFLP and CGH DNA fingerprinting indicate that MDA-231 PH and MDA-231 PL are of the same genetic origin. DNA_{GEN} was isolated from both the MDA-231 PH and the MDA-231 PL cell lines and subjected to DNA fingerprinting analysis. (a) RFLP analysis of the indicated 4 independent chromosomal locations with the *HinfI* restriction enzyme was performed on both samples. TDS, liquid blood human DNA control extracted and treated as were the samples under investigation. CGH analysis was performed on chromosomes 1 through 22 of both samples. DNA from the peripheral blood lymphocytes of a cytogenetically normal female was used as the normal control. Results of CGH evaluation of MDA-231 PL (b) and MDA-231 PH (c) showing a very similar pattern of chromosomal gains and losses. The 5 vertical lines on the right side of the chromosome ideograms reflect different values of the fluorescence ratio between the test and the normal DNA. The values are 0.5, 0.75, 1, 1.25 and 1.5 from left to right. Ratios of 1.25 or higher reflect gains whereas ratios of 0.75 or lower reflect losses. The ratio profile (curve) was computed as a mean value of 8 metaphase spreads (n is the number of chromosomes used to generate each ratio profile).

We then injected MDA-231 PH and MDA-231 PL cells into SCID mice to determine if their differences in PBR expression *in vitro* lead to alterations in their ability to grow *in vivo*. Not surprisingly, MDA-231 PH cells grew well in SCID mice (Fig. 3). In fact, 1 month post-injection several of the 8 MDA-231 PH-injected animals were put down due to too large tumors. The MDA-231 PL cells, however, did not form any detectable tumors in the mice (Fig. 3). To determine if this lack of growth was due to mycoplasma contamination, we submitted the cells to mycoplasma screening. Both the MDA-231 PH and the MDA-231 PL



cell lines were negative for mycoplasma contamination (data not shown).

Given the dramatic differences in the *in vivo* growth of these MDA-231 sub-populations, and to determine if the MDA-231 PH and MDA-231 PL cell lines were derived from the same genetic lineage, we performed DNA fingerprinting using restriction fragment length polymorphisms (RFLP) on both cell lines and compared their chromosomal aberration using comparative genomic hybridization (CGH). Both the RFLP, as evaluated and interpreted by Cellmark Diagnostics Inc., and CGH determined that, indeed, the MDA-231 PH and MDA-231 PL are derived from the same genetic lineage and have similar chromosomal abnormalities (Fig. 4).

DISCUSSION

The MDA-231 human breast cancer cell line is widely used as an *in vitro* model for aggressive breast cancer. Our laboratory has used it to help elucidate the role of PBR in human breast cancer.⁴ During the course of these studies we observed variability in PBR levels of MDA-231 cells obtained from various sources. Using the MDA-231 cell line that we previously used to investigate the role of PBR in cancer progression and aggressive behavior of the cells we isolated 2 sub-populations differing in their expression of PBR ligand binding. The MDA-231 PH and MDA-231 PL cell lines do not differ in expression of the breast cancer markers ER, vimentin, or CD44. Similarly, these cell lines do not differ in their chemotactic or chemoinvasive potentials. They differ markedly, however, in their ability to grow in SCID mice. MDA-231 PH cells grow quite well in SCID mice, whereas MDA-231 PL cells do not.

CGH and RFLP data demonstrated that both subclones are derived from the same genetic lineage suggesting that the MDA-231 human breast cancer cell line is composed of an heterogeneous population. It is difficult to determine whether the differences in PBR expression between the 2 cell lines is due to innate properties of this heterogeneous population or to traits acquired over several passages. In our experience, the MDA-231 cell line has always been a morphologically heterogeneous population consisting of very large, round, flat cells intermixed with thin elongated cells. Both the MDA-231 PH and MDA-231 PL cell lines are morphologically similar, with no difference in the ratio of 1 cell type to another. Therefore, it is unlikely that the reduction of PBR expres-

sion seen in the MDA-231 PL cell line is due to the predominance of 1 cell morphology relative to the other. The data suggests that a reduction of PBR expression may occur over time as the result of multiple passages, however this hypothesis needs to be thoroughly tested before any conclusions may be drawn.

How does the reduction of PBR expression in the MDA-231 PL lead to the inability of these cells to grow in SCID mice? Our laboratory, as well as others, has previously shown that PBR ligands regulate cell proliferation.^{7-11,13-17} The *in vivo* behavior of the cells, however, differs from their *in vitro* behavior where no differences in the rates of cell proliferation between the MDA-231 PH and PL is seen. This may be due to a minimum of PBR levels required for cell proliferation. In our previous study, *in vitro* changes were seen with cells, such as the MCF-7 human breast cancer cells, which contain PBR levels 10-fold lower than the MDA-231 PL cells. This hypothesis is also supported by recent evidence that introduction of PBR into the MCF-7 cell line induces increases in the proliferation rate of these cells (Hardwick and Papadopoulos, unpublished data).

A close correlation between the reduction of MDA-231 cell proliferation and tumor growth in nude mice with PBR expression induced by the treatment of the cells and animals with the standardized *Ginkgo Biloba* extract EGb 761 was also shown.²⁶ Concomitant with the downregulation of PBR in MDA-231 cells by this treatment is the altered expression of several genes with close ties to either cell proliferation, differentiation, or apoptosis.²⁶ The majority of the genes affected by EGb 761 are members of either the Myc family of transcription factors and their effectors, the GTP-binding protein RhoA and its effectors, and members of the MAP/ERK pathway.²⁶ All of these results suggest a role for PBR in 1 if not several cellular pathways that regulate cell proliferation, differentiation, or apoptosis. To better understand PBRs role in the progression of cancer and to begin to realize PBRs cancer therapeutic and prognostic potential, more in depth studies of PBRs ability to either regulate or to be regulated by each of these pathways are necessary.

ACKNOWLEDGEMENTS

We are grateful to Mr. A. Foxworth for excellent assistance with the *in vivo* studies and the Lombardi Cancer Center Animal and Cell Culture Core facilities for their assistance.

REFERENCES

1. Sommers CL, Walker-Jones D, Heckford SE, et al. Vimentin rather than keratin expression in some hormone-independent breast cancer cell lines and in oncogene transformed mammary epithelial cells. *Cancer Res* 1989;49:4258-63.
2. Azzam HS, Arand G, Lippman ME, et al. Association of MMP-2 activation potential with metastatic progression in human breast cancer cell lines independent of MMP-2 production. *J Natl Cancer Inst* 1993;85:1758-64.
3. Culty M, Shizari M, Thompson EW, et al. Binding and degradation of hyaluronan by human breast cancer cell lines expressing different forms of CD44: correlation with invasive potential. *J Cell Phys* 1994;160:275-86.
4. Hardwick M, Fertikh D, Culty M, et al. Peripheral-type benzodiazepine receptor (PBR) in human breast cancer: correlation of breast cancer cell aggressive phenotype with PBR expression, nuclear localization, and PBR-mediated cell proliferation and nuclear transport of cholesterol. *Cancer Res* 1999;59:831-842.
5. Papadopoulos V. Peripheral-type benzodiazepine/diazepam binding inhibitor receptor: biological role in steroidogenic cell function. *Endocr Rev* 1993;14:222-40.
6. Papadopoulos V, Amri H, Boujrad N, et al. Peripheral benzodiazepine receptor in cholesterol transport and steroidogenesis. *Steroids* 1997;62:21-8.
7. Clarke GD, Ryan PJ. Tranquilizers can block mitogenesis in 3T3 cells and induce differentiation in friend cells. *Nature* 1980;287:160-1.
8. Wang JKT, Morgan JJ, Spector S. Benzodiazepines that bind at peripheral sites inhibit cell proliferation. *Proc Natl Acad Sci USA* 1984;81:753-6.
9. Laird HE II, Gerrish KE, Duerson KC, et al. Peripheral benzodiazepine binding sites in Nb 2 node lymphoma cells: effects on prolactin-stimulated proliferation and ornithine decarboxylase activity. *Eur J Pharm* 1989;171:25-35.
10. Ikezaki K, Black KL. Stimulation of cell growth and DNA synthesis by peripheral benzodiazepine. *Cancer Lett* 1990;49:115-20.
11. Bruce JH, Ramirez AM, Lin L, et al. Peripheral-type benzodiazepines inhibit proliferation of astrocytes in culture. *Brain Res* 1991;564:167-70.
12. Cornu P, Benavides J, Scatton B, et al. Increase in peripheral-type benzodiazepine binding site densities in different types of human brain tumors: a quantitative autoradiography study. *Acta Neurochir* 1992;119:146-52.
13. Garnier M, Boujrad N, Oke BO, et al. Diazepam binding inhibitor is a paracrine/autocrine regulator of Leydig cell proliferation and steroidogenesis: action via peripheral-type benzodiazepine receptor and independent mechanisms. *Endocrinology* 1993;132:444-58.
14. Camins A, Diez-Fernandez C, Pujadas E, et al. A new aspect of the antiproliferative action of peripheral-type benzodiazepine receptor ligands. *Eur J Pharm* 1995;272:289-92.
15. Miettinen H, Kononen J, Haapasalo H, et al. Expression of peripheral-type benzodiazepine receptor and diazepam binding inhibitor in human astrocytomas: relationship to cell proliferation. *Cancer Res* 1995;55:2691-5.
16. Neary JT, Jorgensen SL, Oracion A, et al. Inhibition of growth factor-induced DNA synthesis in astrocytes by ligands of peripheral-type benzodiazepine receptors. *Brain Res* 1995;675:27-30.
17. Brown RC, Degenhardt B, Kotoula M, et al. Location-dependent role of the human glioma cell peripheral-type benzodiazepine

- receptor in proliferation and steroid biosynthesis. *Cancer Lett* 2000;162:125-32.
18. Katz Y, Ben-Baruch G, Kloog Y, et al. Increased density of peripheral benzodiazepine-binding sites in ovarian carcinomas as compared with benign ovarian tumors and normal ovaries. *Clin Sci* 1990;78:155-8.
 19. Katz Y, Eitan A, Gavish M. Increase in peripheral benzodiazepine binding sites in colonic adenocarcinoma. *Oncology* 1990;47:139-42.
 20. Batra S, Iosif CS. Peripheral benzodiazepine receptor in human endometrium and endometrial carcinoma. *Anticancer Res* 2000;20:463-6.
 21. Bradford MM. A rapid and sensitive method for the quantification of microgram quantities of protein using the principle of protein-dye binding. *Anal Biochem* 1976;72:248-54.
 22. Munson PJ, Rodbard D. LIGAND: a versatile computerized approach for characterization of ligand binding systems. *Anal Biochem* 1980;107:220-39.
 23. Horwitz KB, Zava DT, Thilagar AK, et al. Steroid receptor analyses of nine human breast cancer cell lines. *Cancer Res* 1978;38:2434-7.
 24. Li H, Yao Z, Degenhardt B, et al. Cholesterol binding at the cholesterol recognition/interaction amino acid consensus (CRAC) of the peripheral-type benzodiazepine receptor and inhibition of steroidogenesis by an HIV TAT-CRAC peptide. *Proc Natl Acad Sci USA* 2001;98:1267-72.
 25. Figueiredo BC, Stratakis CA, Sandrini R, et al. Comparative genomic hybridization (CGH) analysis of adrenocortical tumors of childhood. *J Clin Endocrinol Metab* 1999;84:1116-21.
 26. Papadopoulos V, Kapsis A, Li H, et al. Drug-induced inhibition of the peripheral-type benzodiazepine receptor expression and cell proliferation in human breast cancer cells. *Anticancer Res* 2000;20:2835-47.

Short communication

Peripheral-type benzodiazepine receptor (*PBR*) gene amplification in MDA-MB-231 aggressive breast cancer cellsMatthew Hardwick^a, Luciane R. Cavalli^{b,c}, Keith D. Barlow^a,
Bassem R. Haddad^{b,c}, Vassilios Papadopoulos^{a,c,d,*}^aDivision of Hormone Research, Department of Cell Biology, Georgetown University Medical Center, Washington DC, 20007, USA^bDepartments of Oncology, Obstetrics and Gynecology, Georgetown University Medical Center, Washington DC, 20007, USA^cLombardi Cancer Center, Georgetown University Medical Center, Washington DC, 20007, USA^dDepartment of Pharmacology, Georgetown University Medical Center, Washington DC, 20007, USA

Received 4 March 2002; received in revised form 29 April 2002; accepted 29 April 2002

Abstract

Recent studies using human breast cancer cell lines, animal models, and human tissue biopsies have suggested a close correlation between the expression of the peripheral-type benzodiazepine receptor (*PBR*) and the progression of breast cancer. This study investigates the genetic status of the *PBR* gene in two human breast cancer cell lines: MDA-MB-231 cells, which are an aggressive breast cancer cell line that contains high levels of *PBR*, and MCF-7 cells, which are a nonaggressive cell line that contains low levels of *PBR*. Both DNA (Southern) blot and fluorescence in situ hybridization analyses indicate that the *PBR* gene is amplified in MDA-MB-231 relative to MCF-7 cells. These data suggest that *PBR* gene amplification may be an important indicator of breast cancer progression. © 2002 Elsevier Science Inc. All rights reserved.

1. Introduction

The peripheral-type benzodiazepine receptor (*PBR*) is an 18 kDa high affinity cholesterol-binding protein [1,2] involved in numerous biological functions, including steroid biosynthesis, mitochondrial respiration, and cell proliferation [3,4]. *PBR* is present in most tissues examined [3,4] and up-regulated in various tumors and carcinomas, such as gliomas [5,6], ovarian carcinomas [7], colon adenocarcinomas [8], endometrial carcinomas [9], and hepatomas [10]. Recent studies demonstrated that *PBR* is upregulated in both aggressive human breast cancer cell lines [11,12] and in metastatic human breast tumors [11] compared to non-aggressive tumor cells [11,12] and normal breast tissue [11]. The nature of this up-regulation in breast cancer and other tumors is unknown.

Gene amplification is a well-known mechanism in tumorigenesis. Several well-known oncogenes are found amplified in various cancers such as *ERBB-2* in breast cancer and *N-MYC* in neuroblastomas (reviewed by Savelyeva and Schwab [13]) and the *AIB1* gene in breast and ovarian cancers [14].

In order to determine if the increases in *PBR* expression seen in aggressive breast cancer are due to amplification of the *PBR* gene, we examined the *PBR* gene in the aggressive MDA-MB-231 and the non-aggressive MCF-7 human breast cancer cell lines using both Southern blot and fluorescence in situ hybridization (FISH) analyses.

2. Materials and methods**2.1. Cell culture**

The MDA-MB-231 and MCF-7 cell lines, obtained from the Lombardi Cancer Center, Georgetown University Medical Center, were grown in DMEM, 10% fetal bovine serum as previously described [11]. Cell growth curves for MDA-MB-231 and MCF-7 cells were established by Crystal Violet staining of the cells as previously described [15].

2.2. Southern blot analysis

Genomic DNA from each cell line was isolated using the QIAamp tissue kit (Qiagen Inc., Valencia, CA, USA). Twenty micrograms of each DNA sample was digested with *EcoRI* restriction enzyme, electrophoresed on a 1% agarose gel and transferred to derivatized nylon membranes (Nytran Plus, Schleicher & Schuell, Inc., Keene, NH, USA) [16]. The –317 to +36 bp fragment of the *PBR* gene was radiolabeled with [a-

* Corresponding author. Lombardi Cancer Center, Georgetown University Medical Center, 3900 Reservoir Road, Washington, DC 20007. Tel.: (202) 687-8991; fax: (202) 687-7855.

E-mail address: papadopv@georgetown.edu (V. Papadopoulos).

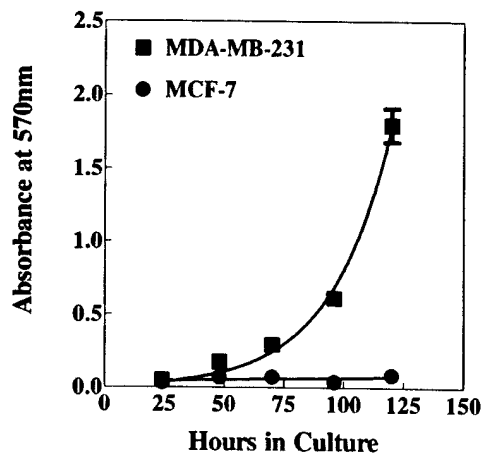


Fig. 1. MDA-MB-231 and MCF-7 cell proliferation rates. Cells were plated at a density of 2000 cells per well on 96 well plates and followed for 5 days. Every 24 hours, cells were stained with Crystal Violet. Absorbance was read at 570 nm. The results shown are means \pm SD. ($n = 8$) is representative of 3–4 independent experiments.

32 P]dCTP using a random primer DNA labeling system (Invitrogen, Inc., Carlsbad, CA, USA). The membrane was first prehybridized overnight at 68°C in 6 \times SSC, 0.5% SDS, and 100 μ g/ml denatured, fragmented, salmon sperm DNA.

After hybridization, the membrane was washed twice with 2 \times SSC, 0.5% SDS, for 10 minutes, once with 0.2 \times SSC, 0.5% SDS, for 30–60 minutes at room temperature, and once with 0.2 \times SSC, 0.5% SDS, for 30 minutes at 60°C. Screen-enhanced autoradiography was performed by exposing the blots to BioMax MS (Kodak, Rochester, NY, USA) film at –80°C for 4 to 48 hours. Densitometric analysis of the signals was performed using the SigmaGel software (Jandel Scientific, San Rafael, CA, USA).

2.3. FISH

Genomic BAC clone dJ526I14 containing a 129-kb fragment of human chromosome 22 known to contain the *PBR* gene was obtained from Sanger Molecular Labs, UK. Presence of the *PBR* gene was verified by DNA (Southern) blot using *PBR* cDNA as probe (data not shown). BAC DNA was purified using the Qiagen Large Construct Kit and preliminary characterization of the *PBR* gene was performed using gene specific primers and fluorescent automated DNA sequencing.

FISH analysis confirmed the correct chromosomal location of the BAC clone on chromosome 22q13.31 (data not shown). Using nick translation, the isolated DNA was labeled with biotin-16-dUTP (Boehringer Mannheim Corporation, Mannheim, Germany) and hybridized to interphase nuclei prepared from the cells as described previously [17]. The biotin-labeled DNA was detected using fluorescein-avidin DCS (FITC) (Vector Lab, Inc., Burlingame, CA, USA). The nuclei were counterstained with 4,6-diamidino-2-phenylindole (DAPI) staining. Over 200 interphase nuclei were counted for each cell line using a Leica DMRBE fluorescent microscope.

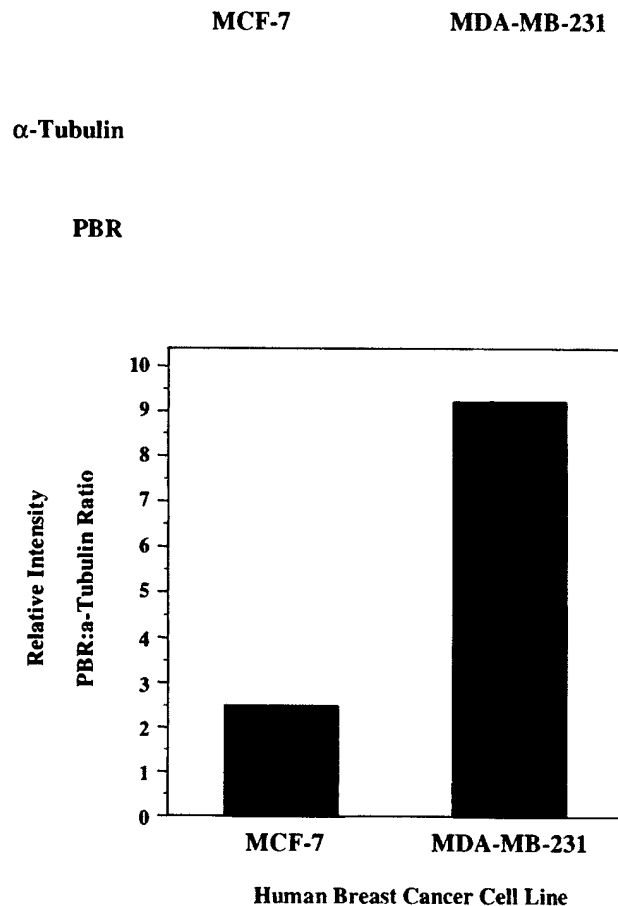


Fig. 2. DNA Southern blot analysis of *PBR* in MCF-7 and MDA-MB-231 (MDA-231) cells. Genomic DNA was digested with *Eco*RI and hybridized to a *PBR* full-length cDNA probe as described in Materials and methods section.

3. Results

In agreement with previously published reports, MDA-MB-231 cells grow very quickly whereas MCF-7 cells, in the absence of exogenously added estrogen, grow very slowly in culture (Fig. 1). The possibility that *PBR* overexpression in aggressive human breast cancer cells is due to *PBR* gene amplification was investigated by both DNA Southern blot (Fig. 2) and FISH analyses (Fig. 3). Southern blot analysis indicated that the aggressive MDA-MB-231 cells contain higher (4-fold) levels of *PBR* gene compared to MCF-7 cells. FISH analysis further confirmed these results. Counting over 200 cells from each cell line showed that 32% of the MDA-MB-231 cells have three or more copies of the *PBR* gene compared to only 4% of the MCF-7 cells (Table 1).

4. Discussion

This study used both FISH and Southern blot analyses to demonstrate amplification of the *PBR* gene in MDA-MB-231 cells, which are an aggressive, estrogen receptor (ER) negative human breast cancer cell line. Conversely, MCF-7 cells, which are a non-aggressive, ER positive human breast cancer cell

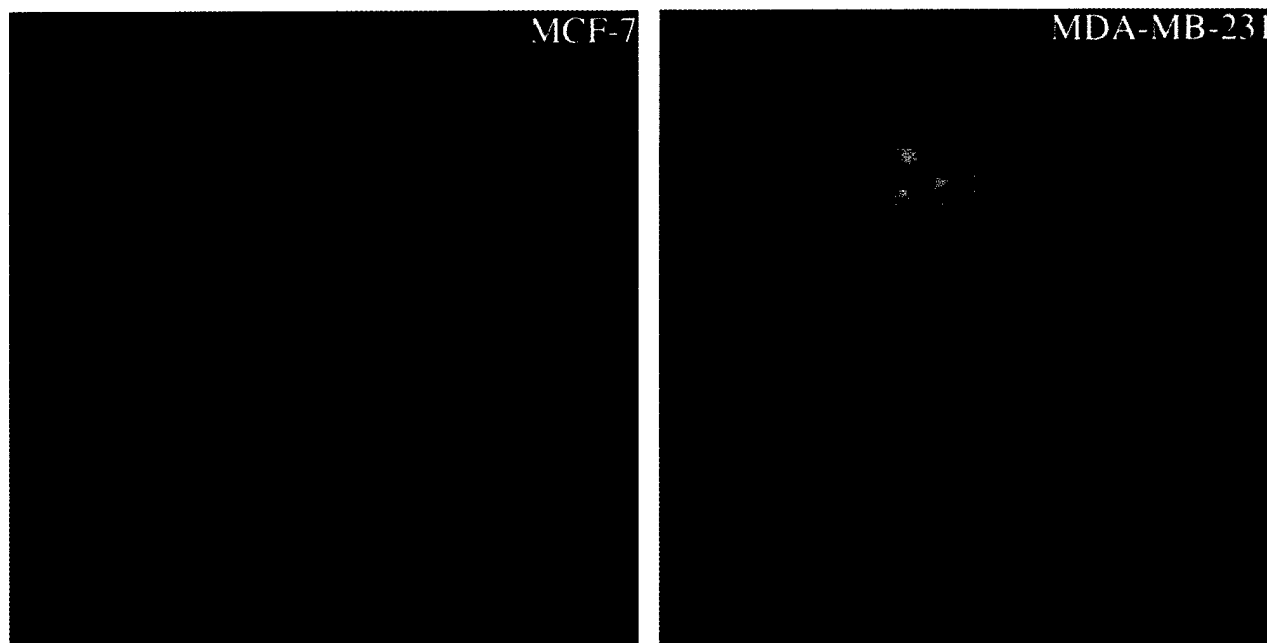


Fig. 3. FISH analysis of *PBR* gene in MCF-7 and MDA-MB-231 (MDA-231) cells. DNA from BAC clone dJ526I14 (Sanger Molecular Labs, UK) was labeled with biotin-16-dUTP and hybridized to interphase nuclei prepared from the two cell lines MCF-7 and MDA-MB-231 as described in Materials and methods. The Biotin-labeled DNA was detected using fluorescein-avidin DCS (FITC). MCF-7 cells showing two FISH signals and MDA-MB-231 cells showing three signals are shown.

line, did not demonstrate amplification of the *PBR* gene. The in vitro growth parameters, invasive and metastatic behavior of the cells used in the present study, as well as their in vivo tumorigenicity in nude mice has been previously reported [11,18]. In agreement with these studies, we observed that MDA-MB-231 cells grow at a much faster rate than the MCF-7 cells in vitro and grew tumors when implanted in SCID mice [15]. In contrast, MCF-7 cells did not grow tumors in this animal model system (Hardwick and Papadopoulos, unpublished data). FISH evaluation showed an increased copy number of the *PBR* gene in over 30% of the cells in MDA-MB-231 compared to only 4% of MCF-7 cells. The FISH assay does not rule out other aberrations of chromosome 22. Southern blot analysis indicated that MDA-MB-231 cells contain higher (4-fold) levels of *PBR* gene compared to MCF-7 cells.

We have recently shown that *PBR* levels are greatly increased in metastatic breast tumors compared to normal mammary epithelium [11]. Further, we showed that *PBR* protein, mRNA, and specific ligand binding is increased in aggressive breast cancer cell lines relative to non-aggressive

breast cancer cell lines [11]. This correlation was most readily seen between the MDA-MB-231 and MCF-7 cell lines and has subsequently been confirmed by others [12]. We also showed that the ability of MDA-MB-231 cells to form tumors in vivo might depend on the amount of *PBR* present in the cells [15]. At the conclusion of these studies we discussed the possibility that these increases may be due either to amplification of the *PBR* gene and/or increased transcription/translation of the gene in aggressive tumors relative to non-aggressive tumors and normal tissue [11].

This study suggests that increases in *PBR* expression seen in previous studies may be at least in part due to amplification of the *PBR* gene. However, gene amplification does not appear to be solely responsible for the increases seen in *PBR* expression due to the fact that the *PBR* gene is increased four-fold and *PBR* mRNA is increased at least 20-fold in MDA-MB-231 cells relative to MCF-7 cells [11]. Therefore, it appears that the increase in *PBR* expression in more aggressive cancers is the result of both gene amplification and increased gene transcription/translation.

Table 1
FISH analysis of MDA-MB-231 and MCF-7 human breast cancer cell lines

Cells	FISH Signals		
	1 (%)	2 (%)	3 or more (%)
MDA-MB-231	3 of 214 cells (1)	143 of 214 cells (67)	68 of 214 cells (32)
MCF-7	16 of 210 cells (7.5)	186 of 210 cells (88.5)	8 of 210 cells (4)

Over 200 interphase nuclei were isolated from both MDA-MB-231 and MCF-7 cells. Nuclei were labeled with a BAC fragment containing a portion of the *PBR* gene as described in Materials and methods section. Nuclei were subsequently counted for the presence of 1, 2, or 3 or more signals.

Given the upregulation of *PBR* in tumors and the correlation between increased *PBR* expression and the aggressive character of breast cancer cell lines, future studies will consider whether *PBR* expression can function as a prognostic indicator of the progression of specific cancers. Presently, we do not know whether the findings presented in this study represent the *in vivo* situation in human biopsies or if they reflect a peculiarity of the cell lines used. We are currently investigating whether *PBR* gene amplification also occurs in human biopsies and whether this amplification could be used as a breast cancer prognostic indicator.

Acknowledgments

This work was supported in part by a grant from the Department of Defense (DAMD17-99-1-9200). The support of the Cell Culture Core of the Lombardi Cancer Center (Georgetown University) is gratefully acknowledged.

References

- [1] Li H, Yao Z, Degenhardt B, Teper G, Papadopoulos V. Cholesterol binding at the cholesterol recognition/interaction amino acid consensus (CRAC) of the peripheral-type benzodiazepine receptor and inhibition of steroidogenesis by an HIV TAT-CRAC peptide. *Proc Natl Acad Sci USA* 2001;98:1267–72.
- [2] Lacapère JJ, Delavoie F, Li H, Pérani G, Maccario J, Papadopoulos V, Vidic B. Structural and functional study of reconstituted peripheral benzodiazepine receptor (PBR). *Biochem Biophys Res Commun* 2001;284:536–641.
- [3] Papadopoulos V. Peripheral-type benzodiazepine/diazepam binding inhibitor receptor: biological role in steroidogenic cell function. *Endocrine Rev* 1993;14:222–40.
- [4] Gavish M, Bachman I, Shoukrun R, Katz Y, Veenman L, Weisinger G, Weizman A. Enigma of the peripheral benzodiazepine receptor. *Pharmacol Rev* 1999;51:629–50.
- [5] Cornu P, Benavides J, Scatton B, Hauw JJ, Philippon J. Increase in peripheral-type benzodiazepine binding site densities in different types of human brain tumors: A quantitative autoradiography study. *Acta Neurochir* 1992;119:146–52.
- [6] Miettinen H, Kononen J, Haapasalo H, Helen P, Sallinen P, Harjuntausta T, Helin H, Alho H. Expression of peripheral-type benzodiazepine receptor and diazepam binding inhibitor in human astrocytomas: relationship to cell proliferation. *Cancer Res* 1995;55:2691–5.
- [7] Katz Y, Ben-Baruch G, Kloog Y, Menczer J, Gavish M. Increased density of peripheral benzodiazepine-binding sites in ovarian carcinomas as compared with benign ovarian tumours and normal ovaries. *Clin Sci* 1990;78:155–8.
- [8] Katz Y, Eitan A, Gavish M. Increase in peripheral benzodiazepine binding sites in colonic adenocarcinoma. *Oncology* 1990;47:139–42.
- [9] Batra S, Iosif CS. Peripheral benzodiazepine receptor in human endometrium and endometrial carcinoma. *Anticancer Res* 2000;20:463–6.
- [10] Venturini I, Zeneroli ML, Corsi L, Avallone R, Farina F, Alho H, Baraldi C, Ferrarese C, Pecora N, Frigo M, Ardizzone G, Arrigo A, Pellicci R, Baraldi M. Up-regulation of peripheral benzodiazepine receptor system in hepatocellular carcinoma. *Life Sci* 1998;63:1269–80.
- [11] Hardwick M, Fertikh D, Culty M, Li H, Vidic B, Papadopoulos V. Peripheral-type benzodiazepine receptor (*PBR*) in human breast cancer: correlation of breast cancer cell aggressive phenotype with *PBR* expression, nuclear localization, and *PBR*-mediated cell proliferation and nuclear transport of cholesterol. *Cancer Res* 1999;59:831–42.
- [12] Beinlich A, Strohmeier R, Kaufmann M, Kuhl H. Relation of cell proliferation to expression of peripheral benzodiazepine receptors in human breast cancer cell lines. *Biochem Pharmacol* 2000;60:397–402.
- [13] Savelyeva L, Schwab M. Amplification of oncogenes revisited: from expression profiling to clinical application. *Cancer Lett* 2001;167:115–23.
- [14] Anzick SL, Kononen J, Walker RL, Azorsa DO, Tanner MM, Guan X-Y, Sauter G, Kallioniemi OP, Trent JM, Meltzer PS. AIB1, a steroid receptor coactivator amplified in breast and ovarian cancer. *Science* 1997;277:965–8.
- [15] Hardwick M, Rone J, Han J, Haddad B, Papadopoulos V. Peripheral-type benzodiazepine receptor levels correlate with the ability of human breast cancer MDA-MB-231 cell line ability to grow in SCID mice. *Int J Cancer* 2001;94:322–7.
- [16] Papadopoulos V, Amri H, Li H, Boujrad N, Vidic B, Garnier M. Targeted disruption of the peripheral-type benzodiazepine receptor gene inhibits steroidogenesis in the R2C Leydig tumor cell line. *J Biol Chem* 1997;272:32129–35.
- [17] Bell KA, Van Deerlin P, Haddad BR, Feinberg RF. Cytogenetic diagnosis of “normal 46,XX” karyotypes in spontaneous abortions may frequently be misleading. *Fertility Sterility* 1999;71:334–41.
- [18] Thompson EW, Paik S, Brunner N, Sommers C, Zugmaier G, Clarke R, Shima TB, Torri J, Donahue S, Lippman ME, Martin GR, Dickson RB. Association of increased basement membrane invasiveness with absence of estrogen receptor and expression of vimentin in human breast cancer cell lines. *J Cell Phys* 1992;150:534–44.

In Vivo and in Vitro Peripheral-Type Benzodiazepine Receptor Polymerization: Functional Significance in Drug Ligand and Cholesterol Binding[†]

Franck Delavoie,^{†,§} Hua Li,^{†,||} Matthew Hardwick,^{†,⊥} Jean-Claude Robert,[§] Christoforos Giatzakis,[†] Gabriel Péranzi,[§] Zhi-Xing Yao,[†] Jean Maccario,[#] Jean-Jacques Lacapère,[§] and Vassilios Papadopoulos^{*,†}

Division of Hormone Research, Departments of Cell Biology and of Pharmacology and Neurosciences, Georgetown University Medical Center, Washington, D.C. 20057, Unité INSERM U410, Faculté de Médecine Xavier Bichat, 16 Rue Henri Huchard, 75870 Paris Cedex 18, France, and Unité INSERM U472, 16 Avenue Paul Vaillant-Couturier, Batiment INSERM, 94807 Villejuif, France

Received August 27, 2002; Revised Manuscript Received February 19, 2003

ABSTRACT: Peripheral-type benzodiazepine receptor (PBR) is an 18 kDa high-affinity drug ligand and cholesterol binding protein involved in various cell functions. Antisera for distinct PBR areas identified immunoreactive proteins of 18, 40, and 56 kDa and occasionally 72, 90, and 110 kDa in testicular Leydig and breast cancer cells. These sizes may correspond to PBR polymers and correlated to the levels of reactive oxygen species. Treatment of Leydig cells with human chorionic gonadotropin rapidly induced free radical, PBR polymer, and steroid formation. UV photoirradiation generates ROS species, which increased the size of intramembraneous particles of recombinant PBR reconstituted into proteoliposomes consistent with polymer formation, determined both by SDS–PAGE and by freeze–fracture electron microscopy. Spectroscopic analysis revealed the formation of dityrosines as the covalent cross-linker between PBR monomers. Moreover, photoirradiation increased PK 11195 drug ligand binding and reduced cholesterol binding capacity of proteoliposomes. Further addition of PK 11195 drug ligand to polymers increased the rate of cholesterol binding. These data indicate that reactive oxygen species induce in vivo and in vitro the formation of covalent PBR polymers. We propose that the PBR polymer might be the functional unit responsible for ligand-activated cholesterol binding and that PBR polymerization is a dynamic process modulating the function of this receptor in cholesterol transport and other cell-specific PBR-mediated functions.

The peripheral-type benzodiazepine receptor (PBR)¹ was initially described as a binding site for the benzodiazepine diazepam present in peripheral tissues (1). Although the tissue and cell distribution, subcellular localization, and pharmacological properties of this receptor have been extensively studied, only recently was it shown that the 18

kDa PBR protein is a high-affinity cholesterol and drug ligand binding protein (2, 3). These properties might explain the reported contribution of PBR and effect of PBR drug ligands in numerous biological functions, including steroid biosynthesis, mitochondrial respiration, cell proliferation, and apoptosis (4–6).

The determining factors in identifying and purifying PBR in various tissues were (i) the successful detergent solubilization of the mitochondrial PBR retaining ligand binding (7–9), (ii) the development of diagnostic high-affinity drug ligands, such as the isoquinolinecarboxamide PK 11195 and the benzodiazepine Ro5-4864 (10, 11), and (iii) the development of a photoaffinity probe specific for PBR, a nitrophenyl derivative of PK 11195 known as PK 14105 (12). This PK 14105 labeled a protein of 18 kDa (12), which was subsequently purified by several groups (13–15). The corresponding cDNA was cloned (16–19) and shown to code for a 169 amino acid protein of an 18.9 kDa molecular size in all species studied, with an approximately 80% homology between mammalian species (5). Despite these findings, there was no information about the structure of non-cross-linked and/or ligand-free PBR.

Additional lines of evidence suggested that the native PBR might be associated with other protein(s). Various groups reported that detergent-solubilized, photolabeled PBR eluted as a 170–210 kDa protein (15, 20) and unlabeled PBR eluted

[†] This work was supported by grants from the National Institutes of Health (Grant ES-07747) and the Department of Defense (DAMD17-99-1-9200).

* Corresponding author. Phone: 202-687-8991. Fax: 202-687-7855. E-mail: papadovp@georgetown.edu.

[†] Georgetown University Medical Center.

[§] Unité INSERM U410, Faculté de Médecine Xavier Bichat.

^{||} Present address: MacroGenics Inc., Rockville, MD 20858.

[⊥] Present address: Department of Urology, James Buchanan Brady Urological Institute Research Laboratories, The Johns Hopkins University Hospital, Baltimore, MD 21287.

[#] Unité INSERM U472.

¹ Abbreviations: CRAC, cholesterol recognition amino acid consensus; PBR, peripheral-type benzodiazepine receptor; recPBR, recombinant PBR; VDAC, voltage-dependent anion channel; 2,7-DCF, 2,7-dichlorofluorescein diacetate; DMEM, Dulbecco's modified Eagle's medium; Ham's F-12, nutrient mixture F-12; DMPC, dimyristoylphosphatidylcholine; DMPE, dimyristoylphosphatidylethanolamine; FBS, fetal bovine serum; hCG, human chorionic gonadotropin; HRP, horseradish peroxidase; L/P, lipid to protein ratio; MDA-231, MDA-MB-231 cells; PK 11195, (2-chlorophenyl)-N-methyl-N-(1-methylpropyl)-3-isoquinolinecarboxamide; promegestone, 17,21-dimethyl-19-norpregn-4,9-diene-3,20-dione; P4, progesterone; RIA, radioimmunoassay; Ro5-4864, 4'-chlorodiazepam; ROS, reactive oxygen species; TTBS, Tween–Tris-buffered saline.

as a larger protein. In addition to the 18 kDa photolabeled protein, various groups identified another protein in the range of 30–35 kDa that could also be photolabeled with PK 14105 (14). This protein could be photolabeled using radiolabeled flunitrazepam (21), AHN 086 (22, 23), and diazepam (24) in tissues devoid of GABA_A/benzodiazepine receptor. In subsequent studies, McEnery et al. (25) presented evidence indicating that the PK 14105 photolabeled 18 kDa mitochondrial PBR was associated with two proteins of 32 and 30 kDa, identified as the voltage-dependent anion channel (VDAC) and the adenine nucleotide carrier, respectively. Moreover, all three proteins migrated as a single peak of 70 kDa on a gel filtration column, consistent with the hypothesis that they are subunits of the same receptor complex (25, 26). It should be noted that in this experiment the 18 kDa protein was also isolated covalently labeled with PK 14105.

In an effort to visualize PBR in Leydig cell mitochondrial membranes, where we showed that PBR drug ligands increase mitochondrial cholesterol transport and steroid formation (4, 27), we used a combination of electron microscopy coupled to atomic force microscopy to study the distribution of gold immunolabeled PBR molecules (28). These studies suggested that the native receptor is a multimeric complex composed on an average of 4–6 18 kDa PBR subunits and possibly one 34 kDa VDAC subunit important to confer benzodiazepine binding (19). Interestingly, addition of the gonadotropin hCG to Leydig cells induced a rapid increase in PBR ligand binding and redistribution of PBR molecules in large clusters (29).

To better understand PBR molecular structure and function, one should approach its native ligand-free structure within the membranes. We recently successfully reconstituted isolated recombinant 18 kDa PBR protein in proteoliposomes and demonstrated that this protein alone could bind with high-affinity cholesterol and PK 11195 (3). In addition, we observed that this protein could also bind the Ro5-4864 with high affinity but with lower capacity, in agreement with a report by Joseph-Liauzun et al. (30). Thus, although the presence of VDAC may be important in conferring a higher capacity to the 18 kDa PBR protein to bind benzodiazepines and may participate in PBR function (19, 25, 31), it does not seem to play a determining role in its ability to bind drug ligands. In addition, other reports failed to observe a role for adenine nucleotide carrier in benzodiazepine ligand binding to the 18 kDa PBR protein (30).

Taken together, these studies indicate that the 18 kDa PBR protein in its native environment exists in various higher molecular mass complexes ranging from 30 to 200 kDa. As noted above, photolabeling of membrane extracts with various probes resulted in the identification of PBRs as 18 and 30–35 kDa proteins as well as a 70 kDa protein complex (25). Considering that the 18 kDa PBR protein has the ability to bind both benzodiazepine and isoquinolinecarboxamide drug ligands and that non-cross-linked and/or ligand-free PBR has not yet been isolated, questions are raised about the identity, formation, and function of the higher molecular mass PBR complexes in drug ligand and cholesterol binding.

We report herein that, in response to reactive oxygen species, the 18 kDa PBR protein forms polymers both in vitro and in vivo. These polymers are 18 kDa PBR monomers linked through dityrosine formation. Cholesterol binds better to PBR monomers than to polymers, whereas PBR drug

ligands exhibit higher binding to PBR polymers. In addition, we suggest that the PBR polymer might be the functional unit responsible for ligand-activated cholesterol binding.

EXPERIMENTAL PROCEDURES

Cell Culture. MA-10 mouse Leydig tumor cells were a gift from Dr. Mario Ascoli (University of Iowa). Cells were plated at low density for 24 h in DMEM/Ham's F-12 medium, 7.5% horse serum, and 5% FBS. After 24 h, the media were changed, and fresh media containing the indicated amounts of hCG for various time periods were added. Purified hCG (batch CR-125 of biological potency 11900 IU/mg) was a gift from National Institutes of Health (NIH). At the end of the incubation period, the cell media were saved for progesterone determination, and the cells were either dissolved in 0.1 N NaOH for protein determination or collected for immunoblot analyses. The MDA-231 cell line, obtained from the Lombardi Cancer Center, Georgetown University Medical Center, was grown in DMEM and 10% FBS as previously described (32). Cell incubations and manipulations were performed in the dark.

Analysis of Oxidative Stress. Levels of cellular oxidative stress were measured using the fluorescent probe 2,7-dichlorofluorescein diacetate (DCF; Molecular Probes, Inc.) as described (33). In brief, MA-10 or MDA-231 cells were cultured in 96-well plates. MA-10 cells were treated for the indicated time periods with or without hCG. At the end of the treatment cells were incubated in the presence of 50 μ M DCF in PBS. Fluorescence was then quantified using the Victor² quantitative detection fluorometer (ECG-Wallac, Inc.). To determine the hCG-induced ROS levels, basal ROS values were subtracted from the hormone-induced values.

Progesterone and Protein Measurements. Progesterone levels were measured by means of RIA using [1,2,6,7-³H]progesterone (specific activity 94.1 Ci/mmol) obtained from DuPont-New England Nuclear (Wilmington, DE) and antibodies from ICN Pharmaceuticals (Costa Mesa, CA). The data were analyzed using the MultiCalc software from EGG-Wallac, Inc. (Gaithersburg, MD). Protein levels were quantified using the dye binding assay of Bradford (34) using bovine serum albumin as the standard.

Antibodies Used and Immunoblot Analyses. Rabbit anti-mouse PBR antibodies were raised against the following peptide sequences: VGLTLVPSLGGFMGAYFVR (ab-PBR-9–27; 2), RGEGLRWYASLQK (ab-PBR-27–39; 35), YIVWKELGGFTE (ab-PBR-65–76; 35), LGGFTEDAM-VPLGLYTGG (ab-PBR-71–88; 36), and LNYVWRDNGS-GRRGGS (ab-PBR-150–166). Ab-PBR-150–166 and antiserum against isolated recombinant mouse PBR protein (ab-recPBR) isolated as previously described (2) were raised in rabbits (Biosynthesis Inc., Lewisville, TX). From these antisera, only ab-PBR-9–27 was affinity purified on a column with immobilized peptide antigen (2). Anti-His tag antiserum was obtained from Novagen (Madison, WI). Cell and tissue protein samples were solubilized in sample buffer [25 mM Tris-HCl (pH 6.8), 1% SDS, 5% β -mercaptoethanol, 1 mM EDTA, 4% glycerol, and 0.01% bromophenol blue], boiled for 5 min, and loaded onto a 15% SDS-PAGE. Separated proteins were electrophoretically transferred to nitrocellulose membrane (Schleicher & Schuell Inc., Keene, NH). Membranes were incubated in blocking TTBS (20 mM

Tris-HCl, pH 7.5, 0.5 M NaCl, and 0.05% Tween-20) buffer containing 10% nonfat milk) at room temperature for 1 h, followed by incubation with a primary antibody against PBR (1:2000) for 2 h. Membranes were then washed with TTBS three times for 10 min each time. After 1 h incubation with the secondary antibody, goat anti-rabbit IgG conjugated with HRP (1:5000) (Transduction Laboratories, Lexington, KY), membranes were washed with TTBS three times for 10 min each time. Specific protein bands were detected by chemiluminescence using the Renaissance Kit (DuPont-New England Nuclear). In some occasions, the specificity of the bands recognized by the antibody was demonstrated using preabsorbed antibody prepared by incubating the antibody with the peptide used for the immunization.

In Vitro Transcription and Translation of PBR. Mouse PBR cDNA (19) was subcloned to the *EcoRI*–*Bam*HI site of pZeoSV2(–) plasmid (Invitrogen). In vitro transcription and translation of PBR were performed using the TNT quick coupled transcription/translation systems (Promega, Madison, WI) in the presence of [³⁵S]methionine (specific activity 1000 Ci/mmol) obtained from DuPont-New England Nuclear following the manufacturer's recommendations. The product of the reaction was incubated with MA-10 Leydig cell mitochondria isolated as previously described (27). Mitochondria were washed twice, and proteins were separated by SDS–PAGE on a 4–20% gradient acrylamide–bis(acrylamide) gel at 125 V for 2 h and transferred to nitrocellulose membrane. The membrane was exposed to a multipurpose phosphor screen for 4 h and analyzed by phosphorimaging using the Cyclone storage phosphor system (Packard BioScience, Meriden, CT) or using X-film for overnight.

Expression and Purification of recPBR. The pET15PBR vector was used to transform the BL21(DE3) *Escherichia coli* strain (Novagen, Madison, WI) where the expression of recombinant mouse PBR protein was induced by 1 mM isopropyl 1-thio- β -D-galactopyranoside as previously described (2, 37). Cells were harvested in 150 mM NaCl and 50 mM phosphate, pH 7.4, washed in 300 mM NaCl and 50 mM phosphate, pH 7.4, and sonicated thoroughly. The pellet was collected at 20000g centrifugation and dissolved in binding buffer containing 0.5% SDS. The recPBR was purified by the His-Bind metal chelation resin (Novagen, Madison, WI) and stored in binding buffer with 1% SDS as previously described (2).

[³H]Promegestone Photolabeling. Various concentrations of recPBR in PBS were incubated with [³H]promegestone (specific activity, 94.1 Ci/mmol; NEN Life Science Products, Boston, MA) at a final concentration of 120 nM in the absence or presence of cholesterol (0.2 mM), progesterone (0.2 mM), pregnenolone (0.2 mM), testosterone (0.2 mM), 17 β -estradiol (0.2 mM), or 22R-hydroxycholesterol (0.2 mM) (Sigma-Aldrich, St. Louis, MO) in a 100 μ L final volume. After 1 h incubation at 4 °C, samples were photoirradiated for 30 min at a distance of <0.5 cm with a 366 nm lamp (UVP Inc., Gabriel, CA) as previously described (2). Sample loading buffer was applied to the samples, and they were submitted to SDS–PAGE. Proteins were transferred to nitrocellulose membranes, which were subsequently exposed to a tritium-sensitive screen and analyzed by the Cyclone storage phosphor system. Image analysis of the phospho-

rimages was performed using the OptiQuant software from Packard Biosciences Inc.

Reconstitution of recPBR in Liposomes. A stock solution of lipids (DMPC/DMPE, 9/1) was added to a SDS-containing buffer (50 mM NaPO₄ at pH 8, 150 mM NaCl) such that the final detergent to lipid ratio was equal to 2 (w/w). The solution was stirred for 30 min at room temperature before addition of the SDS-solubilized isolated recPBR protein at a concentration corresponding to the chosen lipid to protein ratio. The resulting micellar protein–lipid–detergent mixture was stirred for 15 min at room temperature before addition of Bio-Beads SM2, which remove SDS and induce vesicle formation (3). Bio-Beads were added in a two-step process: first, 1 g of Bio-Beads was added per 30 mg of SDS and mixed for 30 min; second, the same Bio-Beads amount was added and left for another 30 min. Bio-Beads were subsequently removed, and the solution was kept in the cold at 4 °C.

Irradiation. Fifty microliters of solubilized or reconstituted recPBR (0.2 mg/mL, i.e., 10^{–5} M), in a microfuge tube ice-cooled in a water bath, was irradiated at 7.5–12 cm distance with a 254 nm UV lamp (Spectrolinker XL1000 UV cross-linker; Spectronics Corp., Rochester, NY) generating an energy of 1.2 mJ/cm². A 10 μ L aliquot was taken at various incubation time periods, and the reaction was stopped by mixing with 5 μ L of nonreducing sample buffer. Ten microliters (1.3 μ g of recPBR) of the preparation was loaded onto SDS–PAGE (12.5% acrylamide). Separated proteins were visualized by silver staining (38). For the spectrofluorometric studies, a 2.5 mL cuvette containing 10^{–8}–10^{–6} M reconstituted recPBR [L/P = 4 (w/w)] used in the fluorometer (Photon Technology Inc., Lawrenceville, NJ) was irradiated as described above; fluorescence spectra were recorded and compared to nonirradiated PBR. Aliquots (250 μ L, 10^{–7} M) were taken and centrifuged for 20 min at 60000g in a TL100 Beckman centrifuge, and pellets containing proteoliposomes were resuspended in 37.5 μ L of nonreducing sample buffer. Samples (15 μ L/0.12 μ g of recPBR) were loaded onto SDS–PAGE (12.5% acrylamide). Separated proteins were visualized by silver staining. For freeze–fracture experiments, 0.35 mL of reconstituted recPBR [0.29 mg/mL; i.e., 1.5 \times 10^{–5} M L/P = 20 (w/w)], in a microfuge tube ice-cooled in a water bath, was irradiated under the same conditions as described above. A 6 μ L aliquot was taken at various incubation times, and the reaction was stopped by mixing with 4 μ L of nonreducing buffer. Samples (8 μ L/1.3 μ g of recPBR) were loaded onto SDS–PAGE (12.5% acrylamide). Separated proteins were visualized by silver staining.

Spectroscopic Measurements. Absorption spectra of tryptophan and tyrosine, added in a 2 mL cuvette containing PBS, were recorded with an UNICAM 300 spectrophotometer (Spectronic UNICAM) at room temperature before and after UV irradiation. Excitation and emission spectra were recorded with a PTI fluorometer (Photon Technology International) at room temperature before and after UV irradiation. Reconstituted recPBR (0.02 mg/mL, i.e., 10^{–6} M), tryptophan, tyrosine, and dityrosine were added in a 2 mL cuvette containing PBS buffer at pH 7.8. The formation of dityrosines was performed at room temperature for 1 h as described by Malencik et al. (39), and the amount was determined by fluorescence spectroscopy determined in a 5 mL borate buffer

(pH 9.1) containing 5 mM tyrosine. Lactoperoxidase (100 μ g) was added, and the reaction was initiated by addition of 14 μ L of H₂O₂ (3%).

Radioligand Binding Assays. Reconstituted recPBR protein (0.5–2.0 μ g/mL) in a 4/1 (w/w) lipid to protein ratio was used for PK 11195 and cholesterol ligand binding studies. Irradiated proteoliposomes were prepared as described above. [³H]PK 11195 (specific activity 83.5 Ci/mmol; NEN Life Science Products) and [1,2-³H]cholesterol (specific activity 43.8 Ci/mmol; NEN Life Science Products) binding studies were performed as previously described (3, 27). Bound [³H]-PK 11195 and [³H]cholesterol were quantified by liquid scintillation spectrometry. Dissociation constants (K_d), the number of binding sites (B_{max}), and Hill coefficients (n_H) for PK 11195 and cholesterol were determined by Curve-Fit (Prism version 3.0; GraphPad Software Inc., San Diego, CA).

Electron Microscopy. Samples (300 μ L) of UV-irradiated proteoliposomes were centrifuged and resuspended in 50 μ L of 10 mM MOPS–KOH (pH 7.0). Samples were freeze-fractured and coated initially with platinum under a 45° angle and then with carbon at a 90° angle in a Balzers apparatus (Balzers, Lichtenstein) with a total deposit calibrated at ca. 20 nm. Biophysical examination of samples was made in a JEOL 1200 EX electron microscope operated at 80 kV accelerated voltage (magnification: 120000 \times). Measurements of the intravesicular particles were made as previously described (3). In brief, measurements of coating shadows (platinum/carbon) over vesicular particles were made directly from the electron microscopic negatives. A Biocom 200 photometric image analysis system and Imagenia software (Imagenia et Instrumentation Biotechnologique, Les Ulis, France) were strictly applied to minimize the possibility of measuring error. The computer program provided isodensitometric contours of all shadows, and in addition, it applied morphometric parameters to the same contours. The population of diameters was a mixture of log normal populations. The parameters of the mixture (i.e., proportions, mean and standard deviation of each component) were estimated by maximum likelihood. The concordance of empirical and estimated distributions was assessed by examination of the PP plot. The best concordance is generally obtained when the plot follows the first diagonal.

Statistics. Statistical analysis was performed by one-way ANOVA and unpaired Student's *t* test using the INSTAT 3.00 package from GraphPad.

RESULTS

Detection of PBR Polymers in Vivo and Correlation with ROS Levels. During the past decade, we developed a number of antisera against various regions of the PBR protein (2, 35, 36) as well as antisera against the entire recPBR protein (present paper). Although these antisera recognized with various degrees of sensitivity the 18 kDa PBR protein, we consistently observed that they recognized additional proteins of 36–40 and 52–56 kDa, and in some cases 72, 90, and 110 kDa with various intensities (data not shown). For example, in MA-10 Leydig cells, ab-PBR-9–27 recognized mostly the 18 kDa PBR protein whereas ab-PBR-71–88 recognized also proteins of 40 and 54 kDa molecular mass (Figure 1A,C). In MDA-231 breast cancer cells, ab-PBR-9–27 and ab-PBR-71–88 recognized predominantly a 40

kDa protein although faint bands at 18 and 56 kDa molecular mass levels were seen (Figure 1A,C). The specificity of the immunoreactivities was demonstrated by preabsorbing ab-PBR-9–27 with the peptide used to generate this antiserum (Figure 1B). Interestingly, recPBR protein, which has a slightly higher molecular size than the native protein because of the presence of the His tag, was also found to generate an immunoreactive band around 40 kDa, which could not be seen with the peptide preabsorbed antiserum (Figure 1A,B). The presence of these complexes was more pronounced when cells or cell lysates were exposed to daylight. Treatment of the samples with increasing concentrations of SDS, ethanol, heat, chaotropic agents such as urea and guanidinium isothiocyanate, and PBR drug ligands failed to break these (40 and 56 kDa) proteins to smaller molecular mass proteins, suggesting that they involve covalent cross-links (data not shown). Because of the abundance of the higher molecular size PBR immunoreactive proteins in breast cancer cells and Alzheimer's disease hippocampus specimens (data not shown) that are known to contain high levels of ROS, we measured ROS in the cells examined to assess whether there were a correlation between ROS levels and the presence of high molecular mass PBR immunoreactive proteins. Indeed, MDA-231 cells contained higher ROS levels compared to MA-10 Leydig cells (Figure 1D).

Polymer Formation by in Vitro Transcribed and Translated PBR. To examine the ability of PBR to form polymers, mouse PBR cDNA was in vitro transcribed and translated and the protein incorporated into MA-10 Leydig cell mitochondria. [³⁵S]Methionine labeling of the protein allowed following the incorporation of PBR into mitochondria. Figure 2A shows that a major 18 kDa radiolabeled protein was formed and incorporated into mitochondria. In addition to the 18 kDa protein, radiolabeled products of 36, 54, and 72 kDa were formed and incorporated into mitochondria. An incomplete 10 kDa PBR protein fragment was also formed, leading to the formation of intermediate 28, 46, and 64 kDa radiolabeled proteins.

Dimer and Polymer Formation by Recombinant PBR in Solution. We recently reported the expression and isolation from bacteria of recombinant mouse PBR with a His tag at the N-terminus (2, 37). As noted above, the addition of the His tag results in the expression of a 20 kDa, instead of 18 kDa, PBR protein (2). During these studies we observed that recombinant PBR appears as both a 20 and a 40 kDa protein identified with antibodies raised against PBR (ab-PBR-9–27) and His tag (Figure 2B). These data suggest that these proteins correspond to PBR monomers and dimers.

To study the interaction of cholesterol with the isolated recombinant PBR, we used the progestin, [³H]promegestone (2). [³H]Promegestone was cross-linked by photoirradiation to the recombinant PBR (Figure 2C–E). [³H]Promegestone cross-linking to the recombinant PBR was displaced by cholesterol (2; Figure 2C). However, in the presence of other steroids (progesterone, pregnenolone, 17 β -estradiol, testosterone), we observed the appearance of 40, 60, and 80 kDa radiolabeled proteins in addition to the 20 kDa PBR protein (Figure 2C). The formation of these PBR polymers, in the presence of progesterone, was increased with a longer exposure to UV light, where additional PBR polymers of 100 and 120 kDa were seen after 30 min exposure. (Figure 2D). The formation of these polymers was also dependent

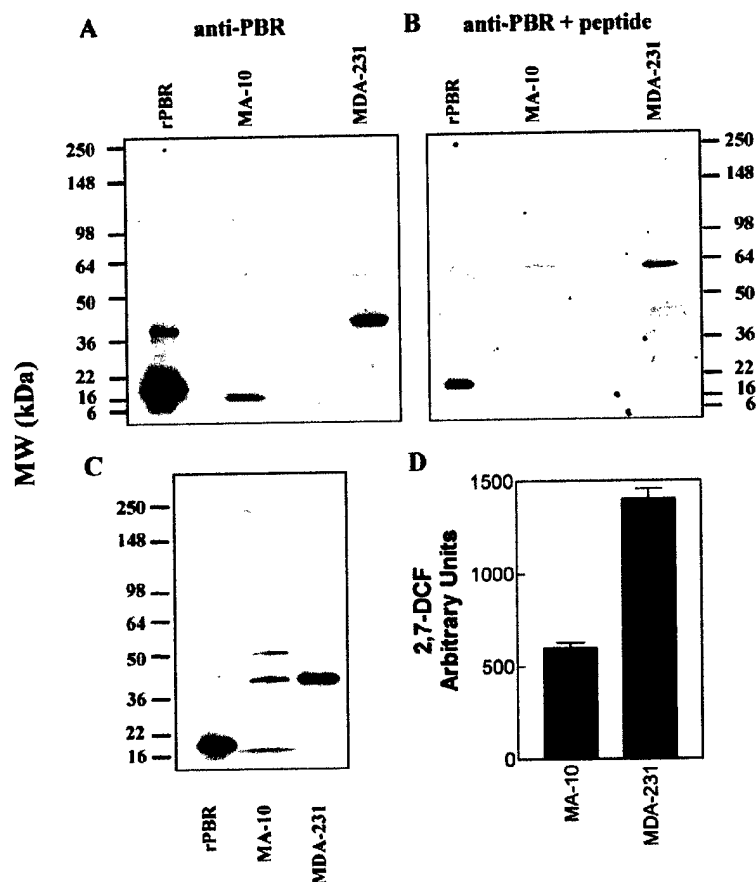


FIGURE 1: Detection of PBR polymers in vivo and correlation with ROS levels. (A) Immunoblot analysis of MA-10 Leydig and MDA-231 breast cancer cell extracts using ab-PBR-9-27 anti-PBR antiserum. (B) Specificity of the immunoreactivities seen in (A) examined by preabsorbing ab-PBR-9-27 with the peptide used to generate the antiserum. (C) Immunoblot analysis of MA-10 Leydig and MDA-231 breast cancer cell extracts using ab-PBR-71-88 anti-PBR antiserum. (D) ROS levels measured in MA-10 Leydig and MDA-231 breast cancer cells as described under Experimental Procedures.

on the amount of progesterone present during the photoirradiation process (Figure 2E). These data suggest that cholesterol, which was otherwise shown to bind with high affinity to PBR (2, 3), prevents covalent PBR cross-linking. In contrast, other steroids and UV light appear to favor this process (Figure 2C).

Dimer and Polymer Formation by recPBR Reconstituted in Proteoliposomes. UV-induced PBR cross-linking was also revealed by silver staining of solubilized PBR preparations (Figure 3, left). We recently reported that solubilized PBR maintained its ability to bind cholesterol, although with low affinity, but failed to bind PBR drug ligands (2). This problem was overcome by reconstitution of the recombinant PBR into proteoliposomes [at a lipid to protein ratio, L/P, of 4 (w/w)] (3). Reconstituted PBR bound with nanomolar affinities both cholesterol and PK 11195 (3). Here, we examined the effect of UV photoirradiation on reconstituted PBR. Figure 3, right, shows that UV exposure induces PBR polymer formation in a time-dependent manner.

Hormonal Induction of PBR Polymers in MA-10 Leydig Cells. The data presented above suggested that UV exposure was the cause of PBR polymer formation. Preliminary experiments indicated that the effect of UV exposure was mostly independent of the wavelength used. UV is a well-known inductor of free radical formation. Isolated protein

oxidation in response to UV and ROS is well documented (40). However, proteins in living cells are exposed to endogenously generated ROS rather than UV light. Considering the data presented in Figure 1, we looked for a physiological mechanism inducing ROS production in MA-10 Leydig cells. Taking into account our previous data on the rapid hCG-induced formation of PBR clusters (29) and reports showing that under physiological conditions LH increases lipid peroxidation in the testis (41) and that in the corpus luteum LH increases progesterone secretion and ROS production (42), we measured ROS and progesterone levels in response to hCG. Indeed, hCG induced both ROS and progesterone formation in a concentration-dependent manner (Figure 4A). Interestingly, the hCG generation of ROS is a very rapid phenomenon (Figure 4B) that occurs much faster than the synthesis of progesterone, because it can be seen within 1 min upon addition of the hormone. Simultaneously, the addition of hCG to MA-10 Leydig cells rapidly induces the formation of PBR polymers within 1 min (Figure 4C), in agreement with our previous data (29).

Spectrophotometric Characterization of PBR Polymers in Proteoliposomes. To characterize the type of covalent bond involved in PBR polymer formation, we performed a series of spectrophotometric studies. Figure 5A shows a silver-stained gel of photoirradiated reconstituted PBR (0.1 μ M)

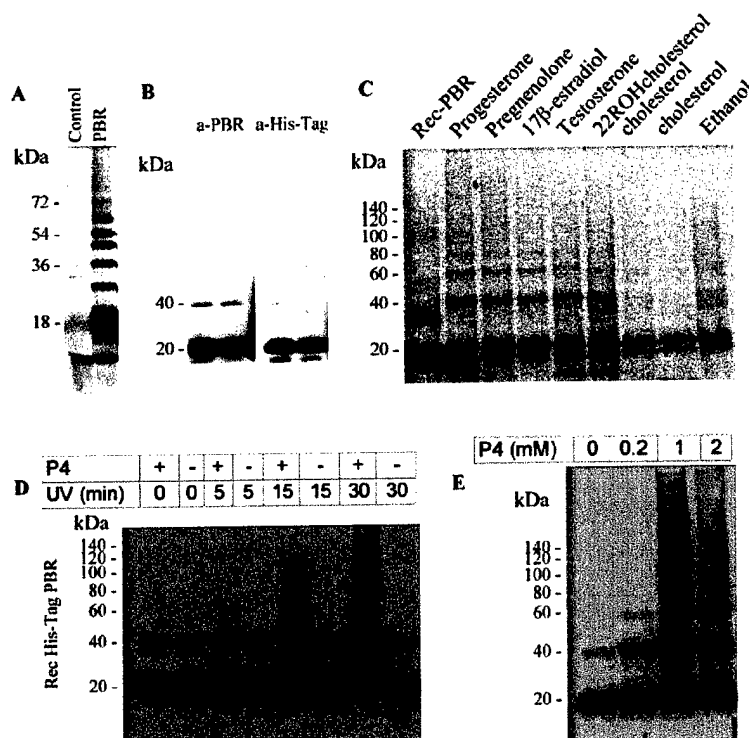


FIGURE 2: Dimer and polymer formation by in vitro transcribed and translated PBR and by recombinant PBR in solution. (A) Mouse PBR cDNA was in vitro transcribed and translated and the radiolabeled protein product(s) incorporated into MA-10 Leydig cell mitochondria. Proteins were separated by SDS-PAGE, and radiolabeled proteins were visualized by phosphorimaging. (B) Immunoblot analysis of recPBR using ab-PBR-9-27 and anti-His tag antisera. (C) Isolated recombinant PBR (5 μM) incubated with $[^3\text{H}]$ promegestone in the presence or absence of the indicated steroids at 0.2 mM concentration. Samples were exposed to UV light, and at the end of the incubation the samples were separated by SDS-PAGE. (D) Isolated recombinant PBR (5 μM) was incubated with $[^3\text{H}]$ promegestone in the presence or absence of the 1 mM progesterone (P4). Samples were exposed to UV light for the indicated time periods, and at the end of the incubation the samples were separated by SDS-PAGE. (E) Isolated recombinant PBR (5 μM) incubated with $[^3\text{H}]$ promegestone in the presence or absence of the indicated concentrations of progesterone (P4). Samples were exposed to UV light for 30 min, and at the end samples were separated by SDS-PAGE. In (B), (C), and (D) photoincorporation of $[^3\text{H}]$ promegestone to recombinant PBR was detected by phosphorimaging.

at L/P 4. Mouse PBR contains 12 tryptophan and 10 tyrosine residues that might be responsible for intrinsic fluorescence of the receptor. Figure 5B shows that PBR intrinsic fluorescence decreased upon UV exposure at 290 nm (excitation), suggesting that some tryptophans might be involved in polymer formation. As a control we examined the effect of UV irradiation on a solution of tryptophan. Panels C and D of Figure 5 show a UV-induced tryptophan fluorescence decrease in the emission spectra when excited at 290 nm (Figure 5C) and a fluorescence increase when excited at 320 nm with a maximum emission wavelength at 440 nm (Figure 5D), which might indicate the formation of dityryptophans (43). To examine whether such phenomenon occurs in the UV-exposed reconstituted PBR, we measured the fluorescence spectra of PBR excited at 320 nm. Figure 5E shows that reconstituted PBR exposed to UV shows a maximum emission wavelength at 380 nm when excited at 320 nm, indicating that dityryptophans are not involved in PBR polymer formation.

Considering that ROS have been shown to lead to covalently stable bond formation via dityrosine formation (40, 44, 45), we further examined if such reaction might occur in our system. Figure 5F shows that UV irradiation of a tyrosine solution induces an increase in fluorescence with a maximum emission at 390 nm when excited at 320 or at 290 nm, in agreement with dityrosine formation (39).

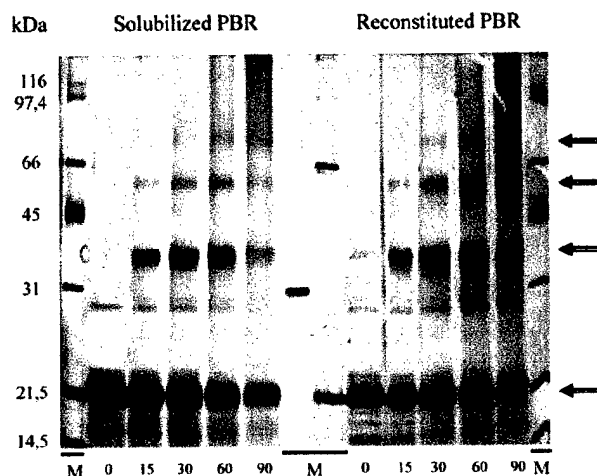


FIGURE 3: Dimer and polymer formation by recPBR reconstituted in proteoliposomes. Silver-stained SDS-PAGE of UV-irradiated PBR (10 μM) either solubilized or reconstituted in liposomes (DMPC/DMPE, 9:1) at a lipid/protein ratio of 4 (w/w) at 4 $^{\circ}\text{C}$. Irradiation times (minutes) are shown at the bottom of the lanes. Molecular mass standards (M) are shown in the first, middle, and last lanes. The middle lanes show carbonic anhydrase (31 kDa), serum albumin (66 kDa), and trypsin inhibitor (21.5 kDa) molecular mass standards in the range of PBR monomers, dimers, and trimers. Arrows on the right indicate the molecular sizes corresponding to PBR monomers, dimers, trimers, and tetramers.

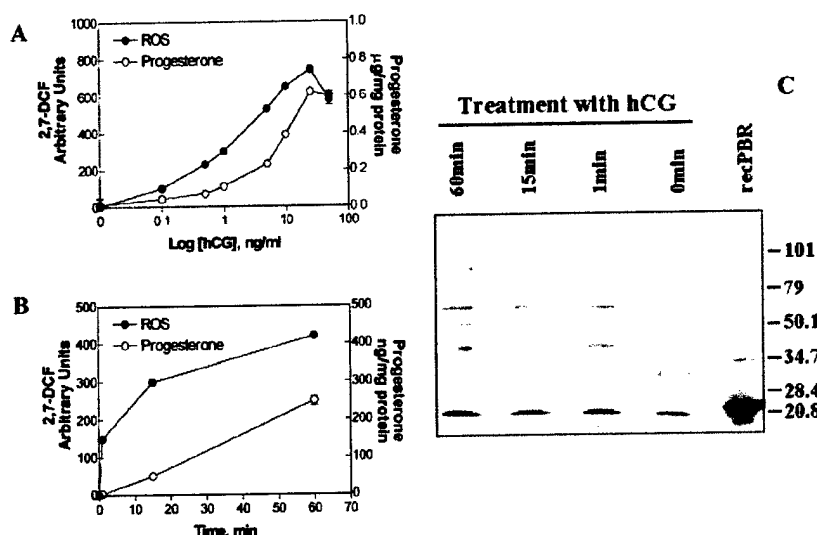


FIGURE 4: Hormonal induction of PBR polymers, ROS formation, and progesterone synthesis in MA-10 Leydig cells. (A) MA-10 Leydig cells were treated with the indicated concentration of hCG for 30 min. (B) MA-10 Leydig cells were exposed to 50 ng/mL hCG for the indicated time periods. For both (A) and (B), at the end of the incubation ROS and progesterone were determined as described under Experimental Procedures. Results shown are means \pm SD from four independent experiments ($n = 12$). (C) Immunoblot analysis of MA-10 Leydig treated for the indicated time periods in the dark with 50 ng/mL hCG using the ab-PBR-9-27 antiserum.

Because the 390 nm maximal emission measured with dityrosine solution is close to the 380 nm observed for UV-irradiated PBR, it is proposed that ROS-induced PBR cross-linking involves dityrosine formation. The amplitude of the dityrosine fluorescence observed with PBR suggests that only one or two tyrosines per monomer are cross-linked.

Morphological Characterization of PBR Polymers in Proteoliposomes. Figure 6A shows a silver-stained gel of reconstituted PBR at L/P 20 (w/w), photoirradiated for 15, 30, 60, and 90 min, respectively. A 90 min irradiation induced the formation of dimers and small amounts of trimers shown by arrows. Freeze-fracture experiments (Figure 6B–I) were performed to characterize the transmembranous domain of nonirradiated (Figure 6B) and 90 min irradiated (Figure 6C) PBR reincorporated in the bilayer. Figure 6D–I shows different types of particles observed in freeze-fractured proteoliposomes. Panels D and E of Figure 6 correspond to typical monomers. Figure 6F–I corresponds to the dimer, trimer, possible tetramer, and higher polymers of PBR, respectively. Figure 7 shows the distribution of the diameter of intravesicular particles in nonirradiated (Figure 7A) and 90 min irradiated (Figure 7B) PBR proteoliposomes. Histograms showing nonirradiated samples (Figure 7A) revealed two populations of particles. The median width of the first group of particles, representing 52% of the population, was of 8.0 ± 1.6 nm apparent diameter. The median width of the second group of particles, representing 48% of the population, was 12.0 ± 2.5 nm. Histograms of data obtained from irradiated samples (Figure 7B) can be analyzed with three populations of particles. The median width of the first group of particles, representing 53% of the population, was 8.0 ± 1.7 nm. The median width of the second group of particles, representing 45% of the population, was 13.0 ± 2.4 nm. The median width of the third group of particles, representing 2% of the population, was 22.0 ± 1.1 nm. The concordance of empirical and estimated distributions of control and irradiated data was assessed by examination of the percentile percentile (PP) plot (panels C and D of Figure

7, respectively). The data presented in Figure 7 show that irradiated and nonirradiated samples contain both PBR monomer and dimer in almost equal proportions. However, under the conditions used (L/P 20), only the irradiated samples contain higher PBR polymer in small proportion. Because of the limited size of this polymeric PBR population, in agreement with the SDS-PAGE shown in Figure 6A, the characterization of trimer and tetramer was difficult to achieve, and for this purpose the respective positions of these PBR polymers are indicated by arrows on Figure 7B. It should be noted that the percentage of each population observed in the freeze-fracture experiments does not directly correspond to the band intensity for PBR monomer and polymers seen on SDS-PAGE (Figure 6A). The diameters measured described mostly monomers and small-size polymers and to a much lesser extent higher molecular mass polymers. A closer look at the histograms shown in Figure 7 indicates the presence of four picks (arrows in Figure 7B) corresponding to monomers, dimers, trimers, and tetramers. Because the percentages of trimer and to a lesser extent tetramer population are very low compared to monomer and dimer PBR, the mathematical analysis used was not able to detect them. This was not due to the number of samples used, because histogram profiles were the same counting either 1000 or 1200 particles. Since these measurements were made directly from the platinum/carbon layers, it was necessary to establish the corrected value of the intravesicular particles alone. The latter value was calculated as the directly measured value minus the thickness of the deposited replica (3, 46, 47). Consequently, the corrected average sizes for the three populations were derived as 3.5, 7.0, and 14 nm, respectively, suggesting the presence of monomers, dimers, and tetramers.

Drug Ligand and Cholesterol Binding Properties of PBR Polymers in Proteoliposomes. Reconstituted PBR (L/P 4) binds with high affinity both PK 11195 (1.5 nM; Figure 8B) and cholesterol (6.0 nM; Figure 8D), in agreement with our previous studies (3). UV photoirradiation of the reconstituted

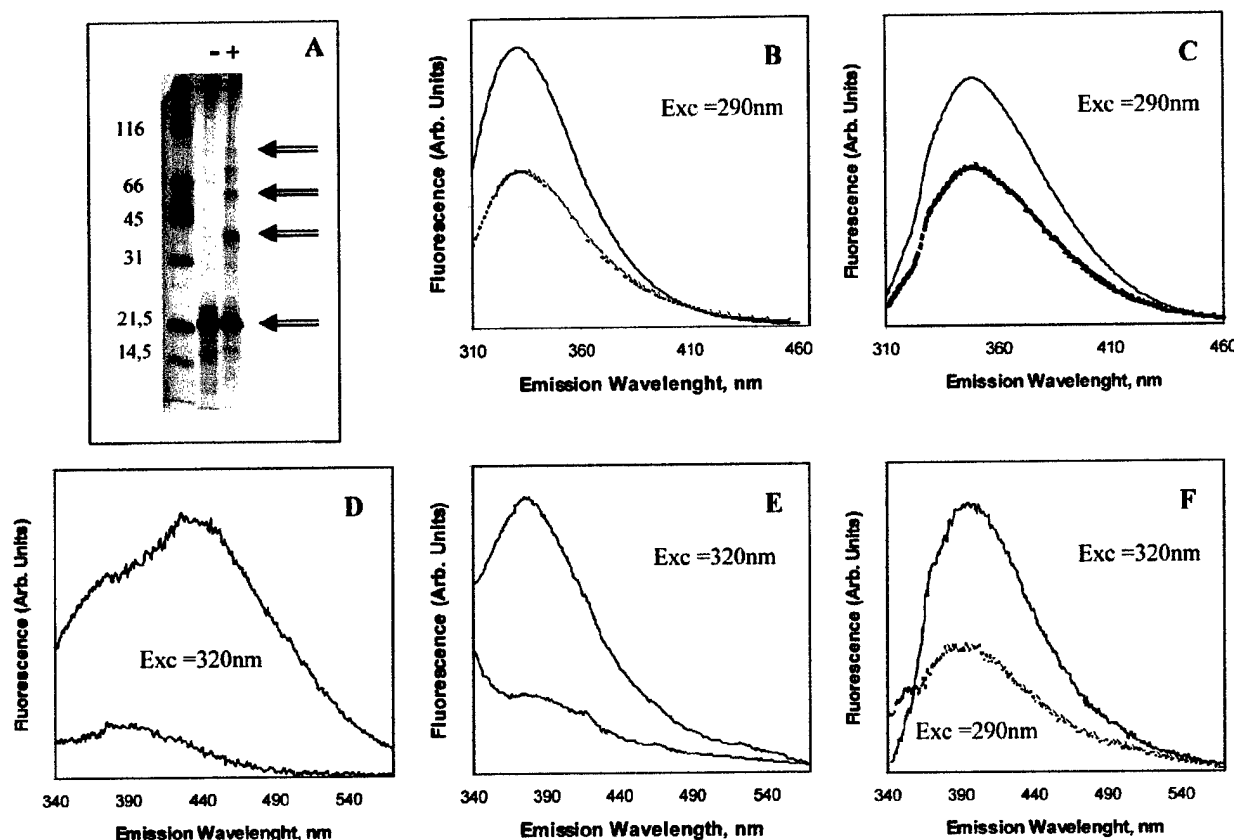


FIGURE 5: Spectrophotometric characterization of PBR polymers in proteoliposomes. (A) Silver-stained SDS-PAGE of PBR reconstituted in liposomes (DMPC/DMPE, 9:1) at a lipid/protein ratio of 4 (w/w) at 4 °C and UV irradiated for 30 min. recPBR (100 nM) was used for photoirradiation. Molecular mass standards are shown in the first lane. Arrows on the right show molecular sizes corresponding to PBR monomers, dimers, trimers, and tetramers. (B) Emission fluorescence spectra of PBR (1 μ M) measured at 290 nm excitation wavelength. Upper line: spectrum before 30 min UV light irradiation in PBS. Bottom line: spectrum after irradiation. (C) Tryptophan (5 μ M) fluorescence emission spectra measured at 290 nm excitation wavelength. Upper line: spectrum before 30 min UV light irradiation in PBS. Bottom line: spectrum after irradiation. (D) Tryptophan (5 μ M) fluorescence emission spectra measured at 320 nm excitation wavelength. Bottom line: spectrum before 30 min UV light irradiation in PBS. Upper line: spectrum after irradiation. (E) Emission fluorescence spectra of PBR (1 μ M) before (bottom line) and after (upper line) UV light irradiation measured at 320 nm excitation wavelength. (F) Tyrosine (10 μ M) fluorescence emission spectra determined at either 320 nm (upper line) or 290 nm (bottom line) excitation wavelengths after 30 min UV light irradiation.

PBR induced a time-dependent increase in PK 11195 ligand binding that reached its maximum at 45 min exposure time and dropped thereafter (Figure 8A). Saturation isotherm analysis of the samples submitted to 45 min irradiation time indicated that the UV-induced increase in PBR ligand binding was due to a 5-fold increase in the PK 11195 ligand binding capacity, with a minor 2-fold decrease in affinity (Figure 8B). In contrast, photoirradiation induced a time-dependent decrease in cholesterol binding (Figure 8C). Saturation isotherm analysis at 45 min irradiation time indicated that the UV-induced decrease in cholesterol binding was due to a 2.7-fold reduction in cholesterol binding capacity, with a significant 6.7-fold increase in affinity (Figure 8D). These data suggest that cholesterol binds to both PBR monomers and polymers and that polymer formation results in increased PBR drug ligand binding associated with a decreased cholesterol binding. On the basis of our previous data on the effect of progesterone on formation of promegestone-radiolabeled PBR polymers upon photoirradiation (Figure 2C), we examined the effect of progesterone on the ability of PBR polymers to bind PK 11195. Progesterone (1 μ M) abolished the ability of PBR polymers to bind PK 11195 in time-dependent manner (Figure 8A, open symbols).

Ligand-Induced Cholesterol Binding by PBR Polymers in Proteoliposomes. One of the most extensively studied and established functions of PBR is its role in mediating the transport of cholesterol into the mitochondria of steroidogenic cells (4, 6). This function, which probably consists of a number of steps including cholesterol binding, uptake, and release, has been shown to be activated by PK 11195 in all steroidogenic cells tested. To investigate the first step of this function of PBR in the *in vitro* reconstituted PBR system, we examined the effect of PK 11195 on the ability of reconstituted PBR to bind cholesterol before and after UV irradiation, i.e., monomeric versus polymeric PBR. Figure 9 shows that PBR polymer formation resulted in a dramatic and rapid ($t_{1/2}$ = 0.5 min) PK 11195 (100 nM) dependent increase in cholesterol binding. This is a transient effect that reaches a maximum at 3 min and decreases thereafter. Conversely, monomeric (i.e., nonirradiated) PBR binds slowly ($t_{1/2}$ = 6 min) cholesterol in response to PK 11195 and in a monoexponential manner (Figure 9, squares). Addition of 1 μ M progesterone in the reaction mixture abolished cholesterol binding by the PBR polymers (Figure 9, open symbols).

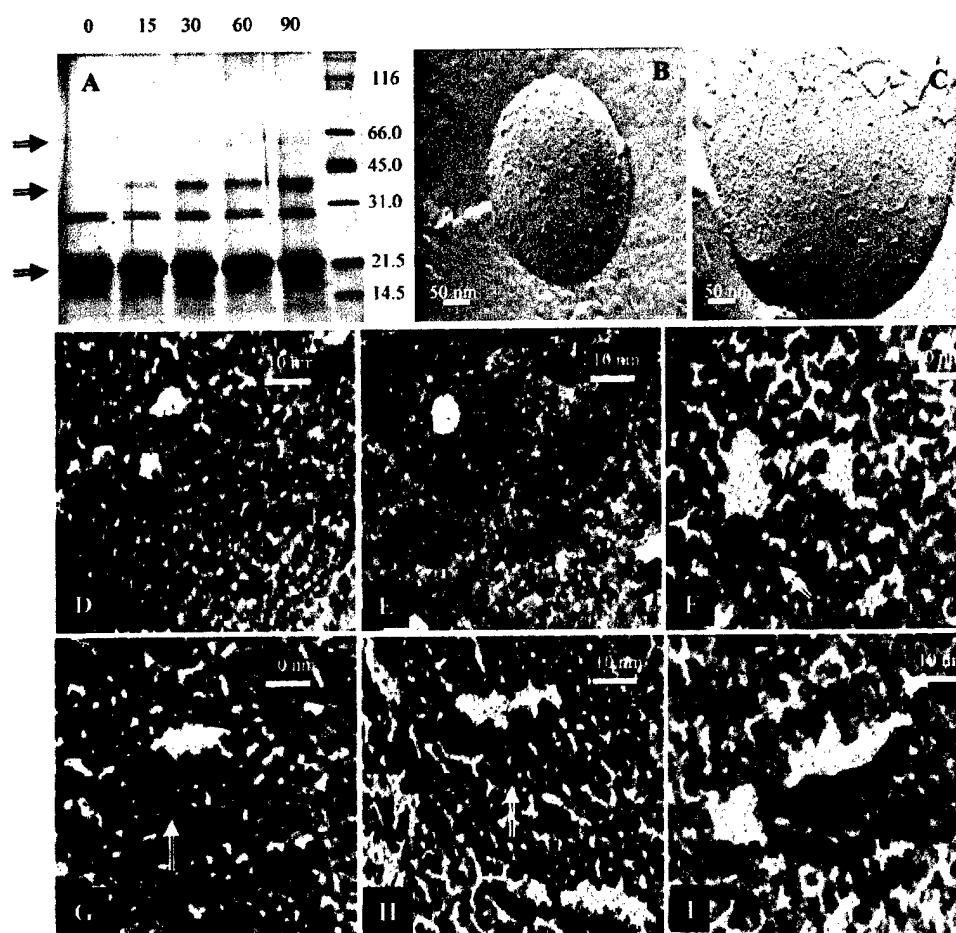


FIGURE 6: Morphological characterization of PBR polymers in proteoliposomes. Silver-stained SDS-PAGE (A) of UV-irradiated PBR reconstituted in liposomes (DMPC/DMPE, 9:1) at a lipid/protein ratio of 20 (w/w) at 4 °C. The different irradiation times used (minutes) are shown on the top of the gel. Molecular mass standards (kDa) are shown in the last lane. Arrows on the left indicate molecular sizes of the PBR monomers, dimers, and trimers. Freeze-fractured control proteoliposomes are shown in (B) and freeze-fractured 90 min UV-photirradiated proteoliposomes are shown in (C). Panels D–I show representative types of objects observed in freeze-fractured proteoliposomes: (D, E) typical monomers; (F) dimer (arrow); (G) trimer (arrow); (H) possible tetramer (arrow); (I) complex structure of oligomer. Please note the shadowing direction from bottom to top; white shadow convention.

DISCUSSION

The synthesis and availability of a number of high-affinity drug ligands for PBR allowed the investigation of the function of this primarily mitochondrial membrane protein in various biological systems. To date, PBR has been described as one of the key proteins in several cell functions including the transport of cholesterol into the mitochondria in steroidogenic tissues (4), mitochondrial respiration (48), and cell proliferation in various tumor cell lines (39, 49, 50). It has also been shown to be a marker of cell growth and tumor formation (32, 49, 50) and a component of the permeability transition pore of the mitochondrial membrane involved in apoptosis (51–54). Moreover, PBR drug ligands are under evaluation for their ability to regulate neurosteroid synthesis and brain function, to detect tumor cells *in vivo*, and to induce or protect against apoptosis with major therapeutic consequences in cancer therapy (55).

It might not be just a coincidence that excessive ROS production occurs in mitochondria, where PBR is mainly found. Indeed, the data presented herein strongly suggest that PBR is a target for ROS. PBR at first reacts by forming

covalent polymers, mediators of physiological functions. Under physiological conditions this could be a cycling process, where newly formed PBR monomers take the place of the polymerized PBR destined to be degraded. However, excessive levels of ROS or continuous exposure to ROS could lead to the continuous covalent polymerization of all of the newly formed PBR, thus leading to the exclusive presence of higher polymers, which could be detrimental to mitochondrial function and ultimately cell viability or, alternatively, to a new pathological state, *i.e.*, in cancer cells.

The serendipitous discovery of PBR polymers was based on the observation that various PBR antisera recognized with various degrees of sensitivity the 18 kDa PBR protein in addition to proteins of 36–40, 52–56, 72, and 110 kDa (see Figures 1 and 4). Despite the observation that these proteins had molecular size multiples of the 18 kDa protein, for a long time our focus was centered either exclusively around the 18 kDa protein or on the presence of other proteins reported to be associated with the 18 kDa PBR protein. Interestingly, there were numerous reports on the presence of a 30–36 kDa protein shown to bind exclusive PBR drug

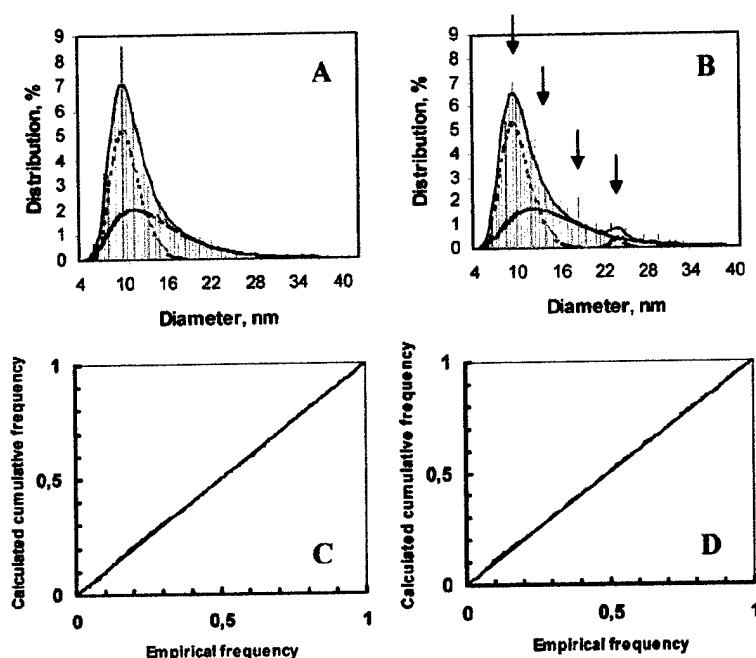


FIGURE 7: Morphometrical analysis of reconstituted recombinant PBR. Distribution of diameters of intravesicular particles from freeze-fractured control (A) and samples irradiated for 90 min (B). The calculated distributions are shown as continuous lines. The upper curves are the sum of the two (control) or the three (irradiated) populations. The other curves in each figure are representative of each individual subpopulation. Percentile percentile (PP) plot of the empirical and calculated models shows the concordance of the empirical (dotted line) and calculated (solid line) distribution of control (C) and irradiated (D) data.

ligands that were dismissed as being due to the association of this protein with PBR (14, 21–24). A careful examination of the PBR literature also unveiled that the first paper reporting the isolation of the photolabeled 18 kDa PBR protein also identified proteins of 32–36 and 50–54 kDa molecular size that were specifically radiolabeled by PK 14105, in addition to the 18 kDa PBR protein, in CHO hamster ovary mitochondrial cell extracts (14).

The observation that the 18 kDa PBR protein was organized in clusters of 2–7 molecules on the Leydig cell mitochondrial membrane suggested for the first time the presence of PBR polymers (28). The hormone-induced appearance of bigger PBR clusters concomitant with the appearance of a higher PBR ligand binding site and initiation of cholesterol transfer into mitochondria and steroidogenesis indicated that the formation of these clusters might be part of a functional process (29).

Considering the abundance of PBR in the mitochondrial membrane and its close association with numerous other proteins, it has been impossible to purify the native PBR protein. Thus, to understand the structure and function of this protein, we focused on isolating and characterizing a functional recombinant protein. The isolation of such a protein allowed us to first demonstrate that it had the ability to bind cholesterol in the carboxy terminus of the molecule (2). However, the absence of the drug ligand binding site in the solubilized PBR protein prompted us to proceed in reconstituting the protein into proteoliposomes. It was not until we succeeded in reconstituting a functional PBR in proteoliposomes (3) that the structure and function of PBR could be studied in a detailed manner.

During our search of PBR function in health and disease we examined PBR protein expression in various normal and pathological cells and tissues, including Leydig cells (27)

and breast cancer cells of various aggressive potential (32). The data obtained indicated the presence of PBR immunoreactive proteins of 18 kDa polymers (dimers and trimers) in breast cancer cells. Interestingly, these samples contained higher levels of free radicals compared to control samples. The presence of increased ROS in human breast cancer cells has been previously described and proposed as one of the determining parameters of breast carcinogenesis and metastasis (56, 57).

Most of our work during the past decade has been focused on the role of PBR in cholesterol transport and steroid production in testicular Leydig cells in response to the gonadotropin hCG. The molecular, pharmacological, and morphological characterization of this receptor in MA-10 mouse tumor Leydig cells has been extensively studied (2, 19, 27, 29). We report herein that PBR exists mainly as an 18 kDa monomer in control samples. However, within 1 min upon addition of hCG the formation of PBR polymers was detected (Figure 4). Interestingly, the formation of polymers parallels the hCG-induced formation of ROS. The induction of ROS formation in response to gonadotropins has been reported (41, 42). This might be due to the initiation of the cytochrome P450 reaction responsible for the metabolism of cholesterol (preexisting in the mitochondria) to pregnenolone and known to generate ROS. The formation of SDS- and mercaptoethanol-resistant (covalent) PBR polymers in response to hCG is also in agreement with our previous studies using transmission electron and atomic force microscopy studies on MA-10 mitochondrial membranes isolated from hormone-treated cells (29). The kinetics of the formation of PBR protein polymers, changes in PBR topography (29), and PBR ligand binding characteristics are similar and rapid (<1 min). The only apparent discrepancy comes from the data reported herein on MA-10 cells, where PBR mostly

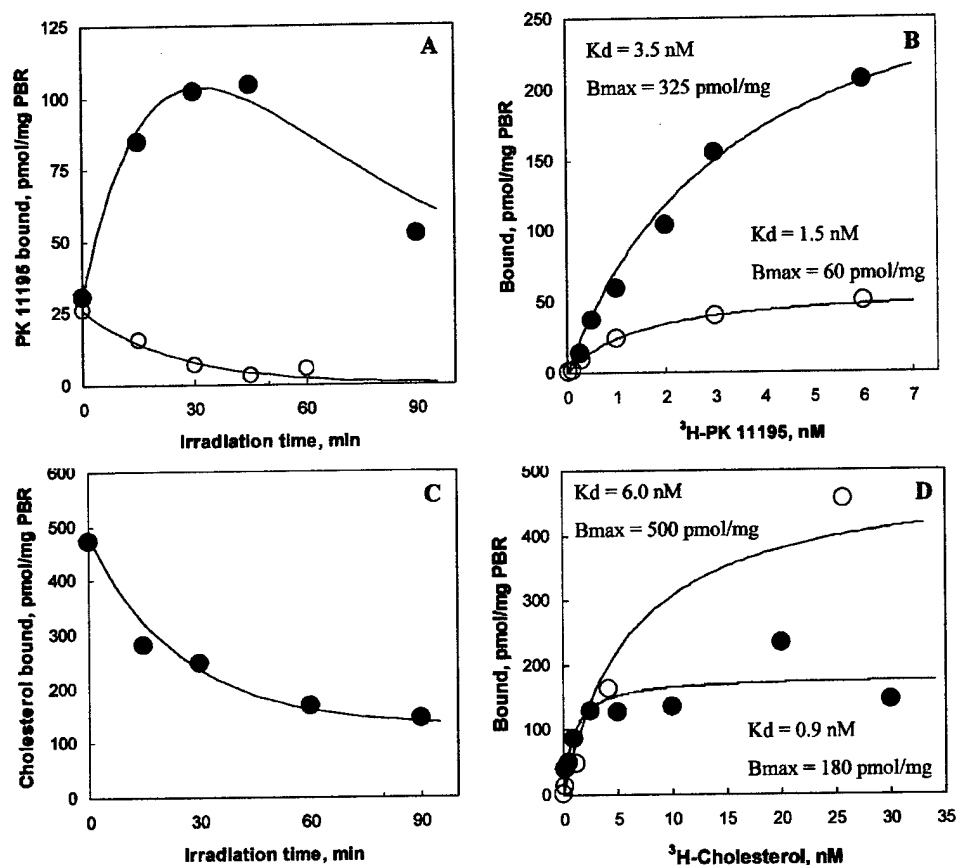


FIGURE 8: Irradiation time dependence and saturation isotherms of [^3H]PK 11195 and [^3H]cholesterol binding to reconstituted recombinant PBR. Recombinant mouse PBR protein (0.5–2.0 $\mu\text{g}/\text{mL}$) reconstituted in a 4/1 (w/w) lipid (DMPC/DMPE, 9/1) to protein ratio was used. (A, C) Proteoliposomes were exposed to UV irradiation for the indicated time points. (B, D) 45 min irradiated (closed circles) and nonirradiated (open circles) proteoliposomes were used for binding experiments using either [^3H]PK 11195 (B) or [^3H]cholesterol (D). Assays were performed and analyzed as described under Experimental Procedures. In (A) the effect of 1 μM progesterone on PK 11195 ligand binding to irradiated proteoliposomes is shown in open circles. In (B) and (D) the saturation curves, K_d , and B_{max} values were obtained by Curve Fit analyses. Results shown are representative of three independent experiments performed in triplicate. The SEM values for K_d and B_{max} were consistently less than 15% of the mean.

exists in its monomeric form in unstimulated cells, and the previous morphological data (28), where in control cells only 40% of PBR was monomeric. This discrepancy could be due to the difference in methodological approaches used in the two studies and the possibility that the polymers seen in control cells by immunogold microscopy were only clustered rather than covalently bound. In contrast, PBR polymers present in Leydig and breast cancer cells seem to involve covalent cross-links resistant to SDS, mercaptoethanol, ethanol, heat, urea, guanidine isothiocyanate, and PBR drug ligands. Moreover, the presence of these complexes was more pronounced when cells or cell lysates were exposed to daylight (data not shown), further indicating the photosensitivity of PBR monomers. These results are in agreement with the data reported by Yeliseev and Kaplan in *Rhodospirillum rubrum*, a bacterium that contains the tryptophan-rich sensory protein (TspO), a PBR homologue, proposed to serve as an oxygen/light sensor (58).

In addition to the studies performed in cells, *in vitro* studies were performed to assess the ability of the mouse PBR cDNA to be transcribed and translated to radiolabeled 18 kDa protein and to be incorporated into mitochondria. During these experiments, we observed that, in addition to the major

radiolabeled 18 kDa PBR protein, radiolabeled proteins of 36, 54, and 72 kDa were formed and incorporated into mitochondria. Although in these studies, as well as in the cell studies, we cannot exclude the possibility that these proteins may not be homopolymers but the results of the association of the 18 kDa PBR protein with other proteins (heteropolymers), the observation that these proteins are multiples of 18 kDa makes this possibility less likely. These data were extended in *in vitro* experiments using His-tagged recombinant PBR protein in solution where PBR dimers were identified by both anti-PBR and anti-His tag antibodies. Furthermore, isolated recPBR protein was shown to form dimers and polymers both in solution and after reconstitution in proteoliposomes *in vitro*. UV irradiation dramatically increased the formation of these polymers. The fact that recPBR protein alone forms polymers further suggests that the *in vivo* seen polymers are homopolymers.

Our spectroscopic studies (Figure 5) strongly suggested that tyrosines are involved in the UV irradiation induced cross-link by formation of dityrosines, linking tyrosines belonging to PBR monomers. The presence of PBR trimers and tetramers suggests that there are at least two tyrosines per monomer involved in the polymer formation in a covalent

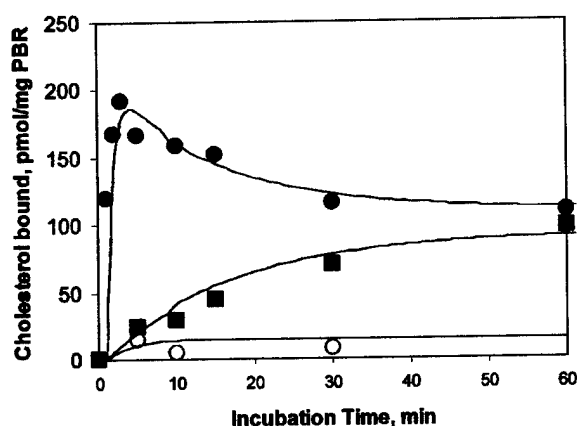


FIGURE 9: Ligand-induced cholesterol binding by PBR polymers in proteoliposomes. Time course of cholesterol binding (6 nM) to either 45 min UV photoirradiated (closed circles) or nonirradiated (closed squares) reconstituted recombinant PBR. Recombinant mouse PBR protein (3.0 $\mu\text{g/mL}$) reconstituted in a 4/1 (w/w) lipid (DMPC/DMPE, 9/1) to protein ratio was used. Open circles indicate the effect of 1 μM progesterone, in the presence of 100 nM PK 11195, on cholesterol binding (6 nM) to irradiated proteoliposomes.

manner. It should be noted that mouse PBR contains 10 tyrosines, some of them located at the amino terminus and others at the carboxy terminus and in the first loop joining the first two transmembrane helices (59, 60). On the basis of secondary structure prediction, six of the tyrosines would be in the transmembrane region and probably less accessible for dityrosine formation. From the remaining tyrosines, the reduction in cholesterol binding observed after polymer formation (Figure 8C,D) suggests that Y152 and/or Y153 are probably involved in PBR polymer formation. Indeed, it has been shown that cholesterol binding occurs at the carboxy-terminal domain of PBR and, more specifically, amino acids 150–156 (2). The decrease (>60%) in the amount of cholesterol bound to PBR polymers (Figure 8C) correlates with the reduction of PBR monomer levels seen under these experimental conditions in SDS–PAGE (Figure 3), suggesting that only the monomer binds cholesterol or, alternatively, that only one monomer among the polymers binds cholesterol. It cannot be excluded that the decreased ability of the polymers to bind cholesterol could also be due to a conformational change in PBR. In addition, the role of tyrosines in PBR polymer formation was further supported by site-directed mutagenesis experiments where specific tyrosines in PBR were replaced by other amino acids, resulting in a dramatic decrease in polymer formation (unpublished data).

In addition, the proximity of PBR monomers seems rather an important factor for the formation of covalent cross-links, as illustrated by the fact that, in reconstituted proteoliposomes, varying L/P from 4 to 20 (for instance) reduces drastically the formation of trimers and tetramers (compare gels in Figures 3 and 6). However, dimers are always present, suggesting that interactions between two monomers occur naturally under physiological conditions. Image analysis of the freeze-fractured proteoliposomes revealed that 50% of PBR are forming dimers, whereas SDS–PAGE followed by silver staining of the separated proteins showed only 10% of covalently cross-linked PBR multimers. Increased levels of ROS induced trimer and higher molecular mass polymer

formation. This can be regarded in the light of freeze–fracture experiments, which clearly show that dimers are observed even in the absence of any irradiation (Figure 7). Thus, it seems that the efficiency of dityrosine formation is dependent, in addition to L/P ratio, on other parameters to be determined. The “natural” formation of PBR dimers was further supported by PBR expression studies in bacteria where recombinant PBR appeared as 20 and 40 kDa proteins identified with antibodies raised against both PBR and the His tag (Figure 2A).

It is of special interest the finding that a higher rate of polymers is formed when solubilized PBR is photoirradiated in the presence of radiolabeled promegestone and other steroids, including progesterone and pregnenolone but not cholesterol. As noted previously, we used radiolabeled promegestone to study the interaction of cholesterol with the isolated recombinant PBR. Under these conditions, PBR in solution has a lower affinity for promegestone (100 μM) compared to its affinity for cholesterol (1 μM) (2). These data suggest that cholesterol might prevent covalent PBR cross-linking and thus polymer formation (Figure 2B), whereas other steroids in the presence of UV light favor this process. Thus, the increased formation of PBR polymers in solution compared to reconstituted PBR might be due to a higher diffusion of the PBR monomers in solution. However, the failure of PBR in solution to bind PK 11195 (2) suggests that this higher diffusion does not allow for the formation of stable polymers required for PBR ligand binding. Indeed, we previously demonstrated that reincorporation of recPBR into proteoliposomes was required for the receptor to recover the drug ligand binding function (3). In the present study we observed that polymer formation increased PK 11195 ligand binding to the receptor (Figure 8A,B) while progesterone abolished the ability of PBR polymers to bind PK 11195 (Figure 8A). To bring this finding into a physiological context, one should consider that, in the steroid biosynthetic pathway, cholesterol is metabolized into pregnenolone, a step occurring into mitochondria, and pregnenolone is then transformed into progesterone by the 3β -hydroxysteroid dehydrogenase enzyme also found in the mitochondria (61). Considering (i) the finding that progesterone does not affect the photoirradiation-induced PBR polymer formation (data not shown), (ii) the data in Figure 2C showing that the UV-photoactivatable derivative of progesterone, promegestone, favors PBR polymer formation in the presence of progesterone, and (iii) the fact that progesterone inhibits drug ligand binding to PBR polymers, it is speculated that progesterone is a critical physiological factor in the regulation of PBR polymerization and function.

We and others have shown that high-affinity PBR drug ligands, such as PK 11195, increase cholesterol transport into mitochondria and the subsequent steroid synthesis by gonadal, adrenal, brain, and liver cells (62). We report here that PK 11195 at nanomolar concentrations induced a dramatic increase of cholesterol binding rate by PBR polymers with a half-life of 30 s (Figure 9). Such a rapid process correlates with the *in vivo* studies on PBR aggregation induced by hCG and its second messenger cAMP in Leydig cells (29) and with the well-characterized acute stimulation of steroid synthesis by peptide hormones (63). Moreover, as described above for PK 11195 binding,

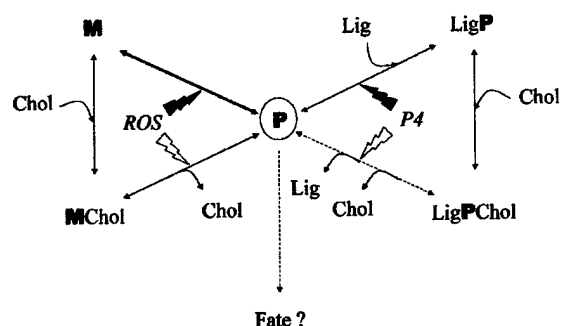


FIGURE 10: Schematic representation of PBR functional states. Additional abbreviations used are PBR monomer (M), polymer (P), cholesterol (Chol), ligands (Lig), reactive oxygen species (ROS), and progesterone (P4).

progesterone, in the presence of PK 11195, was found to inhibit cholesterol binding to PBR polymers (Figure 9).

In aggressive human breast cancer cells, which contain mainly a PBR dimer probably due to the high endogenous free radical levels, PK 11195 increased cholesterol transport into the nucleus and cell proliferation (32). This finding is also in agreement with the PK 11195-induced increase of cholesterol binding rate by PBR polymers in vitro.

In an attempt to summarize the function of the monomeric and polymeric forms of the 18 kDa PBR protein, we propose the scheme shown in Figure 10. PBR monomer (M) to polymer (P) transition is driven by ROS. The monomer binds cholesterol (Chol) with high affinity but not PBR ligands (Lig). The presence of cholesterol on the PBR monomer prevents the ROS-induced polymer formation. The polymer binds PBR ligands with high affinity, and ligand binding induces rapid cholesterol binding. This process would allow a membrane that contains PBR to uptake high levels of cholesterol in a time- and ligand-dependent manner. Since progesterone (P4) inhibits both ligand and cholesterol binding to PBR polymer, we suggest that this cholesterol metabolite might be the key element in releasing cholesterol from PBR. Thus, cholesterol could be taken up and released inside a membrane.

A fraction of ligand- and cholesterol-free covalent polymers would be destined to degradation (Fate), thus avoiding the detrimental effects of the presence of high levels of polymers in the mitochondrial membrane. At the same time, newly synthesized monomers will replace PBR in the membrane. Because such a process might take hours, it is possible that only a fraction of the PBR is used at any given time. In such cases, tissues rich in PBR, such as steroid synthesizing tissues, would have continuously available a pool of PBR monomers available for cholesterol transport. It is evident that further studies are required to validate the above proposed model of PBR cycle.

ACKNOWLEDGMENT

We are grateful to Dr. K. E. Krueger (Georgetown University) for providing ab-PBR-27–39 and ab-PBR-65–76, the National Hormone and Pituitary Program (NICHD, NIH) for the hCG, the Cell Culture Core of the Lombardi Cancer Center (Georgetown University) for the MDA-231 cells, Drs. J.-M. Verbavatz and R. Gobin (CEA, France) for assistance with the freeze–fracture experiments, and Dr. M.

Culty (Georgetown University) for critically reviewing the manuscript.

REFERENCES

1. Braestrup, C., and Squires, R. F. (1977) *Proc. Natl. Acad. Sci. U.S.A.* 74, 3805–3809.
2. Li, H., Yao, Z., Degenhardt, B., Teper, G., and Papadopoulos, V. (2001) *Proc. Natl. Acad. Sci. U.S.A.* 98, 1267–1272.
3. Lacapère, J. J., Delavoie, F., Li, H., Péranski, G., Maccario, J., Papadopoulos, V., and Vidic, B. (2001) *Biochem. Biophys. Res. Commun.* 284, 536–641.
4. Papadopoulos, V. (1993) *Endocrine Rev.* 14, 222–240.
5. Gavish, M., Bachman, I., Shoukrun, R., Katz, Y., Veenman, L., Weisinger, G., and Weizman, A. (1999) *Pharmacol. Rev.* 51, 629–650.
6. Casellas, P., Galiegue, S., and Basile, A. S. (2002) *Neurochem. Int.* 40, 475–486.
7. Benavides, J., Manager, J., Burgevin, M. C., Ferris, O., Uzan, A., Guerey, C., Renault, C., and Le Fur, G. (1985) *Biochem. Pharmacol.* 34, 167–170.
8. Gavish, M., and Fares, F. (1985) *J. Neurosci.* 5, 2889–2893.
9. Awad, M., and Gavish, M. (1989) *J. Neurosci.* 52, 1880–1885.
10. Schoemaker, H., Boles, R. G., Horst, W. D., and Yamamura, H. I. (1983) *J. Pharmacol. Exp. Ther.* 225, 61–69.
11. Le Fur, G., Perrier, M. L., Vaucher, N., Imbault, F., Flamier, A., Uzan, A., Renault, C., Dubroeuq, M. C., and Guerey, C. (1983) *Life Sci.* 32, 1839–1847.
12. Doble, A., Ferris, O., Burgevin, M. C., Menager, J., Uzan, A., Dubroeuq, M. C., Renault, C., Guerey, C., and Le Fur, G. (1987) *Mol. Pharmacol.* 31, 42–49.
13. Antkiewicz-Michaluk, L., Guidotti, A., and Krueger, K. E. (1988) *Mol. Pharmacol.* 34, 272–278.
14. Riond, J., Vita, N., Le Fur, G., and Ferrara, P. (1989) *FEBS Lett.* 245, 238–244.
15. Parola, A. L., Putnam, C. W., Russell, D. H., and Laird, H. E., II (1989) *J. Pharmacol. Exp. Ther.* 250, 1149–1155.
16. Sprengel, R., Werner, P., Seeburg, P. H., Mukhin, A. G., Santi, M. R., Grayson, D. R., Guidotti, A., and Krueger, K. E. (1989) *J. Biol. Chem.* 264, 20415–20421.
17. Riond, J., Mattei, M. G., Kaghad, M., Dumont, X., Guillemot, J. C., Le Fur, G., Caput, D., and Ferrara, P. (1991) *Eur. J. Biochem.* 195, 305–311.
18. Parola, A. L., Stump, D. G., Pepperl, D. J., Krueger, K. E., Regan, J. W., Laird, H. E., II (1991) *J. Biol. Chem.* 266, 14082–14087.
19. Garnier, M., Dimchev, A. B., Boujrad, N., Price, J. M., Musto, N. A., and Papadopoulos, V. (1994) *Mol. Pharmacol.* 45, 201–211.
20. Doble, A., Benavides, J., Ferris, O., Bertrand, P., Menager, J., Vaucher, N., Burgevin, M. C., Uzan, A., Guerey, C., and Le Fur, G. (1985) *Eur. J. Pharmacol.* 119, 153–167.
21. Snyder, S. H., Verma, A., and Trifiletti, R. R. (1987) *FASEB J.* 1, 282–288.
22. Lueddens, H. W. M., Newman, A. H., Rice, K. C., and Skolnick, P. (1986) *Mol. Pharmacol.* 29, 540–545.
23. McCabe, R. T., Schoenheimer, J. A., Skolnick, P., Hauck-Newman, A., Rice, K., Reig, J.-A., and Klein, D. C. (1989) *FEBS Lett.* 244, 263–267.
24. Paul, S. M., Kempner, E. S., and Skolnick, P. (1981) *Eur. J. Pharmacol.* 76, 465–466.
25. McEnery, M. W., Snowman, A. M., Trifiletti, R. R., and Snyder, S. H. (1992) *Proc. Natl. Acad. Sci. U.S.A.* 89, 3170–3174.
26. Golani, I., Weizman, A., Leschiner, S., Spanier, I., Eckstein, N., Limor, R., Yanai, J., Maaser, K., Scherubl, H., Weisinger, G., and Gavish, M. (2001) *Biochemistry* 40, 10213–10222.
27. Papadopoulos, V., Mukhin, A. G., Costa, E., and Krueger, K. E. (1990) *J. Biol. Chem.* 265, 3772–3779.
28. Papadopoulos, V., Boujrad, N., Ikononovic, M., Ferrara, P., and Vidic, B. (1994) *Mol. Cell. Endocrinol.* 104, R5–R9.
29. Boujrad, N., Vidic, B., and Papadopoulos, V. (1996) *Endocrinology* 137, 5727–5730.
30. Joseph-Liauzun, E., Farges, R., Delmas, P., Ferrara, P., and Loison, G. (1997) *J. Biol. Chem.* 272, 28102–28106.
31. Veenman, L., Leschiner, S., Spanier, I., Weisinger, G., Weizman, A., and Gavish, M. (2002) *J. Neurochem.* 80, 917–927.
32. Hardwick, M., Fertikh, D., Culty, M., Li, H., Vidic, B., and Papadopoulos, V. (1999) *Cancer Res.* 59, 831–842.

33. Yao, Z., Drieu, K., and Papadopoulos, V. (2001) *Brain Res.* 889, 181–190.
34. Bradford, M. M. (1976) *Anal. Biochem.* 72, 248–254.
35. Whalin, M., Boujrad, N., Papadopoulos, V., and Krueger, K. E. (1994) *J. Recept. Res.* 14, 217–228.
36. Amri, H., Ogwuegbu, S. O., Boujrad, N., Drieu, K., and Papadopoulos, V. (1996) *Endocrinology* 137, 5707–5718.
37. Li, H., and Papadopoulos, V. (1998) *Endocrinology* 139, 4991–4997.
38. Morrissey, J. H. (1981) *Anal. Biochem.* 117, 307–310.
39. Malencik, D. A., Sprouse, J. F., Swanson, C. A., and Anderson, S. R. (1996) *Anal. Biochem.* 242, 202–213.
40. Davies, M. J., Fu, S., Wang, H., and Dean, R. T. (1999) *Free Radical Biol. Med.* 27, 1151–1163.
41. Peltola, V., Huhtaniemi, I., Metsä-Ketela, T., and Ahotupa, M. (1996) *Endocrinology* 137, 105–112.
42. Sawada, M., and Carlson, J. V. (1996) *Endocrinology* 137, 1580–1584.
43. Morrissey, Z., Rush, J. D., and Koppenol, W. H. (1992) *Arch. Biochem. Biophys.* 296, 514–520.
44. Van der Vlies, D., Pap, E. H., Post, J. A., Celis, J. E., and Wirtz, K. W. (2002) *Biochem. J.* 366, 825–830.
45. Kanwar, R., and Balasubramanian, D. (2000) *Biochemistry* 39, 14976–14983.
46. Peranzi, G., Bayle, D., Telford, J. N., and Soumarmon, A. (1994) *Biol. Cell* 73, 163–171.
47. Maccario, J., Peranzi, G., Bayle, D., Lewin, M. J., and Thomas-Soumarmon, A. (1994) *Biol. Cell* 80, 55–62.
48. Hirsch, J. D., Beyer, C. F., Malkowitz, L., Beer, B., and Blume, A. J. (1988) *Mol. Pharmacol.* 34, 157–163.
49. Ikezaki, K., and Black, K. L. (1990) *Cancer Lett.* 49, 115–120.
50. Miettinen, H., Kononen, J., Haapasalo, H., Helén, P., Sallinen, P., Harjuntausta, T., Helin, H., and Alho, H. (1995) *Cancer Res.* 55, 2691–2695.
51. Papadopoulos, V., Dharmarajan, A. M., Li, H., Culty, M., Lemay, M., and Sridaran, R. (1999) *Biochem. Pharmacol.* 58, 1389–1393.
52. Maaser, K., Hoper, M., Jansen, A., Weisinger, G., Gavish, M., Kozikowski, A. P., Weizman, A., Carayon, P., Riecken, E. O., Zeitz, M., and Scherubl, H. (2001) *Br. J. Cancer* 85, 1771–1780.
53. Decaudin, D., Castedo, M., Nemati, F., Beurdeley-Thomas, A., DePinieux, G., Caron, A., Pouillard, P., Wijdenes, J., Rouillard, D., Kroemer, G., and Poupon, M. F. (2002) *Cancer Res.* 62, 1388–1393.
54. Strohmeier, R., Roller, M., Sanger, N., Knecht, R., and Kuhl, H. (2002) *Biochem. Pharmacol.* 64, 99–107.
55. Brown, R. C., and Papadopoulos, V. (2001) *Int. Rev. Neurobiol.* 46, 117–144.
56. Szatrowski, T. P., and Nathan, C. F. (1991) *Cancer Res.* 51, 794–798.
57. Brown, N. S., and Bicknell, R. (2001) *Breast Cancer Res.* 3, 323–327.
58. Yeliseev, A. A., and Kaplan, S. A. (1995) *J. Biol. Chem.* 270, 21167–21175.
59. Joseph-Liauzun, E., Delmas, P., Shire, D., and Ferrara, P. (1998) *J. Biol. Chem.* 273, 2146–2152.
60. Culty, M., Li, H., Boujrad, N., Amri, H., Vidic, B., Bernassau, J. M., Reversat, J. L., and Papadopoulos, V. (1999) *Steroid Biochem. Mol. Biol.* 69, 123–130.
61. Cherradi, N., Defaye, G., and Chambaz, E. M. (1994) *Endocrinology* 134, 1358–1364.
62. Papadopoulos, V. (1998) *Proc. Soc. Exp. Biol. Med.* 217, 130–142.
63. Jefcoate, C. R., McNamara, B. C., Artemenko, I., and Yamazaki, T. (1992) *J. Steroid Biochem. Mol. Biol.* 43, 751–767.

BI0267487

Peripheral-type benzodiazepine receptor (PBR) overexpression and knockdown in human breast cancer cells indicate a role in tumor cell proliferation mediated by activation of p21^{WAF1/CIP1} expression

Wenping Li¹, Matthew J. Hardwick¹, Vassilios Papadopoulos^{1,2,3,4}

Division of Hormone Research, Departments of Cell Biology¹, Pharmacology² & Neurosciences³, and the Lombardi Cancer Center⁴, Georgetown University Medical Center, Washington, DC 20057, USA

Present address of M. Hardwick: Department of Urology, James Buchanan Brady Urological Institute Research Laboratories, The Johns Hopkins University Hospital, Baltimore, MD 21287

Correspondence: Dr. V. Papadopoulos, Department of Biochemistry and Molecular Biology, Georgetown University Medical Center, 3900 Reservoir Road, NW, Washington, DC 20057, USA; Phone: 202-687-8991; Fax: 202-687-7855; e-mail: papadopv@georgetown.edu

Grant support: This work was supported by a grant from the Department of Defense (DAMD17-99-1-9200).

Running Title: PBR and tumor cell proliferation

Key words: Gene expression, MCF-7, MDA-231, RNA interference, Transfection

Abbreviations and acronyms:

Akt1: A serine/threonine protein kinase, Protein kinase B (PKB)

B_{max}: Maximal binding capacity, or density

BrdU: 5-Bromo-2'deoxyuridine

Cdk: Cyclin-dependent protein kinase

DMEM: Dulbecco's modified Eagle medium

Dox: Doxycyclin

Erk1: Extracellular-signal related/regulated kinase-1; identical to mitogen-activated protein kinase-1 (MAPK1)

FBS: Fetal bovine serum

GAPDH: Glyceraldehyde 3-phosphate dehydrogenase

HIV: Human immunodeficiency virus

Kd: Dissociation constant

MAPK: Mitogen-activated protein kinase

MCF-7 Tet-Off cells: Tetracycline-repressible MCF-7 cell line

MDA-231: MDA-MB-231 cells

MIP cells: MCF-7 Tet-Off cells with induced expression of PBR

MIP1 and MIP2 cells: MIP cells that were stably transfected with PBR cDNA

MOM cells: Mock-transfected MCF-7 Tet-Off cells

mRNA: Messenger RNA

p21^{WAF/CIP1}: Cyclin-dependent protein kinase inhibitor p21

PAGE: Polyacrylamide gel electrophoresis

pBI-EGFP: Bi-directional expression vector possessing cDNA for enhanced green fluorescent protein (EGFP) PBR:

PBS: Phosphate-buffered saline

PBR: Peripheral-type benzodiazepine receptor

PCNA: Proliferating cell nuclear antigen

PK 11195: 1-(2-Chlorophenyl)-N-methyl-N-(1-methylpropyl)

-3-isoquinoline-carboxamide

PKC: Protein kinase C

pTK-Hyg vector: Vector that confers hygromycin resistance

Q-PCR: Quantitative polymerase chain reaction

RNAi: RNA interference

shRNA: small hairpin RNA

siRNA: small interfering RNA

ABSTRACT

The peripheral-type benzodiazepine receptor (PBR), an 18-kDa high affinity drug and cholesterol binding protein, has been shown to be expressed at high levels in various forms of cancer, and its expression is positively correlated with aggressive metastatic behavior in human breast cancer cells. The effects of PBR drug ligands on cell proliferation and apoptosis have been described, but the role of the PBR protein in these processes has not yet been examined. Therefore, we have used transfection of the tetracycline-repressible MCF-7 cell line (MCF-7 Tet-Off) with human PBR cDNA, transfection of MDA-MB-231 cells with small interfering RNAs (siRNAs) targeting human PBR, radioligand binding assays and real-time quantitative PCR to examine the role of PBR protein in cell proliferation. The human breast cancer cell line MCF-7 is normally non-aggressive and expresses extremely low PBR levels. Induction of PBR expression in MCF-7 Tet-Off cells increased PBR ligand binding and cell proliferation. Multiple siRNAs complementary to PBR (PBR-siRNAs) enabled us to evaluate the role of PBR in cell proliferation in PBR-enriched, aggressive MDA-MB-231 human breast cancer cells. Transfection of MDA-MB-231 cells with PBR-siRNAs targeting different sites of PBR mRNA led to different levels of mRNA and protein knockdown. The decreased PBR expression was associated with decreased cell proliferation, and with increased levels of the cyclin-dependent protein kinase inhibitor p21^{WAF/CIP1} which is known to be involved in tumor-suppression. Collectively, these results indicate that PBR protein expression is directly involved in regulating cell proliferation in human breast cancer cells, probably by influencing a mechanism involved in cell cycle control.

INTRODUCTION

Breast cancer is the most common neoplasm and the leading cause of cancer-related deaths in women in most developing countries [1]. In breast cancer, tumor progression occurs via a multi-step process in which normal cells gradually acquire more malignant phenotypes, including the ability to invade tissues and form distal metastases, the primary cause of mortality. Considering that the first step of tumor progression is cell proliferation, it can be envisaged that tumorigenesis and malignancy are related to the proliferative potential of tumoral cells. Therefore, a search for cellular components that are involved in enhancing such proliferative potential seems warranted.

The peripheral-type benzodiazepine receptor (PBR) may be one cellular component that is involved in regulating cell proliferation, and therefore it could be involved in the increased cell proliferation that occurs in cancer cells. PBR was identified because of its ability to bind the benzodiazepine diazepam in tissues that do not express the central benzodiazepine receptor [2,3]. It is an 18-kDa receptor protein that is abundant in steroid-synthesizing tissues, such as gonads, adrenal gland, placenta and brain [2,3]. PBR resides primarily in the outer mitochondrial membrane where it regulates the transport of cholesterol to the mitochondrial inner membrane, this transport process being the rate-determining step in steroidogenesis [2]. Recent studies have shown that PBR is a high-affinity cholesterol-binding protein [4,5]. Considering its widespread distribution [2,3] and its ability to bind cholesterol [4,5], PBR might affect cholesterol compartmentalization and membrane biogenesis, events known to be involved in cell proliferation and cell death. Indeed, a role for PBR in mitochondrial respiration has been suggested [6], an anti-apoptotic (cell survival) role of the 18-kDa PBR protein has been

demonstrated [7-11], and the use of PBR as a therapeutic target has been suggested [12,13].

Numerous studies conducted during the last decade have indicated that PBR may also play a role in carcinogenesis. The receptor is highly expressed in testicular and adrenocortical cells and in brain gliomas, and PBR drug ligands (e.g., benzodiazepines) have been shown to regulate the proliferation of such cells [14]. PBR expression has been correlated with the high metastatic potential of human astrocytomas and other types of human brain tumors [15,16], and PBR ligands have been shown to influence the proliferation of various tumors, such as gliomas and lymphomas [17-21]. Increases in the density of PBR binding sites have been found in colonic adenocarcinoma, ovarian carcinoma [22-25], and in human brain gliomas, as compared to normal tissue [25,26]. Also, recent studies have indicated that antitumoral drugs that act via PBR (e.g., PBR ligand-drug conjugates) may be useful in treating pancreatic and brain tumors [27,28], that pharmacological concentrations of high-affinity PBR drug ligands can induce apoptosis in various cancer cell lines [29-32], and that PBR ligands may act as chemosensitizing agents for the treatment of human neoplasms [33].

In previous studies, we examined the expression, characteristics, localization, and function of PBR in a battery of human breast cancer cell lines that differed with respect to their invasive and chemotactic potentials [29]. PBR ligand-binding and PBR mRNA levels were much higher in highly aggressive cell lines, such as MDA-MB-231 (MDA-231) than in non-aggressive cell lines, such as MCF-7, a difference that may be due, at least in part, to PBR gene amplification [34,35]. PBR was also found to be expressed at high levels in aggressive metastatic human breast tumor biopsies, as compared to normal

breast tissue [25,29]. In further studies, we found that the ability of aggressive breast tumor cells to form tumors *in vivo* might depend on the amount of PBR present in the cells. Furthermore, exposure of MDA-231 cells to high-affinity PBR drug ligands increased the incorporation of bromodeoxyuridine into the cells, indicating that PBR plays a role in regulating cell proliferation in this aggressive cancer cell line [35].

Taken together, the results mentioned above support a role for PBR in cell proliferation in showing that levels of the protein are increased in tumor cells and in aggressive cell lines with high metastatic potential, and that PBR ligands can influence the proliferation of various tumors. However, two major questions remain to be answered: Does PBR play a direct role in regulating cell proliferation? What mechanism underlies the effect of PBR?. Results provided herein indicate that the 18-kDa PBR protein is directly involved in regulating cell proliferation, probably by activating a mechanism that influences cell cycle control.

MATERIALS AND METHODS

Cell Culture. MCF-7 and MDA-231 human breast cancer cell lines were obtained from the Lombardi Cancer Center, Georgetown University Medical Center. They were grown in Dulbecco's modified Eagle medium (DMEM) supplemented with 10% fetal bovine serum (FBS) plus 100 U/ml penicillin and 10 µg/ml streptomycin (Invitrogen Life Technologies, Carlsbad, CA). The commercially available tetracycline-repressible MCF-7 cell line, designated "MCF-7 Tet-Off" BD Biosciences Clontech (Palo Alto, CA) was used for stably transfecting human PBR cDNA. MCF-7 Tet-Off mock-transfected cells

(designated "MOM") and MCF-7 Tet-Off-Induced expression of PBR cells (designated "MIP") were maintained in DMEM supplemented with 10% Tet-Approved FBS (Clontech). Stable MIP transfectants were later termed "MIP1" and "MIP2". Plasticware was purchased from Corning (Corning, NJ).

Stable Transfection of MCF-7 Tet-Off Cells with PBR cDNA. Approximately 8×10^5 MCF-7 Tet-Off cells were co-transfected with 40 μ g of either the pBI-EGFP vector alone (mock-transfected MCF-7 Tet-Off, or MOM cells) or with the vector plus the full-length human PBR cDNA (MIP cells) and 2 μ g of the pTK-Hyg vector via electroporation (220 V, 950 μ F). pBI-EGFP is a bi-directional expression vector from Clontech possessing both the enhanced green fluorescent protein (EGFP) cDNA and a multi-cloning sequence under the expression of a bi-directional minimal cytomegalovirus promoter. Thus, pBI-EGFP permits the simultaneous expression of the PBR gene and EGFP. The pTK-Hyg vector (Clontech) confers hygromycin resistance and served as a negative selection marker in this study. After electroporation, cells were plated in DMEM supplemented with 10% Tet System Approved FBS (BD Biosciences Clontech) without antibiotics for two days at 37°C, 6% CO₂. The cells were then maintained in DMEM, 10% Tet System Approved FBS supplemented with 100 μ g/ml hygromycin and 1 μ g/ml doxycyclin (Dox) (Sigma Aldrich, St. Louis, MO). After several weeks, colonies over 2 mm in size were isolated and amplified in DMEM, 10% Tet System Approved FBS supplemented with 100 μ g/ml hygromycin and 1 μ g/ml Dox.

Doxycyclin-Induced Reduction of EGFP Expression. Selected stably-transfected MIP clones, MIP1 and MIP2, were plated onto 96-well plates (Corning) at a concentration of 5,000 cells/well and allowed to grow for 3 days in DMEM supplemented with 10% Tet System Approved FBS in the presence of 0, 0.0001, 0.01, or 1.0 $\mu\text{g/ml}$ Dox. [In this gene expression system, the Tet-controlled transcriptional transactivator activates transcription in the absence of the inducer (Dox).] After incubation, cells were washed twice with PBS, and EGFP fluorescence was determined at 485 nm excitation and 510 nm emission.

Crystal Violet Cell Proliferation Assay. Cells that were grown to confluency were trypsinized and plated on 96-well plates at a concentration of 5,000 cells/well and maintained in DMEM supplemented with 10% Tet System Approved FBS. Dox was added to the designated samples at a concentration of 1 $\mu\text{g/ml}$. Media were changed every two days. At the specified time points, cells were stained and fixed in Crystal Violet solution (100 $\mu\text{l/well}$ of 0.5% Crystal Violet, 25% methanol) for 10 minutes at room temperature. Plates were then thoroughly washed in 1 x PBS, dried, and read dry at 600 nm.

Chemical Determination of Vimentin. Approximately 20,000 cells per well of each cell line were loaded onto poly-D-lysine slides (Becton Dickinson Labware, Bedford, MA) and incubated overnight at 37°C, 6% CO₂. Cells were then fixed in 10% formaldehyde for 10 minutes at room temperature. After washing thoroughly with distilled H₂O, anti-vimentin (Chemicon International, Inc., Temecula, CA), diluted 1:3 in

PBS supplemented with 10% FBS, was added to each well and samples were incubated overnight at 4°C. After thoroughly rinsing the slides in PBS, horseradish peroxidase-conjugated goat anti-mouse secondary antibody, diluted 1:1,000 in PBS supplemented with 10% FBS, was added to each well and immunoreactivity was revealed as previously described [35].

Preparation of siRNAs. Small interfering RNAs (siRNAs) consisting of 21 nucleotides were synthesized by Dharmacon Research (Lafayette, CO) using 2'-ACE protection chemistry. The siRNA strands were deprotected according to the manufacturer's instructions, mixed in equimolar ratios and annealed at 60°C for 45 minutes and at ambient temperature for 30 min. The GeneBank accession number for human PBR is gi 21536444. siRNA duplexes with the following sense and antisense sequences were used:

PBR	361	siRNA	targeting	human	PBR	exon	3,5'-
							5'-
AACTGGGCATGGCCCCCATCCCTGTCTC-3'(sense),							
AAGATGGGGGGCCATGCCCAGCCTGTCTC-3'(antisense);							
PBR	537	siRNA	targeting	human	PBR	exon	4,5'-
							5'-
AACTACTGCGTATGGCGGGACCCTGTCTC-3'(sense),							
AAGTCCCGCCATACGCAGTAGCCTGTCTC-3'(antisense);							
PBR	548	siRNA	targeting	human	PBR	exon	4, 5'-
							5'-
AACCATGGCTGGCATGGGGGACCTGTCTC-3'(sense),							
AATCCCCCATGCCAGCCATGGCCTGTCTC-3'(antisense);							

Scrambled siRNA, 5'-AAGGCTACTATGCGGCGACTGCCTGTCTC-3'(sense), 5'-AACAGTCGCGGCATAGTAGCCCCTGTCTC-3'(antisense). PBR 361, 537 and 548 siRNAs correspond to PBR coding regions and scrambled siRNA served as the control.

Sequences for the siRNAs were selected as follows: 75 bases downstream from the start codon the first AA dimer was located and the next 19 nucleotides were selected. The percentage of guanosines and cytidines (G/C content) of the AA(N19) 21-base sequence was calculated. Ideally the G/C content should be ~50% (less than 70% and greater than 30%). If the sequence does not meet this criterion, the search continues downstream to the next AA dimer until this condition is met. Each 21-base sequence was subjected to a BLAST-search (NCBI Database) against EST libraries to ensure that only one gene was targeted. The base-pairing region for each siRNA was selected carefully to avoid chance complementarity to an unrelated mRNA.

Transfection of MDA-231 Human Breast Cancer Cells with PBR-siRNA Duplexes. A single transfection of siRNA duplexes was performed using the Oligofectamine reagent (InVitrogen), and the cells were assayed for silencing 3 days later. Cells had been seeded the previous day in DMEM supplemented with 10% FBS in the absence of antibiotics. The siRNA duplex was mixed with Opti-MEM (InVitrogen), and in a separate tube, the Oligofectamine reagent was mixed with Opti-MEM and incubated for 10 minutes at room temperature. The two solutions were combined, gently mixed by inversion, incubated for 20 minutes at room temperature, and then the resulting siRNA-Oligofectamine was added to cells that were cultured at 30-50% confluency. Twenty-four hours later, fresh DMEM

supplemented with 30% FBS was added to transfected cells to obtain a final concentration of 10% FBS.

Real-time Quantitative PCR (Q-PCR). Following incubation with or without siRNA, cells were washed three times with 1 x PBS (pH 7.4), and total RNA was isolated using the Qiagen RNeasy Mini kit (Qiagen, Valencia, CA) according to the manufacturer's specifications. Total RNA was submitted to On-Column DNase I digestion with RNase-free DNase in order to remove genomic DNA contamination. Q-PCR was performed using the ABI PRISM 7700 Sequence Detection System (Applied Biosystems, Foster City, CA) as previously described [36]. Briefly, total RNA was reverse-transcribed into cDNA, and the resulting cDNA was then processed for amplification of the PBR gene using specific primers. Each sample was run in triplicate. Direct detection of the PCR products was achieved by measuring the increase in fluorescence caused by the binding of SYBR® Green I Dye to double-stranded (ds) DNA. The Comparative C_T Method was used to analyze the data. The amount of PBR mRNA expression was normalized to the endogenous reference (18S rRNA).

Radioligand Binding Assays. [³H]PK11195 (specific activity, 85.5 Ci/mmol) was obtained from NEN Life Science Products (Boston, MA). Cells were scraped from 150-mm culture dishes into 6 ml of phosphate buffered saline (PBS), dispersed by trituration, and assayed for protein concentration. [³H]PK11195 binding to samples representing 40 µg of protein from cell suspensions was determined as previously described [37]. Specific [³H]PK11195 binding was analyzed using the iterative non-linear curve-fitting

program Radlig 4.0 (KELL suite, Biosoft, Cambridge, UK). Protein levels were measured according to Bradford [38] using the Bio-Rad Protein Assay Kit (Bio-Rad Laboratories, Hercules, CA), bovine serum albumin serving as the standard.

BrdU Cell Proliferation Assay. MDA-231 cells were plated on 96-well plates in DMEM supplemented with 10% FBS containing various concentrations of siRNAs and incubated for 72 hrs. After incubation, differences in cell proliferation were analyzed by measuring the amount of 5-bromo-2'deoxyuridine (BrdU) incorporation using the BrdU Cell Proliferation ELISA (Roche Molecular Biochemicals, Indianapolis, IN). Incorporation of BrdU was measured at 450 nm (reference at 690 nm) [39].

Soft Agar Colony Formation Assay. For this assay, 5,000 cells were suspended in 1.5 ml top agar (0.35% agar, DMEM supplemented with 10% Tet System Approved FBS) and plated on 1.5 ml base agar (0.5% agar, DMEM plus 10% Tet System Approved FBS) in one well of a 6-well plate and incubated at 37°C, 6% CO₂ for 14 days. On day 2, a thin layer of liquid DMEM supplemented with 10% Tet System Approved FBS was added to each well. At the end of the assay, colony formation was determined by reading each plate using an Omnicon 3800 Tumor Colony Analyzer (Imaging Products International, Inc., Chantilly, VA).

Immunoblots. After subjecting cells to the above-described protocol, whole-cell extracts were prepared in lysis buffer (100 mM dithiothreitol, 2% sodium dodecyl sulfate, 50 mM Tris-HCl pH 6.8, 50% glycerol, 0.1% bromophenol blue). Equal amounts of protein were

separated by SDS-PAGE in 4-20% Tris-Glycine Gels and electrotransferred onto a nitrocellulose membrane. Antibodies to p21^{WAF1/CIP1}, Akt1 protein kinase (Akt1), phosphorylated Akt (P-Akt), extracellular signal-regulated kinase-1 (Erk1) and phosphorylated Erk1 (P-Erk1) were obtained from BD Biosciences (San Jose, CA), and anti-glyceraldehyde 3-phosphate dehydrogenase (anti-GAPDH) was from Trevigen Inc. (Gaithersburg, MD). Proteins were visualized using an ECL kit (Amersham Biosciences, Arlington Heights, IL), and images were developed and analyzed using Fujifilm LAS-1000 (FUJIFILM Medical Systems USA, Inc., Stamford, CT).

Statistics. Multiple means were compared using InStat's one-way analysis of variance (ANOVA) (Prism v. 3.0, GraphPad Inc., San Diego, CA). All F statistics and *P* values for one-way ANOVAs are provided in the text. Comparisons between individual drug treatments and control treatments were made using an unpaired t-test. All *P* values for unpaired t-tests are provided in the text.

RESULTS

PBR Overexpression in Non-Aggressive MCF-7 Human Breast Cancer Cells. After stably transfecting human PBR cDNA and the pBi-EGFP bi-directional vector as described above, MOM and MIP cells were analyzed. While several (approximately 20) MOM stable transfectants were isolated, only 2 MIP stable transfectants (MIP1 and MIP2) could be isolated. EGFP expression was completely repressed by 1.0 µg/ml Dox in both

MIP1 (Fig. 1A and B) and MIP2 cells (Fig. 1A), indicating that the Tet-off system is fully functional in this cell line.

Ligand Binding to PBR in MCF-7 Tet-Off, MOM, MIP1 and MIP2 cells. As shown in Table 1, the MCF-7 Tet-Off cell line expressed approximately 10-fold less PBR ligand binding sites than the MDA-231 cell line ($B_{\max} = 0.8$ vs 8.7 pmol/mg protein, respectively). MOM cells also had a low capacity for PBR ligand binding (B_{\max} of 0.5 pmol/mg protein). MIP1 and MIP2 cells achieved maximal PBR ligand binding (B_{\max}) of 4.9 and 2.1 pmol/mg protein, respectively. In the presence of 1.0 $\mu\text{g/ml}$ Dox, the B_{\max} values for both MIP1 and MIP2 decreased to levels approximating those of MCF-7 Tet-Off and MOM (0.6 and 0.8 pmol/mg protein, respectively). K_d values, which represent reciprocals of ligand-binding affinities, were nearly identical (approximately 1.0 nM) for all of the cell lines under all conditions employed (Table 1).

Expression of Vimentin in MIP1 and MIP2 Cells. Expression of the developmentally regulated intermediate filament protein, vimentin, is a marker of enhanced invasiveness and increased metastatic potential, and therefore it serves as an indicator of increased aggressive phenotype in breast cancer cells [40,41]. Immunocytochemical data showing the expression of vimentin in the MCF-7 Tet-Off, MDA-231, MIP1, and MIP2 cells are provided in Figure 1C. As MCF-7 cells are vimentin-negative and as MDA-231 cells are vimentin-positive [40], the latter were used as a positive control in these experiments. Light vimentin immunostaining was found in MCF-7 Tet-Off, MIP1 and MIP2 cell lines,

whereas strong immunostaining occurred in MDA-231 cells (Fig. 1C). However, there were no gross differences in vimentin expression among these cell lines.

Effects of PBR Transfection on the Proliferation of MCF-7 Tet-Off Cells.

Further functional studies were performed to examine whether increased PBR expression may lead to increased cell proliferation, as our previous studies had indicated [29,34,35]. Indeed, even in the presence of 10% FBS, MIP1 cells proliferated at a much greater rate than MCF-7 Tet-Off cells in the absence of Dox (Fig. 1D). This effect was abrogated by the addition of 1.0 $\mu\text{g/ml}$ Dox. No differences were seen between MIP2 and MCF-7 Tet-Off cells. Preliminary studies did not show any significant difference between the MCF-7 Tet-Off and the original MCF-7 cell line (data not shown). In additional experiments, proliferation of MOM cells did not differ from that of MCF-7 Tet-Off cells, and neither the MIP1 nor the MIP2 cell line displayed any more ability to grow in soft agar than the MCF-7 Tet-Off parental cell line (data not shown). Upon testing the chemotactic potential, we found no differences among MCF-7 Tet-Off, MIP1, and MIP2 cell lines (data not shown).

siRNAs Targeting PBR Down-Regulate PBR mRNA and Radioligand Binding in MDA-231 Breast Cancer Cells. siRNAs targeting various PBR coding regions decreased PBR mRNA expression by about 50% (Fig. 2A). This inhibition of PBR mRNA expression resulted in an inhibition of ligand binding to PBR (Fig. 3).

Silencing PBR Expression Inhibits the Proliferation of MDA-231 Cells. Following treatment of MDA-231 cells with the various PBR-specific siRNAs for 72 hours, the amount of BrdU incorporation also decreased in a manner parallel to the decrease in PBR mRNA expression (Fig. 2B).

Silencing PBR Expression Increases the Expression of p21^{WAF1/CIP1}. In search of the mechanism underlying the translation of changes in PBR levels into changes in cell proliferation, we examined the expression of key proteins involved in regulating cell proliferation. Inhibition of PBR mRNA expression by 50% by treatment of MDA-231 cells with PBR-siRNAs was correlated with a 2.5-fold increase in p21^{WAF1/CIP1} protein levels (Fig. 4). No major effects on Akt1, Erk1 and P-Erk1 protein expression were observed (Fig. 4). The anti P-Akt1 signal was too weak for analysis (data not shown).

DISCUSSION

The results presented herein which were obtained using two human breast cancer cell lines, MCF-7 which is non-aggressive and has extremely low levels of PBR and MDA-231 which is aggressive and expresses high levels of PBR (29), provide convincing evidence in support of the view that PBR is involved in regulating cell proliferation in breast cancer cells. Thus, PBR could play a role in mediating the increased cell proliferation that occurs in breast cancer and in certain other forms of cancer. With regard to MCF-7 cells, we found that stable transfection of the MCF-7 Tet-Off derivative of this cell line with the full-length human PBR cDNA resulted in cells (MIP1 and MIP2) that exhibited an increase in PBR ligand binding. Our PBR transfectants, MIP1 and MIP2

cells, expressed increases in PBR ligand binding of 4.9- and 2-fold, respectively, relative to the parental MCF-7 Tet-Off cells. Growth assays showed that MIP1 cells grew at a faster rate than MCF-7 Tet-Off cells. The finding that Dox abolished this difference in growth rate strongly indicates that the increases in cell proliferation were a *direct* result of increased PBR expression and not a by-product of transfection. Further, the finding that no differences in cell proliferation existed between MCF-7 Tet-Off and MIP2 cells (which differed from MIP1 cells in expressing lower levels of PBR ligand binding; see above) indicates that a certain threshold level of PBR expression must be surpassed in order for increased cell proliferation to occur.

The finding that cell proliferation rate could be enhanced by increasing the expression of PBR in MIP1 cells is of interest in that it supports other findings which have revealed that PBR site densities are as much as 12-fold higher in high-grade astrocytomas and glioblastomas than in normal brain tissue [15], that PBR is highly up-regulated in high-grade human astrocytomas relative to low grade tumors [16], and that the binding of the PBR-specific ligand, PK11195 (determined by Positron Emission Tomography), is two-fold greater in glioblastomas than in normal human gray matter [26]. In this regard, it is also noteworthy that other recent results have indicated that the expression of PBR is correlated with carcinogenic potential. As examples, we have shown that PBR binding occurs to a much greater extent in aggressive, estrogen receptor (ER)-negative MDA-231 cells than in non-aggressive, ER-positive MCF-7 cells [29], and the results of Beinlich and colleagues [42] have indicated that specific high-affinity binding of [3H]Ro5-4864 (a PBR agonist) to PBR occurred with highest capacity in the ER-negative, progesterone receptor (PR)-negative BT-20 and MDA-MB-435-5 breast cancer cell lines but with only

low capacity in ER-positive, PR-positive MCF-7, T47-D and BT-474 breast cancer cell lines. All of these findings may be relevant to understanding mechanisms involved in human breast cancer, a view that is further substantiated by our previous demonstration that PBR protein expression and ligand binding are up-regulated in aggressive metastatic human breast tumor biopsies [29] by a mechanism(s) that may related to PBR gene amplification [34,35].

Taken together, these transfection data provide crucial evidence in support of the view that PBR *directly* influences the regulation of cell proliferation in cancer cells. We do conclude, however, that although the amount of PBR protein per cell may serve as the index of carcinogenesis, the level of PBR expression does not appear to account for other phenotypic differences that exist between non-aggressive and aggressive human breast cancer cells. This latter point is substantiated by our finding that no difference in the expression of the cancer marker vimentin existed between PBR-transfected MIP1 and MIP2 cells and the parental MCF-7 Tet-Off cells, and that PBR transfection did not affect the ability of MCF-7 Tet-Off cells to grow in soft agar (anchorage-independent cell growth; the hallmark of uncontrolled tumorigenic proliferation).

In the present study, we also used the method of "RNA interference" (RNAi). PBR-siRNA duplexes were used to evaluate the role of PBR in cell proliferation in aggressive, PBR-enriched MDA-MB-231 human breast cancer cells in an effort to determine the contribution of PBR to invasiveness and metastatic potential, other phenotypic characteristics of breast cancer cell lines. This method is based on the finding that double-stranded RNA (dsRNA) silences the expression of a gene(s) that is highly homologous to either of the RNA strands in the duplex via degradation of mRNA

sequences, and serves as a powerful technology that permits the post-transcriptional silencing of mammalian genes with great target-specificity [43,44]. RNAi can be elicited very effectively by well-defined 21-base duplex siRNAs [45-47]. When the siRNA duplex is added together with a transfection agent to mammalian cell cultures it acts in concert with cellular components to silence the gene with sequence homology to one of the siRNA strands. Our finding that inhibition of PBR mRNA expression by PBR-siRNAs led to reduced proliferation of MDA-231 cells agrees with our previous results which showed that *in vitro* treatment of these cells or treatment of nude mice bearing xenografts of these cells with the standardized leaf extract of *Ginkgo biloba* (Egb 761) and ginkgolide B inhibited PBR gene expression and cell proliferation [36,39].

Using PBR-siRNA treatment, we also observed that inhibition of PBR expression and cell proliferation is linked to a significant increase in p21^{WAF1/CIP1} protein in MDA-231 cells (see Fig. 4). p21^{WAF1/CIP1} was initially identified as an inhibitor of cyclin-dependent protein kinase (cdk) activity in a quaternary complex that also included Cyclin D, Cdk4, and proliferating cell nuclear antigen (PCNA), and was subsequently shown to directly bind to, and inhibit each member of the cdk family of proteins that is involved in cell cycle control [48,49]. Related studies have revealed that p21^{WAF1/CIP1} is a downstream mediator of the p53 tumor-suppressor and that p21^{WAF1/CIP1} may play a prominent role in inducing apoptosis and cell cycle arrest [48,50-53]. Thus, our finding that inhibition of PBR expression is associated with increased expression of p21^{WAF1/CIP1} is of interest, particularly because it links PBR inhibition (via p21^{WAF1/CIP1} up-regulation) to mechanisms involved in apoptosis and tumor suppression.

The results of several recent studies are useful in amplifying this latter contention. Studies concerning the overexpression of p21^{WAF1/CIP1} seem particularly noteworthy. As an example, it has been shown that transfection of the p21^{WAF1/CIP1} gene into a human hepatocellular carcinoma cell line (HCC-9204) bearing a p53 mutation caused an increase in cell number in the G1 phase of the cell cycle (an indicator of cellular differentiation), decreased anchorage-independent growth in soft agar, reduced BrdU incorporation, inhibited cell proliferation, and induced apoptosis [54]. As another example, transfection of human breast cancer cell lines MCF-7 and T47-D leading to overexpression of p21^{WAF1/CIP1} caused growth suppression that was associated with apoptosis [51]. As a third example, overexpression of p21^{WAF1/CIP1} in p53-defective human glioma cells resulted in an accumulation of cells in G1, altered morphology, growth arrest, and cell differentiation [55]. Also, many studies have shown that various anticancer drugs enhance the transcription of p21^{WAF1/CIP1}. Treatment with tamoxifen, a drug that is used very extensively in breast cancer patients, resulted in G1 arrest in two head and neck squamous cell carcinoma cell lines, HN5 and HN6, this growth suppression being independent of p53 status but resulting in an up-regulation of cyclin-dependent kinase inhibitors, including p21^{WAF1/CIP1} [56]. Another study showed that treatment of PC3, PC3-M and DU145 prostate cancer cells with micromolar concentrations of tamoxifen was associated with inhibition of protein kinase C (PKC), which was followed by an induction of p21^{WAF1/CIP1}, dephosphorylation of retinoblastoma protein, and cell cycle arrest at the G1/S phase [57]. Recent studies have also indicated that an important mode of apoptosis induction by the anticancer taxanes (paclitaxel, docetaxel) involves their up-regulation of p53 and p21^{WAF1/CIP1} [58]. In this

regard, it has been shown that increased expression of p21^{WAF1/CIP1} in anaplastic thyroid cancer cells (KAT-4 cells) by stable transfection with p21^{WAF1/CIP1} cDNA enhanced the antineoplastic activity of paclitaxel and its capacity to induce apoptosis [59]. With further regard to anticancer drugs, it has also been shown that transcription of p21^{WAF1/CIP1} was increased in human breast cancer cell lines MCF-7 and MDA-MB-468 by treatment with the DNA topoisomerase I inhibitors 10-hydroxycamptothecin and camptothecin, both of which have been shown to have therapeutic effects in various models of human breast cancer [60], and that phenylacetate (a member of a new class of antineoplastic drugs) induced growth arrest in MCF-7 cells that was associated with overexpression of p21^{WAF1/CIP1} [61].

Upon considering these latter findings, it seems that it may be worthwhile to test whether *in vivo* treatment with siPBR leads to increased expression of p21^{WAF1/CIP1}, since such an effect could provide a means for increasing the pro-apoptotic (antineoplastic) activity of certain anticancer drugs (e.g., taxanes), especially in those cancers that express high levels of PBR. Such *in vivo* testing of siPBR seems feasible in view of the recent demonstration that siRNAs are indeed functional *in vivo* in mice [62]. In their studies, McCaffrey and colleagues [62] co-injected luciferase expression constructs and luciferase-specific or control siRNAs into mouse livers. After 72 hours, the mice were sacrificed and luciferase levels in the liver were measured. It was found that luciferase-specific siRNAs, but not control siRNAs, were able to silence the injected luciferase gene (by 81%). In addition, these workers showed that an even higher level of silencing (93%) could be achieved using small hairpin RNA (shRNA) expression-constructs. The next challenge will be to develop viral or non-viral vectors that can deliver siRNAs or

shRNAs to their specific targets. Creation of such vectors could represent an important new method for cancer treatment.

We found no significant effect of PBR-siRNA treatment on Akt1 and Erk1, proteins known to be involved in signal transduction, as well as in cell survival, apoptosis and carcinogenesis. Akt [PKB (Protein kinase B)] is a family of serine/threonine kinases containing a pleckstrin-homology domain [63] that is considered to link extracellular survival signals (growth factors) to the apoptotic mechanism [64]. Phospho-Akt promotes cell survival by inhibiting apoptosis, and more specifically, P-Akt1 has been shown to phosphorylate and thereby inactivate Bad, a member of the Bcl-2 family that promotes cell death [64]. The family of serine/threonine kinases known as Erks or MAPKs (mitogen-activated protein kinases) is activated following cell stimulation by a variety of growth factors and hormones [65]. A myriad of proteins represent the downstream effectors for activated Erk and implicate it in the control of cell proliferation and differentiation [66]. Many studies have shown that elevated Erk activity is associated with certain forms of cancer, including breast cancer [67]. The lack of effect of PBR-siRNA treatment of MDA-231 cells on Akt1 and Erk1 may be indicating that inhibition of PBR expression has some degree of selectivity; i.e., a pronounced influence on cell cycle control involving mainly changes in factors that can alter the expression of p21^{WAF1/CIP1}, but no appreciable influence on growth factor pathways involving Akt or Erk as mediators. Further study is required in this area, but it does seem noteworthy that a recent study has implied that a link may exist between Erk activation and p21^{WAF1/CIP1} induction with respect to terminal differentiation of the human promyelocytic leukemia cell line HL60 [68].

With specific regard to PBR and the cell cycle, Sanger et al. [69], in showing that a strong correlation exists between increased expression of PBR ligand binding and the increase in the percentage of cells in the S phase, have provided evidence that PBR regulates cell proliferation by influencing cell cycle function. A previous study, conducted by this same group, showed that low concentrations of PBR ligands stimulated, whereas high micromolar concentrations inhibited, proliferation of the aggressive BT-20 breast cancer cell line [42]. Thus, it appears that nanomolar concentrations of PBR ligands may enhance the entry of these cells into the S phase of the cell cycle, whereas high micromolar concentrations may lead to an accumulation of cells in the Go/G1 phase [69]. Carmel and colleagues [70] found that high micromolar concentrations of PBR ligands also inhibit the proliferation of non-aggressive MCF-7 cells by inducing the cells to accumulate in the Go/G1 phase. These studies [69,70] provide persuasive evidence that PBR influences cell proliferation by regulating cell cycle staging .

Considering the foregoing discussion, it is clear that there is a great deal more to learn about PBR and its role in cell proliferation. It seems likely that PBR is one of the most basic proteins known to biology and that it has the versatility required to perform many different cellular functions while maintaining its identity as the major site involved in mediating the incorporation of cholesterol into cellular membranes. We envision that the development of methods based on regulating tumor cell proliferation by PBR manipulation opens up many new avenues for developing anticancer therapies. In showing that PBR-siRNAs can inhibit the proliferation of human breast cancer cells, the results provided herein represent a first step toward achieving this goal. This view that siRNAs may be useful as therapeutic agents has been substantiated in recent studies. For

example, in two recent studies, siRNAs targeting HIV proteins (Gag, Rev) and the HIV-receptor (CD4) have been shown to reduce virus infections in cultured mammalian cells [71,72]. As indicated by Sharp and colleagues [44,72], these experiments serve as a "proof-of-principle" that siRNA technology can be useful in suppressing multiple steps of the HIV-1 life cycle. Given that PBR expression is increased in colonic, brain, ovarian, and, as we have shown, breast cancer, it seems that manipulation of PBR by treatment with PBR-siRNAs could be useful in treating a broad variety of cancers.

ACKNOWLEDGEMENTS

We thank the Tissue Culture core facility of the Lombardi Cancer Center for assistance in this project and Dr. F. DeFeudis (Institute for Biosciences, Westboro, MA) for critically reviewing the manuscript.

REFERENCES

1. Lippman, ME. The Development of Biological Therapies for Breast Cancer. *Science* 1993;259: 631-632.
2. Papadopoulos V. Peripheral-type benzodiazepine/diazepam binding inhibitor receptor: biological role in steroidogenic cell function. *Endocr Rev* 1993;14:222-240.
3. Gavish M, Bachman I, Shoukrun R et al. Enigma of the peripheral benzodiazepine receptor. *Pharmacol Rev* 1999; 51:629-650.
4. Lacapère JJ, Delavoie F, Li H, Péranski G, Maccario J, Papadopoulos V, Vidic B. Structural and functional study of reconstituted peripheral benzodiazepine receptor (PBR). *Biochem Biophys Res Commun* 2001; 284:536-641.
5. Li H, Yao Z, Degenhardt B, Teper G, Papadopoulos V. Cholesterol binding at the cholesterol recognition/interaction amino acid consensus (CRAC) of the peripheral-type benzodiazepine receptor and inhibition of steroidogenesis by an HIV TAT-CRAC peptide. *Proc Natl Acad Sci USA* 2001; 98:1267-1272.

6. Hirsch JD, Beyer CF, Malkowitz L, Beer B, Blume AJ. Mitochondrial benzodiazepine receptors mediate inhibition of mitochondrial respiratory control. *Mol. Pharmacol.* 1989;35:157-163.
7. Papadopoulos V, Dharmarajan AM, Li H, Culty M, Lemay M, Sridaran R. Mitochondrial peripheral-type benzodiazepine receptor expression: correlation with the GnRH-agonist induced apoptosis in the corpus luteum. *Biochem Pharmacol* 1999; 58:1389-1393.
8. Carayon P, Portier M, Dussossoy D et al. Involvement of peripheral benzodiazepine receptors in the protection of hematopoietic cells against oxygen radical damage. *Blood* 1996; 87:3170-3178.
9. Rey C, Mauduit C, Naureils O, Benahmed M, Lousiot P, Gasnier F. Up-regulation of mitochondrial peripheral benzodiazepine receptor expression by tumor necrosis factor alpha in testicular Leydig cells. Possible involvement in cell survival. *Biochem Pharmacol* 2000; 60:1639-1646.
10. Hardwick M, Rone J, Han J, Haddad B, Papadopoulos V. Peripheral-type benzodiazepine receptor levels correlate with the ability of human breast cancer MDA-MB-231 cell line ability to grow in SCID mice. *Int J Cancer* 2001; 94:322-327.
11. Hauet T, Han Z, Wang Y et al. Modulation of peripheral-type benzodiazepine receptor levels in a perfusion injury pig kidney-graft model. *Transplantation* 2002;74:1507-1515.

12. Morin D, Papadopoulos V, Tillement J-P. Prevention of cell damage in ischemia: novel molecular targets in mitochondria. *Expert Opin Therap Target* 2002;6:315-334.
13. Castedo M, Perfettini JL, Kroemer G. Mitochondrial apoptosis and the peripheral benzodiazepine receptor: a novel target for viral and pharmacological manipulation. *J Exp Med*. 2002;96:1127-1139.
14. Garnier M, Dimchev AB, Boujrad N, Price JM, Musto NA, Papadopoulos V. *In Vitro* Reconstitution of a functional peripheral-type benzodiazepine receptor from mouse Leydig tumor cells. *Mol Pharmacol* 1994;45:201-211.
15. Cornu P, Benavides J, Scatton B, Hauw JJ, Philippon J. Increase in omega 3 (peripheral-type benzodiazepine) binding site densities in different types of human brain tumors. A quantitative autoradiography study. *Acta Neurochir* 1992;119:146-152.
16. Miettinen H, Kononen J, Haapasalo H et al. Expression of peripheral-type benzodiazepine receptor and diazepam binding inhibitor in human astrocytomas: relationship to cell proliferation. *Cancer Res*. 1995;15: 2691-2695.
17. Ikezaki K, Black KL. Stimulation of cell growth and DNA synthesis by peripheral benzodiazepine. *Cancer Lett* 1990;49:115-120.
18. Bruce JH, Ramirez AM, Lin L, Oracion A, Agarwal RP, Norenberg MD. Peripheral-type benzodiazepines inhibit proliferation of astrocytes in culture. *Brain Res* 1991;564:167-170.

19. Neary JT, Jorgensen SL, Oracion AM, Bruce JH, Norenberg MD. Inhibition of growth factor-induced DNA synthesis in astrocytes by ligands of peripheral-type benzodiazepine receptors. *Brain Res* 1996;675:27-30.
20. Clarke GD, Ryan PJ. Tranquillizers can block mitogenesis in 3T3 cells and induce differentiation in Friend cells. *Nature* 1980;287:160-161.
21. Laird HE 2nd, Gerrish KE, Duerson KC, Putnam CW, Haddock-Russell D. Peripheral benzodiazepine binding sites in Nb 2 node lymphoma cells: Effects on prolactin-stimulated proliferation and ornithine decarboxylase activity. *Eur J Pharm* 1989;171:25-35.
22. Katz Y, Eitan A, Amiri Z, Gavish M. Dramatic increase in peripheral benzodiazepine binding sites in human colonic carcinoma as compared to normal colon. *Eur J Pharmacol* 1988;148:483-484.
23. Katz Y, Eitan A, Gavish M. Increase in peripheral benzodiazepine binding sites in colonic adenocarcinoma. *Oncology* 1990;47:139-142.
24. Katz Y, Ben-Baruch G, Kloog Y, Menczer J, Gavish M. Increased density of peripheral benzodiazepine-binding sites in ovarian carcinomas as compared with benign ovarian tumours and normal ovaries. *Clin Sci (Lond)* 1990;78:155-158.
25. Han Z, Slack RS, Li W, Papadopoulos V. Expression of peripheral benzodiazepine receptor (PBR) in human tumors: relationship to breast, colon and prostate tumor progression. *J Rec Res Sign Transd* 2003; in press.

26. Pappata S, Cornu P, Samson Y et al. A PET study of carbon-11-PK 11195 binding to peripheral-type benzodiazepine sites in glioblastoma: A case report. *J Nuclear Med* 1991;32:1608-1610.
27. Ratcliffe SL, Matthews EK. Modification of the photodynamic action of delta-aminolaevulinic acid (ALA) on rat pancreatoma cells by mitochondrial benzodiazepine receptor ligands. *Br. J Cancer* 1995;71:300-305.
28. Kupczyk-Subotkowska L, Siahaan TJ, Basile AS et al. Modulation of mephalan resistance in glioma cells with a peripheral benzodiazepine receptor ligand-mephalan conjugate. *J Med Chem* 1997;40:1726-1730.
29. Hardwick M, Fertikh D, Culty M, Li H, Vidic B, Papadopoulos V. Peripheral-type benzodiazepine receptor (PBR) in human breast cancer: correlation of breast cancer cell aggressive phenotype with PBR expression, nuclear localization, and PBR-mediated cell proliferation and nuclear transport of cholesterol. *Cancer Res* 1999; 59:831-842.
30. Maaser K, Höpfner M, Jansen A et al. Specific ligands of the peripheral benzodiazepine receptor induce apoptosis and cell cycle arrest in human colorectal cancer cells. *Br J Cancer* 2001;85:1771-1780.
31. Sutter AP, Maaser K, Hopfner M et al. Specific ligands of the peripheral benzodiazepine receptor induce apoptosis and cell cycle arrest in human esophageal cancer cells. *Int J Cancer*. 2002;102:318-327.

32. Camins A, Diez-Fernandez C, Pujadas E, Camarasa J, Escubedo E. A new aspect of the antiproliferative action of peripheral-type benzodiazepine receptor ligands. *Eur J Pharmacol* 1995;272:289-292.
33. Decaudin D, Castedo M, Nemati F et al. Peripheral benzodiazepine receptor ligands reverse apoptosis resistance of cancer cells in vitro and in vivo. *Cancer Res* 2002;62:1388-1393.
34. Hardwick M, Rone J, Han J, Haddad B, Papadopoulos V. Peripheral-type benzodiazepine receptor levels correlate with the ability of human breast cancer MDA-MB-231 cell line ability to grow in SCID mice. *Int J Cancer* 2001;94:322-327.
35. Hardwick M, Rone J, Barlow K, Haddad B, Papadopoulos V. Peripheral-type benzodiazepine receptor (PBR) gene amplification in MDA-231 aggressive breast cancer cells. *Cancer Genet Cytogen* 2002; in press.
36. Li W, Pretner E, Shen L, Drieu K, Papadopoulos V. Common gene targets of Ginkgo biloba extract (EGb 761) in human tumor cells :relation to cell growth. *Cell Mol Biol (Noisy-le-grand)*. 2002;48:655-662.
37. Garnier M, Boujrad N, Oke BO et al. Diazepam binding inhibitor is a paracrine/autocrine regulator of Leydig cell proliferation and steroidogenesis. Action via peripheral-type benzodiazepine receptor and independent mechanisms. *Endocrinology* 1993;132:444-458.

- 38 Bradford MM. A rapid and sensitive method for the quantification of microgram quantities of protein using the principle of protein-dye binding. *Anal Biochem* 1976;72: 248-254.
39. Papadopoulos V, Kapsis A, Li H et al. Drug-induced inhibition of the peripheral-type benzodiazepine receptor expression and cell proliferation in human breast cancer cells. *Anticancer Res* 2000;20:2835-2848.
- 40 Sommers CL, Walker-Jones D, Heckford SE et al. Vimentin rather than keratin expression in some hormone-independent breast cancer cell lines and in oncogene transformed mammary epithelial cells. *Cancer Res* 1989;49:4258-4263.
- 41 Thompson EW, Paik S, Brunner N et al. Association of increased basement membrane invasiveness with absence of estrogen receptor and expression of vimentin in human breast cancer cell lines. *J Cell Physiol* 1992;150:534-544.
- 42 Beinlich A, Strohmeier R, Kaufmann M, Kuhl H. Specific binding of benzodiazepines to human breast cancer cell lines. *Life Sci* 1999;65:2099-2108.
- 43 Hammond SM, Caudy AA, Hannon GJ. Post-transcriptional gene silencing by double-stranded RNA. *Nat Rev Genet.* 2001;2:110-119.
- 44 Sharp PA. RNA interference - 2001. *Genes Dev.* 2001;15:485-490.
- 45 Elbashir SM, Lendeckel W, Tuschl T. RNA interference is mediated by 21- and 22-nucleotide RNAs. *Genes Dev* 2001;15:188-200.
- 46 Elbashir SM, Harborth J, Lendeckel W, Yalcin A, Weber K, Tuschl T. Duplexes of 21-nucleotide RNAs mediate RNA interference in cultured mammalian cells. *Nature* 2001;411:494-498.

- 47 Elbashir SM, Martinez J, Patkaniowska A, Lendeckel W, Tuschl T. Functional anatomy of siRNAs for mediating efficient RNAi in *Drosophila melanogaster* embryo lysate. *EMBO J* 2001;20:6877-6888.
- 48 Zhang H, Hannon GJ, Beach D. p21-containing cyclin kinases exist in both active and inactive states. *Genes Dev* 1994;15:1750-1758.
- 49 Dulic V, Stein GH, Far DF, Reed SI. Nuclear accumulation of p21Cip1 at the onset of mitosis: a role at the G2/M-phase transition. *Mol Cell Biol* 1998;18:546-557.
- 50 el-Deiry WS, Tokino T, Velculescu VE et al. WAF1, a potential mediator of p53 tumor suppression. *Cell* 1993;75:817-825.
- 51 Sheikh MS, Rochefort H, Garcia M. Overexpression of p21WAF1/CIP1 induces growth arrest, giant cell formation and apoptosis in human breast carcinoma cell lines. *Oncogene* 1995;11:1899-1905.
- 52 Strasser A. Dr. Josef Steiner Cancer Research Prize Lecture: the role of physiological cell death in neoplastic transformation and in anti-cancer therapy. *Int J Cancer* 1999;81:505-511.
- 53 Gómez-Navarro J, Arafat W, Xiang J. Gene therapy for carcinoma of the breast: Pro-apoptotic gene therapy. *Breast Cancer Res* 1999;2:32-44. [Complete electronic version is online at: <http://breast-cancer-research.com/content/2/1/032>]
- 54 Yang F, Wang W. Effects of overexpression of p21WAF1/CIP1 on the malignant phenotype and apoptosis of human hepatocellular carcinoma cells. *Zhonghua Zhong Liu Za Zhi* 1999;21:99-101. [Article in Chinese]

- 55 Kokunai T, Izawa I, Tamaki N. Overexpression of p21WAF1/CIP1 induces cell differentiation and growth inhibition in a human glioma cell line. *Int J Cancer* 1998;75:643-648.
- 56 Tavassoli M, Soltaninia J, Rudnicka J, Mashanyare D, Johnson N, Gaken J. Tamoxifen inhibits the growth of head and neck cancer cells and sensitizes these cells to cisplatin induced-apoptosis: role of TGF-beta. *Carcinogenesis* 2002;23:1569-1575.
- 57 Rohlff C, Blagosklonny MV, Kyle E et al. Prostate cancer cell growth inhibition by tamoxifen is associated with inhibition of protein kinase C and induction of 21(waf1/cip1). *Prostate* 1998;37:51-59.
- 58 Ganansia-Leymarie V, Bischoff P, Bergerat JP, Holl V. Signal transduction pathways of taxanes-induced apoptosis. *Curr Med Chem Anti-Canc Agents* 2003;3:291-306.
- 59 Yang HL, Pan JX, Sun L, Yeung SC. p21 Waf-1 (Cip-1) enhances apoptosis induced by manumycin and paclitaxel in anaplastic thyroid cancer cells. *J Clin Endocrinol Metab* 2003;88:763-772.
- 60 Liu W, Zhang R. Upregulation of p21WAF1/CIP1 in human breast cancer cell lines MCF-7 and MDA-MB-468 undergoing apoptosis induced by natural product anticancer drugs 10-hydroxycamptothecin and camptothecin through p53-dependent and independent pathways. *Int J Oncol* 1998;12:793-804.

- 61 Gorospe M, Shack S, Guyton KZ, Samid D, Holbrook NJ. Up-regulation and functional role of p21Waf1/Cip1 during growth arrest of human breast carcinoma MCF-7 cells by phenylacetate. *Cell Growth Differ* 1996;7:1609-1615.
- 62 McCaffrey AP, Meuse L, Pham TT, Conklin DS, Hannon GJ, Kay MA. RNA interference in adult mice. *Nature*. 2002;418:38-39.
- 63 Ferrigno P, Silver PA. Regulated nuclear localization of stress-responsive factors: how the nuclear trafficking of protein kinases and transcription factors contributes to cell survival. *Oncogene* 1999;18:6129-6134.
- 64 Alessi DR, Downes CP. The role of PI-3- kinase in insulin action. *Biochim Biophys Acta* 1998;436:151-164.
- 65 Anderson NG, Maller JL, Tonks NK, Sturgill TW. Requirement for integration of signals from two distinct phosphorylation pathways for activation of MAP kinase. *Nature*. 1990;343:651-653.
- 66 Clark EA, Hynes RO. Ras activation is necessary for integrin-mediated activation of extracellular signal-regulated kinase 2 and cytosolic phospholipase A2 but not for cytoskeletal organization. *J Biol Chem* 1996;271:14814-14818.
- 67 Sivaraman VS, Wang H, Nuovo GJ, Malbon CC. Hyperexpression of mitogen-activated protein kinase in human breast cancer. *J Clin Invest*. 1997;99:1478-1483.
- 68 Das D, Pintucci G, Stern A. MAPK-dependent expression of p21(WAF) and p27(kip1) in PMA-induced differentiation of HL60 cells. *FEBS Lett* 2000;472:50-52.

- 69 Sanger N, Strohmeier R, Kaufmann M, Kuhl H. Cell cycle-related expression and ligand binding of peripheral benzodiazepine receptor in human breast cancer cell lines. *Eur J Cancer* 2000;36:2157-2163.
- 70 Carmel I, Fares FA, Leschiner S, Scherubl H, Weisinger G, Gavish M. Peripheral-type benzodiazepine receptors in the regulation of proliferation of MCF-7 human breast carcinoma cell line. *Biochem Pharmacol* 1999;58:273-278.
- 71 Lee NS, Dohjima T, Bauer G et al. Expression of small interfering RNAs targeted against HIV-1 rev transcripts in human cells. *Nat Biotechnol* 2002;20:500-505.
- 72 Novina CD, Murray MF, Dykxhoorn DM et al. siRNA-directed inhibition of HIV-1 infection. *Nat Med* 2002;8:681-686.

Table 1. PBR Ligand Binding Characteristics of MCF-7 Tet-Off, MOM, and MIP Cells.

Scatchard analyses of 40 µg of cell protein from MCF-7 Tet-Off, MOM, MIP1 and MIP2 cells were performed as described in *Materials and Methods*. Scatchard analyses were also performed on MIP1 and MIP2 cells grown in the presence of 1.0 µg/ml Dox for 3 or more days.

Cell Line	Kd, nM	Bmax, pmol/mg protein
MCF-7 Tet-Off	1.2 ± 0.23	0.8 ± 0.92
MOM	0.7 ± 0.16	0.5 ± 0.03
MIP1 - Dox	1.2 ± 0.20	4.9 ± 0.23
MIP1 + Dox	0.9 ± 0.21	0.6 ± 0.04
MIP2 - Dox	1.3 ± 0.06	2.1 ± 0.03
MIP2 + Dox	1.2 ± 0.01	0.8 ± 0.03

Figure Legends

Figure 1. Repression of EGFP Fluorescence by Increasing Doxycyclin Concentrations in MIP1 and MIP2 Cells. (A) MIP1 and MIP2 cells were seeded at a density of 5,000 cells/well on a 96-well plate and grown for 4 days in medium containing 0.0, 0.0001, 0.1, or 1.0 $\mu\text{g/ml}$ Dox. After 4 days, cells were washed in PBS and fluorescence was determined at 485 nm excitation, 510 nm emission. Data points represent the means \pm SEM of three independent experiments carried out in quadruplicate. (B) MIP1 cells were layered on poly-D-lysine coated slides and grown under the same conditions as in (A). After 4 days, cells were fixed in 10% formaldehyde. The slides were then rinsed in distilled H_2O before mounting with Crystal/Mount. Phase-contrast images are beneath their corresponding fluorescent images. Each photograph was taken at 10x magnification. The higher background seen in the fluorescent images exposed to 0.01 and 1.0 $\mu\text{g/ml}$ Dox was due to the low intensity of the signal. (C) Vimentin Immunocytochemistry in MCF-7 Tet-Off, MIP1, and MIP2 Cell Lines. 20,000 cells per well for each cell line (5,000 cells per well for MDA-231 cells) were loaded onto poly-D-lysine coated 8-well slides and incubated for 2 days at 37°C, 6% CO_2 . Cells were fixed in 10% formaldehyde for 10 minutes at room temperature. After washing thoroughly with distilled H_2O , vimentin immunostaining was carried out as described in *Materials and Methods*. Each phase-contrast image was taken at 10x magnification. (D) Cell Proliferation Curves for MCF-7 Tet-Off, MIP1, and MIP2 Cells. Six-day growth curves were obtained for MCF-7 Tet-Off, MIP1, and MIP2 cell lines in the presence or absence of 1.0 $\mu\text{g/ml}$ Dox. Cells were incubated at 37°C, 6% CO_2 . Media with or without Dox were changed every 2 days.

Cells were stained with Crystal Violet. The experiment was performed three times with eight replications for each cell line.

Figure 2. siRNAs Targeting PBR Decrease PBR mRNA and Proliferation in MDA-231

Breast Cancer Cells. (A) MDA-231 cells were either mock-transfected or transfected with siRNAs targeting different coding regions of PBR or scrambled siRNA, and analyzed 72 hours later for PBR mRNA expression by Q-PCR. Results shown are means \pm SEM from three independent experiments ($n = 9$). (B) Silencing Expression of PBR Inhibits MDA-231 Cell Proliferation. After treatment with PBR-siRNAs for 72 hours, the amount of BrdU incorporation was determined as described in *Materials and Methods*. Results shown are means \pm SEM from three independent experiments ($n = 9$).

Figure 3. siRNAs Targeting PBR Decrease PBR Radioligand Binding in MDA-231

Breast Cancer Cells. MDA-231 cells were either mock-transfected or transfected with 100 nM siRNAs targeting different PBR coding regions or scrambled siRNA. Cells were analyzed 72 hours later for PBR expression using a [3 H]PK11195 ligand binding assay. Results shown are means \pm SEM from two independent experiments ($n = 6$). MDA-231 cells were either mock-transfected or transfected with the indicated concentrations of siRNAs targeting different PBR coding regions or scrambled siRNA. Cells were analyzed 72 hours later for the expression of the indicated proteins by immunoblot analysis as described in *Materials and Methods*.

Figure 4. Effect of PBR-siRNA Treatment on p21^{WAF1/CIP1} Expression. MDA-231 cells were either mock-transfected or transfected with siRNAs targeting different PBR coding regions or with scrambled siRNA, and analyzed 72 hours later by immunoblotting for changes in proteins involved in signal transduction pathways (p21^{WAF1/CIP1}, Akt1, Erk1). Equal loading was assessed using anti-GAPDH.

Fig. 1

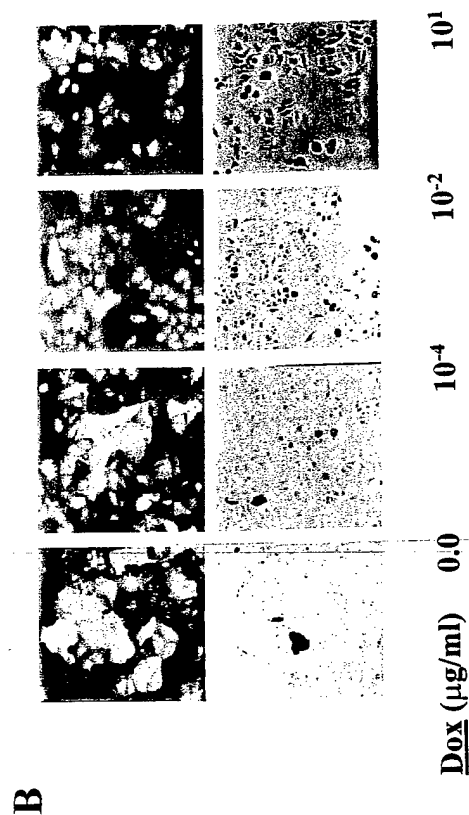
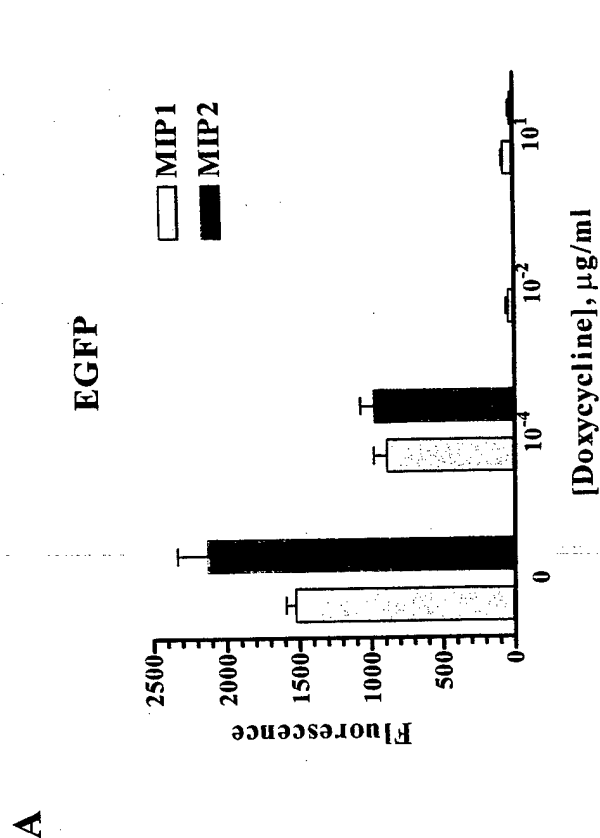
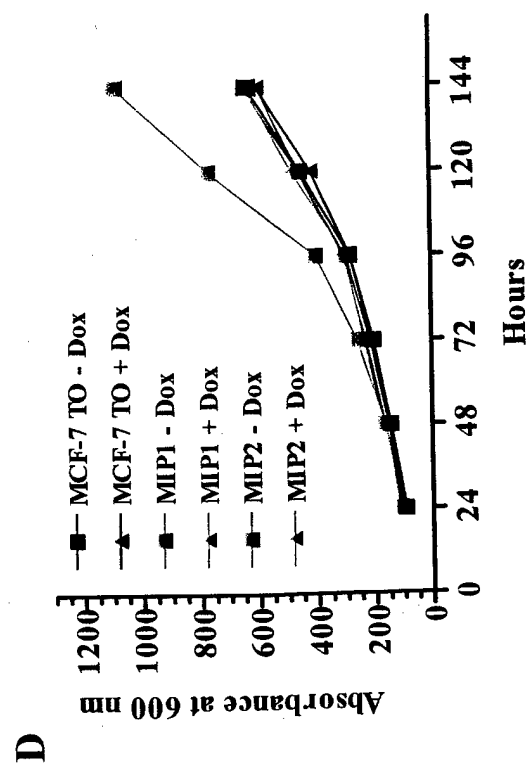
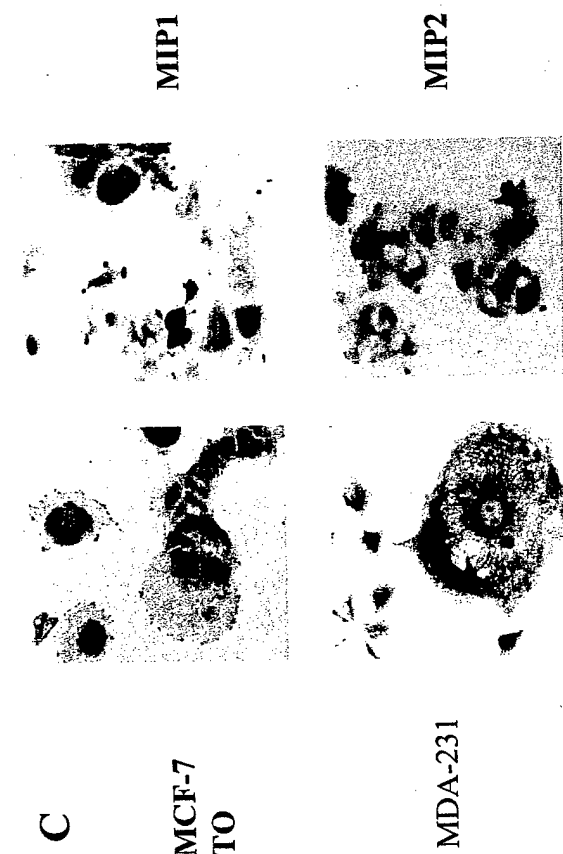


Fig. 2

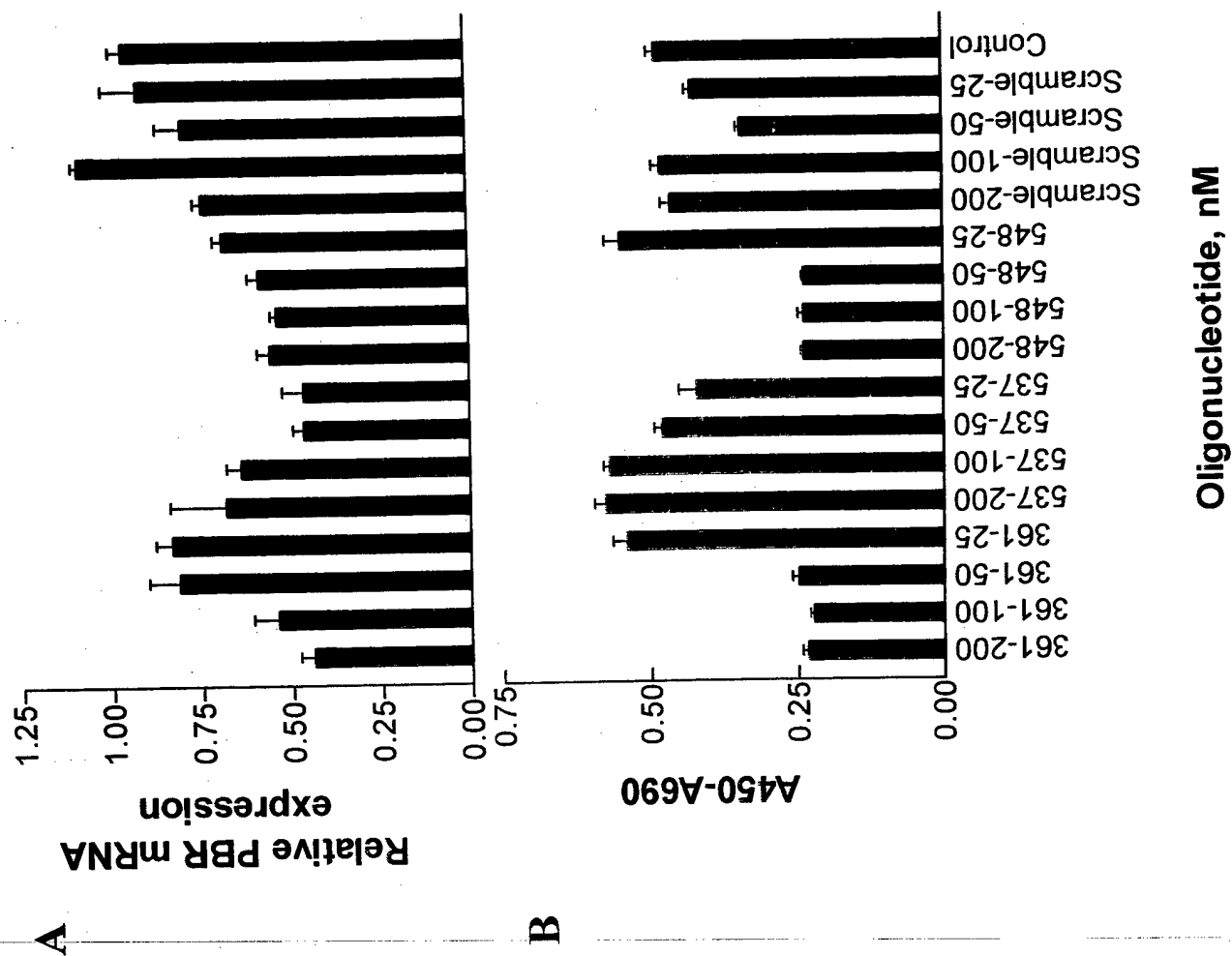


Fig. 3

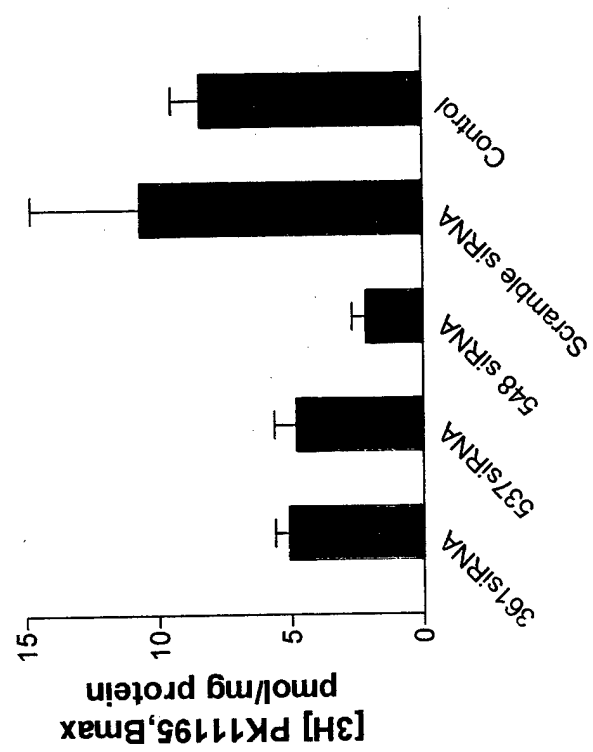
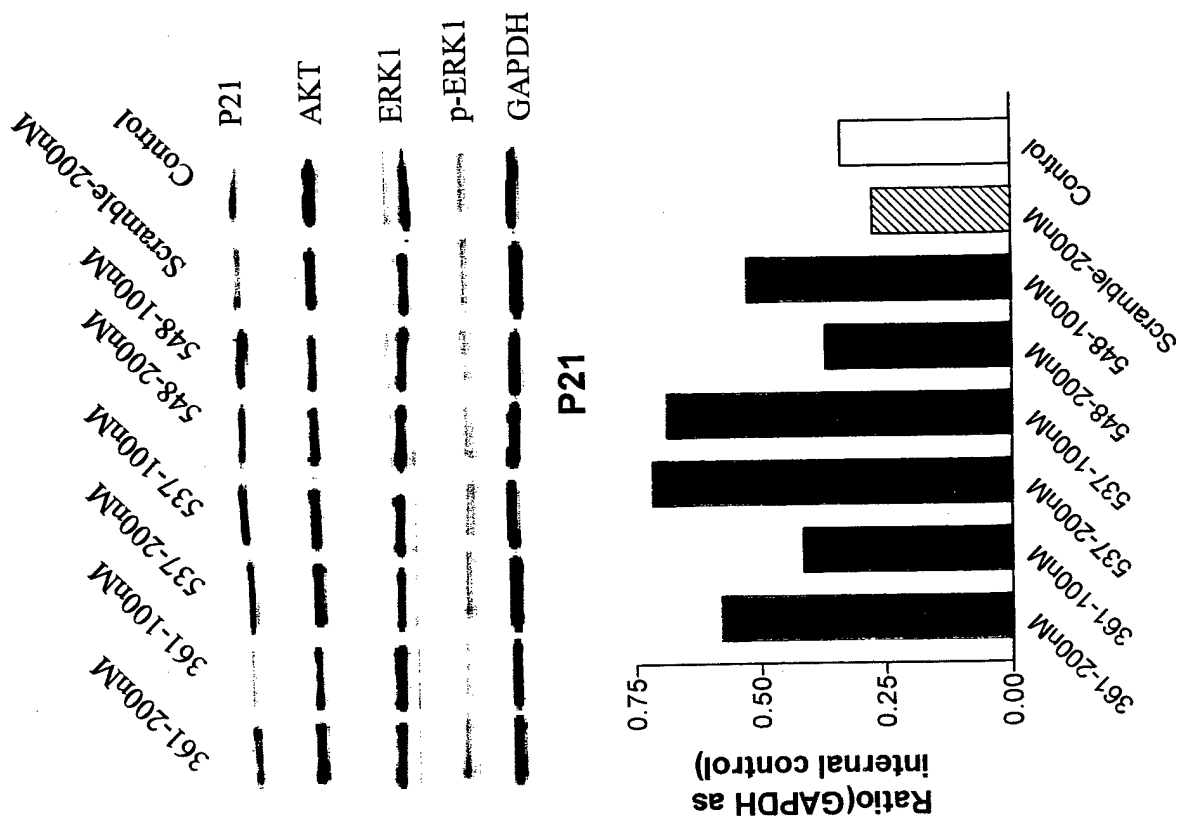


Fig. 4



**Peripheral-type benzodiazepine receptor (PBR) and PBR drug ligands
in fibroblast and fibrosarcoma cell proliferation: Role of ERK, c-jun
and ligand-activated PBR-independent pathways**

Dimitris Kletsas¹, Wenping Li², Zeqiu Han², Vassilios Papadopoulos^{2,3}

Laboratory of Cell Proliferation and Ageing, Institute of Biology, National Center of Scientific Research "Demokritos", Athens, Greece¹; Department of Biochemistry and Molecular Biology² and the Lombardi Comprehensive Cancer Center³, Georgetown University Medical Center, Washington, DC 20057, USA

Correspondence:

Dr. D. Kletsas

Laboratory of Cell Proliferation and Ageing, Institute of Biology, National Centre of Scientific Research "Demokritos", Athens, Greece

Tel: + 30 210 6503565

Fax: + 30 210 6511767

E-mail: dkletsas@bio.demokritos.gr

ABSTRACT

Peripheral-type benzodiazepine receptor (PBR) is a 18-kDa high-affinity drug and cholesterol binding protein, that has been implicated in several physiological processes, such as cholesterol transport and mitochondrial respiration. Specific PBR ligands regulate cell proliferation, although their action is controversial and probably cell-type specific. The aim of the present study was to examine the expression of PBR in cells of mesenchymal origin, i.e. human fibroblast and fibrosarcoma cells, as well as its role in the regulation of their proliferation. Both mesenchymal cell types express high levels of PBR, localized exclusively in mitochondria. The PBR-specific drug ligands, the isoquinoline carboxamide PK 11195 and the benzodiazepine Ro5-4864, at relative high concentrations (10^{-4} M), exert a strong inhibitory effect on cell proliferation by arresting the cells at the G0/G1 phase of the cell cycle, in a calcium-independent manner, while no apoptotic cell death was observed. In normal fibroblasts, this inhibition was correlated with a decrease in the activation of ERK and c-Jun. PBR knockdown by RNA inhibition did not affect the proliferation of either cell type and did not influence the inhibitory effect of PK 11195 and Ro5-4864 on cell growth. Our data suggest that in fibroblasts and fibrosarcoma cells PBR drug ligands inhibit cell proliferation in a PBR-independent manner. These results are in contrast to data reported on epithelial human breast cancer cells, suggesting that the origin of the cell type, epithelial or mesenchymal, is crucial in defining the role of PBR in cell proliferation.

Introduction

Benzodiazepines exert their anxiolytic, hypnotic and anticonvulsant action by binding to the central-type benzodiazepine receptor, located on the neuronal plasma membrane, where they interact with the GABA_A receptor [1]. A second receptor, with distinct pharmacological and molecular properties, is the peripheral-type benzodiazepine receptor (PBR) [2, 3]. PBR is a 18 kDa hydrophobic protein, primarily localized in the outer mitochondrial membrane, associated with the voltage-dependent anion channel and the adenine nucleotide transporter [2, 4]. PBR is abundantly expressed in steroid-synthesizing tissues, but it is also widely expressed throughout the body [2].

Although the exact function of PBR has not been defined, it seems to be involved in numerous physiological processes, such as steroid production [2, 5], mitochondrial respiration [6], immunomodulation [7], porphyrin transport and heme biosynthesis [8], apoptosis [9, 10], as well as cell proliferation [11]. It was recently demonstrated that a basic biological function of PBR is to bind cholesterol with nanomolar affinity [12-14], that could explain its role in mitochondrial cholesterol transport, the rate-determining step in steroidogenesis [15].

The role of PBR in cell proliferation was mainly investigated using PBR-specific high affinity drug ligands, such as the benzodiazepine Ro5-4864 and the isoquinoline carboxamide PK 11195 [16]. However, the data on the effect of these compounds on cell proliferation seems to be concentration-dependent and contradictory, ranging from stimulatory to inhibitory, probably reflecting the tissue-specificity of PBR function [17-23]. Moreover, it has been suggested that the effect of these drug ligands on cell

proliferation could be independent of their ability to bind to PBR [24]. Recently, using gene silencing approaches, we reported that the presence of PBR is required for human epithelial breast cancer cell proliferation [25]. Although the effect of PBR drug ligands, and par extension PBR, in the proliferation of several cancer cells has been extensively investigated, less attention had been devoted on stroma cells, such as fibroblasts. Accordingly, the aim of the present study was to examine in normal and cancer cells of mesenchymal origin, i.e. human fibroblasts and fibrosarcoma cells, the presence of PBR and its role in their proliferation.

Materials and Methods

Cells and Cell Culture Conditions. Normal human fibroblasts (HFFF2, ECACC, Salisbury, UK) and human fibrosarcoma cells (HT-1080, ATCC, Manassas, VA) were cultured on polystyrene culture dishes (Corning; Corning, NJ) in MEM (HFFF2) or DMEM (HT-1080) supplemented with 10% FCS, in an environment of 5% CO₂, at 37°C, and were subcultured once a week at 1:2 split ratio using a trypsin-EDTA solution. All media were from Sigma (St. Louis, MO). Normal fibroblasts were arrested quiescent as follows: they were grown until confluency and the medium was changed to MEM supplemented with 0.1% FCS. Two days later fresh medium was added, along with the compounds to be tested [26].

Laser Scanning Confocal Microscopy. Cells grown on glass coverslips, previously incubated for at least 2 hours with FCS to achieve better attachment, were washed twice with sterile phosphate buffered saline (PBS) and incubated for 1 hour with 2 µM of compound 4, a fluorescent high-affinity PBR ligand [27]. Subsequently, the cells were washed with PBS and incubated with MitoTracker Red (Molecular Probes, Eugene, OR) 1:5000 in PBS for 5 min. Then, the cells were washed in PBS and fixed with 4% formaldehyde in PBS and analyzed in a Olympus laser scanning confocal microscope, equipped with a Fluoview software, as previously described [54].

Immunoblot Analysis. For the collection of whole-cell lysates, cell monolayers were washed with Tris-buffered saline (TBS) and scraped immediately in hot SDS-PAGE sample buffer containing β -mercaptoethanol, as well as protease and phosphatase inhibitors (Sigma). Following sonication (10 sec) the samples were centrifuged and supernatants were stored at -80°C until further use. Samples were separated on a 4-20% acrylamide gels and the proteins were transferred onto nitrocellulose membranes. Membranes were blocked with 5% non-fat milk (or 1% BSA, in the case of phosphotyrosine antibodies) in TBS containing 0.1% Tween-20 (T-TBS) for 1 hour and subsequently incubated with the primary and HRP-conjugated secondary antibodies (diluted in the same blocking buffer), with a 3x10 min washing step in between. Immunoreactive bands were visualized on Kodak-X-OMAT AR films by chemiluminescence (ECL kit) according to the manufacturer's (Amersham, Staffordshire, UK) instructions.

DNA Synthesis Assay. Cells were plated on 96-well plates (Corning) at a cell density of 10,000 cells/well, in MEM supplemented with 10% FCS. 24 hours later the compounds to be tested were added at the indicated concentrations and after another 24-h incubation period DNA synthesis was measured by BrdU incorporation by using the BrdU ELISA kit (Boehringer Mannheim; Indianapolis, IN). Incorporation of BrdU was measured at 450 nm (reference at 690 nm) using the Victor 1420 Multilabel Counter (Perkin Elmer Life Sciences, Boston, MA). Alternatively, DNA synthesis was measured in cells arrested quiescent in serum-deprived confluent cultures, as mentioned above.

Cell Cycle Analysis. Cell cycle distribution was estimated by flow cytometry. Cultures were treated with and without 10^{-4} M PK 11195 and Ro5-4864 for 24 hours. Cells were collected by trypsinization, washed in ice-cold PBS, fixed in 50% ethanol and stained with a solution containing propidium iodide (50 μ g/ml) and RNase (10 μ g/ml). Flow cytometric analysis was performed in a FACS Scan flow cytometer (Becton Dickinson, Menlo Park, CA) equipped with a Modfit software program at the Lombardi Cancer Center, Georgetown University flow cytometry facility.

RNA Analysis. PBR mRNA analysis was estimated with quantitative real-time-PCR (Q-PCR) as follows. Total cellular RNA was isolated by using the Quiagen Rneasy Mini kit (Quiagen, Valencia, CA). For reverse transcription of 18S amplicon, 0.4 μ g total RNA was incubated in 1x TaqMan RT buffer, 5.5mM MgCl₂, 500 μ M dNTP, 2.5 μ M random hexamers, 3.125U/ μ l MultiScribe™ reverse transcriptase, 0.4U/ μ l RNase inhibitor, in a total volume of 20 μ l. The reaction mixture was sequentially incubated at 25°C for 10min, 37°C for 60 min, and 95°C for 5 min. For reverse transcription of the target genes, 0.4 μ g total RNA was incubated in a total volume of 20 μ l 1x TaqMan RT buffer, 5.5mM MgCl₂, 500 μ M dNTP, 2.5 μ M oligo d(T)16 , 1.25U/ μ l MultiScribe™ reverse transcriptase, and 0.4U/ μ l RNase inhibitor. Incubation was performed successively at 25°C for 10min, 48°C for 30 min, and 95°C for 5 min. The resulting cDNAs were then processed for amplification of the genes of interest using specific primer sets designed according to Primer Express guidelines. For target genes and endogenous reference, the forward/reverse primers' final concentrations were 250nM. 2 μ l cDNA was used as a template. Each sample was run in triplicates. The reaction was incubated in the ABI

PRISM 7700 Sequence Detector (Applied Biosystems, Foster City, CA) at 50°C for 2min, 95°C for 10min, and 95°C (15sec) / 60°C (1min) for 40 cycles, successively. Direct detection of the PCR products was achieved by measuring the increase in fluorescence caused by the binding of SYBR® Green I Dye to double-stranded (ds) DNA. The Comparative C Method was used to analyze the data. The amount of target genes was normalized to the endogenous reference (18S rRNA). Target genes and endogenous reference genes were run separately.

siRNA Preparation. 21-nucleotide RNAs were chemically synthesized by Dharmacon Research (Lafayette, Colorado) using 2'-ACE protection chemistry. The siRNA strands were deprotected according to manufacturer's instructions, mixed in equimolar ratios and annealed by 60°C 45 min, ambient temperature 30 min. The accession number for human PBR is gi 21536444. siRNAs with the following sense and antisense sequences were used:

PBR	361siRNA	targeting	human	PBR	exon	3,5'-
AACTGGGCATGGCCCCCATCCCTGTCTC-3'(sense),5'-						
AAGATGGGGGGCCATGCCAGCCTGTCTC-3'(antisense);						
PBR	537siRNA	targeting	human	PBR	exon	4,5'-AACTACTGCGTATGGCGGGACCCTGTCTC-
3'(sense), 5'-AAGTCCCGCCATACGCAGTAGCCTGTCTC-3'(antisense);PBR						
PBR	548siRNA	targeting	human	PBR	exon	4, 5'-
AACCATGGCTGGCATGGGGGACCTGTCTC-3'(sense), 5'-						
AATCCCCCATGCCAGCCATGGCCTGTCTC-3'(antisense); scrambled siRNA, 5'-						
AAGGCTACTATGCGGCGACTGCCTGTCTC-3'(sense), 5'-						

AACAGTCGCCGCATAGTAGCCCCTGTCTC-3'(antisense). PBR 361,537,548

siRNAs corresponded to the PBR coding regions, scramble siRNA was used as control.

Transfection of Cells with PBR siRNA Duplexes. Single transfections of siRNA

duplexes were performed using OLIGOFECTAMINE Reagent (Invitrogen/Life Technologies) and assayed for silencing 3 days after transfection. The cells were seeded the previous day using DMEM tissue culture medium supplemented with 10% FBS without antibiotics. siRNA duplex with Opti-MEM (Invitrogen/Life Technologies) solutions were mixed, incubated for 20 minutes at room temperature and the siRNA-Oligofectamine mixture was then added to the cells grown at 30 to 50% confluency. 24 hours later, fresh medium supplemented with 30% FBS was added to transfected cells to get final FBS concentration of 10%.

Radioligand Binding Assays. Cells were scrapped from 150-mm culture dishes into 5 ml PBS, dispersed by trituration and centrifuged at 500xg for 15 min. Cell pellets were resuspended in PBS and assayed for protein concentration by the Bradford method, using the Bio-Rad Protein Assay kit (Bio-Rad Laboratories, Hercules, CA) with bovine serum albumin as a standard. [³H]PK 11195 binding studies on 50 µg of protein from cell lysates were performed as previously described [28]. Scatchard plots were analyzed by the Ligand program [28].

Results

PBR expression and subcellular localization. PBR expression in normal human fibroblasts and fibrosarcoma cells was first examined at the mRNA level by Q-PCR. As can be seen in Fig. 1, young cycling human fibroblasts contain PBR mRNA at a near equal amount compared to that of the human breast cancer MDA-MB-231 cell line, known to express high PBR mRNA levels among non-steroidogenic cells [17]. Furthermore, arrested fibroblasts express comparable mRNA levels. Although it has been previously shown that an aggressive epithelial cancer cell phenotype is correlated with an increased expression of PBR [17], HT-1080 fibrosarcoma cells produce significantly reduced PBR mRNA levels, in comparison to normal fibroblasts. Subsequently, we have investigated the subcellular localization of PBR in these cell lines by confocal laser microscopy. In order to avoid problems associated with antibody specificity and sensitivity, we have used compound 4, a high affinity fluorescent PBR drug ligand [27]. As can be seen in Fig. 2, PBR appears to be localized to the cytoplasmic/perinuclear region, in both normal and fibrosarcoma cells. No nuclear staining was found in either cell line. Interestingly, an identical pattern can be seen by the use of the specific mitochondrial probe MitoTracker. Superposition of these images resulted in a yellow color, indicating the co-localization of mitochondria and PBR in these cells.

PBR ligands inhibit the proliferation of human fibroblasts and fibrosarcoma cells.

The effect of PBR ligands PK 11195 and Ro5-4864 on the proliferation of normal human fibroblasts and fibrosarcoma cells was examined by using bromodeoxyuridine

incorporation into newly synthesized DNA. As opposite results have been published by several investigators depending on the dose used, we have tested a wide range of concentrations, ranging from 10^{-4} M to 10^{-11} M. Fig. 3 shows that concentrations ranging from 10^{-5} M to 10^{-11} M of PK 11195 and Ro5-4864 exerted no significant alteration in cell proliferation of either normal (HFFF2; Fig. 3A) or cancer (HT-1080; Fig. 3B) cells. However, at the concentration of 10^{-4} M a strong inhibition of BrdU incorporation was observed in both cell types, with the effect provoked by PK 11195 being more intense than that induced by Ro5-4864. This action of PBR ligands can be considered cytostatic, because no signs of cytotoxicity were observed. This was further reinforced by experiments performed in quiescent normal fibroblasts, where the PBR-ligand-mediated inhibition is only modest at the same concentration used (Fig. 3C). The effect of PBR drug ligands, tested at 10^{-4} M concentration, on cell cycle was further assessed by flow cytometry. As can be seen in Table 1, both PK 11195 and Ro5-4864 provoke a significant accumulation of HFFF2 cells in the G0/G1 phase of the cell cycle, with a concomitant reduction in the proportion of cells being in the S and the G2/M phases. On the other hand, in HT-1080 cells also PK 11195 and Ro5-4864 induce an increase in the percentage of cells being in the G0/G1 phase and a reduction of those in the S phase, however no significant alterations in the G2/M phase has been observed. Interestingly, no sub-G1 peak was observed in any case, indicating that the inhibition in DNA synthesis is not due to apoptotic cell death. Finally, we have tested another three benzodiazepines, i.e. clonazepam and flurinazepam that bind preferentially to central-type benzodiazepine receptors and diazepam that can bind with a mixed affinity to both peripheral- and central-type receptors. Clonazepam and flurinazepam had no effect on the proliferation of

both normal and cancer cells, while diazepam provoked a significant inhibitory effect (Fig. 4), suggesting the involvement of PBR in the regulation of the proliferation of fibroblasts and fibrosarcoma cells.

The ability of PK 11195 to inhibit strongly cell proliferation was further tested at the level of cell cycle-markers expression. As can be seen in Fig. 5, in normal human fibroblasts after a 24-hour incubation with 10^{-4} M PK 11195 we observed a significant reduction of the activated (phosphorylated) forms of ERK (member of the MAPK family) and c-Jun (one of the components of the AP-1 transcription factor), both being involved in the regulation of proliferation. On the other hand, the levels of cyclin-dependent kinase inhibitor p21^{WAF1} were found to be unaffected. Interestingly, the changes in the activation of pERK and p-c-Jun were not observed in fibrosarcoma cells (data not shown), implying the presence of an alternative regulation of proliferation in these cells.

Effect of PBR RNAi on PBR expression. To further access the involvement of PBR on the proliferation of human fibroblasts and fibrosarcoma cells, we inhibited the expression of this protein by dsRNAs. To this end, three 21-nucleotide RNAs were constructed (see Materials and Methods) and their effect on the expression of PBR mRNA has been tested. As can be seen in Fig. 6A, all three siRNAs significantly inhibited the production of PBR mRNA in both cell types, as shown by Q-PCR. The PBR 548siRNA was found to be the more potent, as it decreased the mRNA expression by more than 90% and consequently it was used in all subsequent functional experiments. A scrambled siRNA had no effect on PBR mRNA expression. Beyond the reduction of PBR mRNA, we further tested the effect of PBR 548 siRNA on PK 11195 binding. Ligand binding studies followed by

Scatchard analysis in HT-1080 cells has shown that treatment with PBR 548 siRNA inhibited by 80% the PK 11195 binding (B_{max}) to PBR, compared to control and scrambled siRNA (Fig. 6B). Interestingly, treatment with the 548 siRNA oligo increased the affinity of the receptor (Control, $K_d = 13.9$ nM; scrambled siRNA, $K_d = 9.3$ nM, and 548 siRNA, $K_d = 3.1$ nM). Similar results were observed in HFFF2 cells (data not shown).

PBR does not mediate the inhibitory effect of PBR drug ligands on cell proliferation.

Subsequently, we investigated the effect of PBR silencing on the inhibition of DNA synthesis induced by benzodiazepines. HFFF2 cells were transfected with the 548 siRNA (or a scrambled siRNA) and two days later cells were treated with 10^{-4} M PK 11195. As can be seen in Fig. 6C, both dsRNAs had a negligible effect on DNA synthesis. On the other hand, PK 11195 significantly decreased DNA synthesis (as shown above). Surprisingly, PK 11195 decreased at the same extent the 548- and scrambled-siRNA-treated cells. The same effect was also observed in HT-1080 cells, although in these cells both dsRNAs when added alone had also a significant inhibitory effect (Fig. 6D). Similar results have been obtained with Ro5-4864 (data not shown). These data suggested that the effect of specific PBR drug ligands on cell proliferation could be independent from their interaction with the 18 kDa PBR protein.

We further tested this hypothesis by direct cell counting. To this end, transfected human fibroblasts and fibrosarcoma cells were allowed to proliferate and we measured the increase in cell numbers between days 2 and 6 after transfection. As can be seen in

Fig. 7, transfected HFFF2 and HT-1080 cells proliferate at the same ratio as untransfected cells, suggesting that PBR may be unrelated with the regulation of their proliferation.

It has been previously proposed that the antiproliferative effect of peripheral-type benzodiazepine ligands on cell proliferation could be reversed by high calcium chloride concentrations. Accordingly, we have studied the effect of PK 11195 and Ro5-4864 on DNA synthesis in the presence of $5 \times 10^{-3} \text{M}$ CaCl_2 . As can be seen in Fig. 8, in human fibroblasts and fibrosarcoma cells the presence of calcium was unable to revert the inhibition provoked by PBR ligands, indicating the presence of an alternative regulatory mechanism.

DISCUSSION

The role of PBR and its specific drug ligands on several highly differentiated and cancer cells has been extensively studied. However, much less attention has been devoted to the stromal cells. Considering the crucial role of these cells in tissue homeostasis, as well as tumor development and the role of PBR in cell proliferation we investigated the presence and function of PBR and PBR drug ligands in the regulation of the proliferation of cells of mesenchymal origin and, in particular, human fibroblast and fibrosarcoma cells.

PBR expression has been shown to be up-regulated in intensely proliferating cells [17, 30, 31]. However, we have found that normal human fibroblasts contain near equal levels of PBR mRNA with the highly aggressive breast cancer cell line MDA-MB-231, a cell line of epithelial origin known to express increased PBR levels. PBR expression in fibroblasts was found to be unrelated to their proliferative status, as cycling and arrested cells produce similar amounts of PBR mRNA. Even more, the highly-proliferative fibrosarcoma cell line express slightly lower mRNA levels from normal fibroblasts. This seems unexpected in the light of previous data showing that intensely proliferating and aggressive cancer cell lines overexpress PBR [31, 31, 17]. However, we have recently shown that while in breast, colon-rectum and prostate tissues elevated PBR expression is associated with tumor progression, malignant skin tumors express lower PBR levels than normal skin [32]. These data, being in accordance to those presented herein, indicate that the relation between enhanced PBR levels and increased proliferation is tissue-specific.

Initial studies from the 80's involved PBR in the regulation of cellular proliferation. This issue was mainly addressed using specific PBR ligands, such as the isoquinoline carboxamide PK 11195 and the benzodiazepine Ro5-4864. The majority of the reported data point to a strong inhibitory effect of these compounds for several cell types, such as rat glioma and human neuroblastoma and astrocytoma cells [33, 21], Chinese hamster lung cells [34], mouse thymoma cells [35], mouse melanoma cells [20], mouse fibroblasts [36], as well as in breast, colon and esophageal cancer cell lines [17, 19, 22, 23]. In the majority of these cases, this inhibition was dose-dependent, at relatively high (micromolar) concentrations. On the other hand, a slight but still significant stimulatory effect of nanomolar concentrations of PK 11195, close to the affinity of the receptor for this compounds, was reported in Swiss 3T3 cells, and human breast cancer and glioblastoma cell lines [17, 18, 37]. Interestingly, in human breast cancer cells this effect was associated with high levels of PBR expression and nuclear/perinuclear localization. In particular, PK 11195 was found to stimulate the proliferation of human breast cancer cells MDA-MB-231 and the glioblastoma cell line MGM-1. Both cell lines are characterized by high levels of PBR expression localized around and in the cell nucleus. On the other hand, in two separate tumor cell lines (MCF-7 and MGM-3), where PBR was found to located in mitochondria, PK 11195 had no stimulatory effect. Even more, higher concentrations of this PBR ligand (10^{-4} M) inhibited MCF-7 proliferation [17, 18]. The data presented herein indicate that both PK 11195 and Ro5-4864 at high concentrations, i.e. 10^{-4} M, induce a strong inhibitory effect on human fibroblast and fibrosarcoma cells. Interestingly, confocal laser microscopy has revealed that in both normal fibroblasts and fibrosarcoma cells PBR is localized exclusively in the

cytoplasmic/perinuclear region, in a matching distribution with that of mitochondria, while no nuclear staining was found in either cell line. Furthermore, the effect of PBR ligands seems to be specific, as the central-type benzodiazepine receptor ligands clonazepam and flurazepam were unable to affect fibroblast or fibrosarcoma cell proliferation, while diazepam that can bind both peripheral- and central-type benzodiazepine receptors exerts a significant inhibitory effect. Moreover, although PK 11195 and Ro5-4864 were found to induce or to facilitate apoptosis in several cell lines [6, 22, 23, 37, 38], no signs of cell death were found either microscopically or by FACS analysis, indicating that their effect on DNA synthesis is cytostatic rather than cytotoxic. This is further substantiated by the more modest inhibitory effect exerted on serum-starved fibroblasts. Having in mind that in contrast to intensely proliferating cancer cells, normal stromal cells are arrested within the tissue, the differential inhibitory effect of PBR drug ligands on fibrosarcoma cells and on arrested fibroblasts could suggest a possible usefulness of these compounds in growth inhibitory treatment regimes.

It is important to note that the mechanism underlying this inhibitory action of PK 11195 and Ro5-4864 is not unique for all cell types tested. It has been reported that their inhibitory effect is accompanied by an arrest in G2/M [20, 34], in G0/G1 [22, 23] or in both [19]. Moreover, we report herein that the mechanism of cell cycle arrest in normal and tumor mesenchymal cell lines seems to be different. In normal human fibroblasts we observed an increase of the percentage of cells being in G0/G1, followed by a decrement of those being in the S and G2/M phases. In contrast, in fibrosarcoma cells the enlargement of G0/G1 is the result of the reduction of S phase, while the G2/M remains practically unaltered.

In addition, we have also studied for the first time the effect of PK 11195 on the expression and activation of central cell-cycle regulators. Mitogen-activated protein kinase (MAPK) pathways represent a key link between the transmembrane receptors of serum growth factors and changes in gene expression. In mammalian cells, three MAPK cascades have been identified: the extracellular signal-regulated kinase (ERK) cascade, the stress-activated protein kinase/c-jun-N-terminal kinase (SAPK/JNK) cascade and the p38MAPK cascade [39]. All these target an overlapping set of immediate early genes, most important being the c-fos and c-jun proto-oncogenes, whose protein products form the AP-1 transcriptional complex, a mediator of the regulation of cell proliferation [40, 41]. In particular, activated (phosphorylated) ERK activates Elk-1, the major component of the ternary complex factor (TCF) that binds to the serum response element (SRE) on c-fos promoter, thus regulating its transcription. In addition, ERK can contribute in the phosphorylation of the c-Fos protein. On the other hand, JNK and p38 can induce c-jun transcription and even more JNK can phosphorylate the c-Jun protein, an important determinant of dimeric AP-1 activation and function [39, 42, 43, 44, 45]. Accordingly, we have tested the effect of PK 11195 on the activation of these pivotal signaling molecules, e.g. p-ERK (phosphorylated ERK) and p-c-Jun (phosphorylated c-Jun). In normal human fibroblasts, both p-ERK and p-c-Jun were found to be drastically down-regulated, in accordance to the inhibitory action of PK 11195 on the serum-dependent proliferation of these cells. Interestingly, in fibrosarcoma cells none of the above changes was observed, indicating once again the different mechanisms underlying the inhibitory effect of these PBR ligands in these two cell types. Further downstream, we have also studied the regulation of p21^{WAF1}, that inhibits the cyclin-dependent kinases (Cdks),

whose action is necessary to drive the cell cycle [46]. In human fibroblasts, PK 11195 has no significant effect on p21^{WAF1} levels, indicating that it exerts its function on cell cycle upstream, most probably at the level of MAPKs (see above). Interestingly, we have recently shown that in the human breast cancer cell line MDA-MB-231 a decreased expression of PBR was associated with an inhibition in their proliferation and with an increase of the p21^{WAF1} levels. These data suggest that either the function of PBR on cell proliferation is cell type-specific or PK 11195 exerts a PBR-independent effect on human fibroblast proliferation.

Although in clinical use high benzodiazepine levels (up to 50µM) can be found in plasma [33, 47] the high doses of PBR ligands required to inhibit proliferation, i.e. 10⁻⁵M - 10⁻⁴M, raises the question of whether the 18-KDa PBR protein is involved in the regulation of human fibroblast and fibrosarcoma cell proliferation. Using siRNAs we were able to nearly annihilate PBR expression, as shown by Q-PCR and PK 11195 ligand binding experiments. However, under these conditions PK 11195 and Ro5-4864 were still able to inhibit the proliferation of both cell types. Even more, siRNA, and the subsequent inhibition of PBR expression, did not disturb the proliferation of these cells under standard culture conditions. These results are in agreement with data reported in mouse MA-10 Leydig cells where PBR levels were decreased using a PBR antisense knockout approach [48]. It should be noted that like fibroblast and fibrosarcoma cells, Leydig cells are also of mesenchymal origin [49]. These findings suggest that the 18-kDa PBR protein may not be crucial for the regulation of proliferation of human fibroblast and fibrosarcoma cells. Nevertheless, the effect of PBR ligands is specific as we have shown that the central-type benzodiazepine receptor ligands clonazepam and flurazepam are

unable to affect fibroblast or fibrosarcoma cell proliferation, while diazepam that can bind in both peripheral- and central-type benzodiazepine receptors exhibits a significant inhibitory effect. Thus, it can be hypothesized that specific PBR drug ligands may act or activate a yet unidentified, PBR-independent, pathway.

It has been proposed that PBR ligand benzodiazepines can inhibit cell proliferation by blocking Ca^{2+} -influx through voltage activated channels. Indeed, it has been shown that micromolar concentration of PBR agonists can hinder Ca^{2+} influx through voltage-activated calcium channels [47, 50, 51] and, in addition, the inhibitory effect of Ro5-4864 on rat pituitary tumor cells can be reversed by increased calcium concentrations [52]. However, in the case of fibroblast and fibrosarcoma the addition of the same calcium concentrations had no effect on the inhibitory effect of PBR ligands, such as PK 11195 and Ro5-4864, suggesting an alternative intracellular target for these compounds.

In conclusion, we have shown that PBR is present in the mitochondria of cells of mesenchymal origin, such as human fibroblast and fibrosarcoma cells and that specific PBR drug ligands, at relatively high concentrations, exert a strong inhibitory effect on these cells by arresting them at the G0/G1 phase of the cell cycle. In normal fibroblasts, this inhibition correlated with a decrease in the activation of ERK and c-Jun. Moreover, the data presented herein indicates that PBR-devoid cells still respond to PBR drug ligands, suggesting that in these mesenchymal cells this event may be PBR-independent, in contrast to reported findings in cells of epithelial origin. Finally, further supports the future use of PBR drug ligands in cancer therapy either alone or in combination with other treatment regimens.

Acknowledgments

This work was supported by a grant from the Department of Defense (DAMD17-99-1-9200) to VP and a Fullbright scholarship to DK. The authors wish to thank the members of the Lombardi Comprehensive Cancer Center, Georgetown University flow cytometry facility.

References

1. Costa E, Guidotti A, Mao SS and Suria A. New concepts of the mechanism of action of benzodiazepines. *Life Sci.* 1975; 17: 167-186.
2. Papadopoulos V. Peripheral-type benzodiazepine/diazepam binding inhibitor receptor: biological role in steroidogenic cell function. *Endocr. Rev.* 1993; 14: 222-240.
3. Gavish M, Bachman I, Shoukrun R, Katz Y, Veenman L, Weisinger G, Weizman A. Enigma of the peripheral benzodiazepine receptor. *Pharmacol. Rev.* 1999; 51:629-650.
4. McEnery MW, Snowman AM, Trifiletti RR and Dwyer SH. Isolation of the mitochondrial benzodiazepine receptor: Association with the voltage-dependent anion channel and the adenine nucleotide carrier. *Proc. Natl. Acad. Sci USA* 1992; 89: 3170-3174.
5. Lacapere JJ, Papadopoulos V. Peripheral-type benzodiazepine receptor: Structure and function of a cholesterol binding protein in steroid and bile acid biosynthesis. *Steroids*, 2003; 68:569-585.
6. Hirsch JD, Beyer CF, Malkowitz L, Beer B and Blume AJ. Mitochondrial benzodiazepine receptors mediate inhibition of the mitochondrial respiratory control. *Mol. Pharmacol.* 1989; 35: 157-163.
7. Zavala F. Benzodiazepines, anxiety and immunity. *Pharmacol. Therap.* 1997; 75: 199-216.

8. Taketani S, Kohno H, Furukawa T and Tokunaga R. Involvement of peripheral-type benzodiazepine receptors in the intracellular transport of heme and porphyrins. *J. Biochem.* 1995; 117: 875-880.
9. Papadopoulos V, Dharmarajan AM, Li H, Culty M, Lemay M and Sridaran R. Mitochondrial peripheral-type benzodiazepine receptor expression: correlation with the GnRH-agonist induced apoptosis in the corpus luteum. *Biochem. Pharmacol.* 1999; 58: 1389-1393.
10. Costantini P, Jacotot E, Decaudin D, Kroemer G. Mitochondrion as a novel target of anticancer chemotherapy. *J Natl Cancer Inst.* 2000; 92:1042-53.
11. Beurdeley-Thomas A, Miccoli L, Oudard S, Dutrillaux B, Poupon MF. The peripheral benzodiazepine receptors: a review. *J. Neurooncol.* 2000; 46: 45-56.
12. Li H, Yao Z, Degenhardt B, Teper G and Papadopoulos V. Cholesterol binding at the cholesterol recognition/interaction amino acid consensus (CRAC) of the peripheral-type benzodiazepine receptor and inhibition of steroidogenesis by an HIV TAT-CRAC peptide. *Proc. Natl. Acad. Sci. USA* 2001; 98: 1267-1272.
13. Lacapere JJ, Delavoie F, Li H, Macarion J, Papadopoulos V and Vidic B. Structural and functional study of reconstituted peripheral benzodiazepine receptor (PBR). *Biochem. Biophys. Res. Commun.* 2001; 284: 536-541.
14. Delavoie F, Li H, Hardwick M, Robert J-C, Giatzakis C, Péranzi G, Yao Z-X, Maccario J, Lacapère JJ, and Papadopoulos V. In vivo and in vitro peripheral-type benzodiazepine receptor polymerization: functional significance in drug ligand and cholesterol binding. *Biochemistry*, 2003; 42:4506-4519.

15. Lacapere JJ, and Papadopoulos V. Peripheral-type benzodiazepine receptor: Structure and function of a cholesterol binding protein in steroid and bile acid biosynthesis. *Steroids*, 2003; 68:569-585.
16. Casellas P, Galiegue S and Basile AS. Peripheral benzodiazepine receptors and mitochondrial function. *Neurochem. Int.* 2002; 40: 475-486.
17. Hardwick M, Fertikh D, Culty M, Li H, Vidic B and Papadopoulos V. Peripheral-type benzodiazepine receptor (PBR) in human breast cancer: Correlation of breast cancer cell aggressive phenotype with PBR expression, nuclear localization, and PBR-mediated cell proliferation and nuclear transport of cholesterol. *Cancer Res.* 1999; 59: 831-842.
18. Brown RC, Degenhardt B, Kotoula M and Papadopoulos V. Location-dependent role of the human glioma cell peripheral-type benzodiazepine receptor in proliferation and steroid biosynthesis. *Cancer Lett.* 2000; 15: 125-132.
19. Carmel I, Fares FA, Leschiner S, Scherubel H, Weisinger G and Gavish M. Peripheral-type benzodiazepine receptors in the regulation of proliferation of MCF-7 human breast carcinoma cells. *Biochem. Pharmacol.* 1999; 58: 273-278.
20. Landau M, Weizman A, Zoref-Shani E, Beery E, Wasseman L, Landau O, Gavish M, Brenner S and Nordenberg J. Antiproliferative and differentiating effects of benzodiazepine receptor ligands on B16 melanoma cells. *Biochem. Pharmacol.* 1998; 56: 1029-1034.
21. Zisterer DM, Hance N, Campiani G, Garofalo A, Nacci V and Clive Williams D. Antiproliferative action of pyrrolobenzoxazepine derivatives in cultured cells:

Absence of correlation with binding to the peripheral-type benzodiazepinebinding site. *Biochem. Pharmacol.* 1998; 55: 397-403.

22. Maaser K, Höpfner M, Jansen A, Weisinger G, Gavish M, Kozikowski AP, Weizman A, Carayon P, Riecken E-O, Zeitz M and Scherubl H. Specific ligands of the peripheral benzodiazepine receptor induce apoptosis and cell cycle arrest in human colorectal cancer cells. *Br. J. Cancer* 2001; 85: 1771-1780.
23. Sutter AP, Maaser K, Höpfner M, Barthel B, Grabowski P, Faiss S, Carayon P, Zeitz M and Scherubl H. Specific ligands of the peripheral benzodiazepine receptor induce apoptosis and cell cycle arrest in human esophageal cancer cells. *Int. J. Cancer* 2002; 102: 318-327.
24. Beinlich A, Strohmeier R, Kaufmann M and Kuhl H. Specific binding of benzodiazepines to human breast cancer cell lines. *Life Sci.* 1999; 20: 2099-2108.
25. Li W, Hardwick MJ, Papadopoulos V. Peripheral-type benzodiazepine receptor (PBR) overexpression and knockdown in human breast cancer cells indicate a role in tumor cell proliferation mediated by activation of p21^{WAF1/CIP1} expression. Submitted.
26. Kletsas D, Stathakos D, Sorrentino V, Philipson L. The growth-inhibitory block of TGF- β is located close to the G1/S border in the cell cycle. *Exp. Cell Res.* 1995; 217: 477-485.
27. Kozikowski AP, Kotoula M, Ma D, Boujrad N, Tuckmantel W and Papadopoulos V. Synthesis and biology of 7-nitro-2,1,3-benzoxadiazol-4-yl derivative of 2-

- phenylindole-3-acetamide: a fluorescent probe for the peripheral-type benzodiazepine receptor. *J. Medicinal Chem.* 1997; 40: 2435-2439.
28. Garnier M, Dimchev AB, Boujard N, Price JM, Musto NA and Papadopoulos V. In vitro reconstitution of a functional peripheral-type benzodiazepine receptor from mouse Leydig tumor cells. *Mol. Pharmacol.* 1994; 45: 201-211.
29. Munson PJ, Rodbard D. LIGAND. A versatile computerized approach for characterization of ligand binding systems. *Anal. Biochem.* 1980; 107: 220-239.
30. Miettinen H, Kononen J, Haapasalo H, Helen P, Sallinen P, Harjuntausta T, Helin H, Alho H. Expression of peripheral-type benzodiazepine receptor and diazepam binding inhibitor in human astrocytes: relationship to cell proliferation. *Cancer Res.* 1995; 55: 2691-2695.
31. Beinlich A, Strohmeier R, Kaufmann M and Kuhl H. Relation of cell proliferation to expression of peripheral benzodiazepine receptors in human breast cancer cell lines. *Biochem. Pharmacol.* 2000; 60: 397-402.
32. Han Z, Slack SR, Li W, and Papadopoulos V. Expression of peripheral benzodiazepine receptor (PBR) in human tumors: relationship to breast, colon and prostate tumor progression. *Journal of Receptor Research and Signal Transduction*, in press, 2003.
33. Gorman AMC, O'Beirne GB, Regan CM and Clive Williams D. Antiproliferative action of benzodiazepines in cultured brain cells is not mediated through the peripheral-type benzodiazepine receptor. *J. Neurochem.* 1998; 53: 849-855.

34. Camins A, Diez-Fernandez C, Pujadas E, Camarasa J, Escubedo E. A new aspect of the antiproliferative action of peripheral-type benzodiazepine receptor ligands. *Eur. J Pharmacol.* 1995; 272: 289-292.
35. Wang JKT, Morgan JI and Spector S. Benzodiazepines that bind to peripheral sites inhibit cell proliferation. *Proc. Natl. Acad. Sci USA* 1998; 81: 753-756.
36. Clark GD and Ryan PJ. Tranquillizers can block mitogenesis in 3T3 cells and induce differentiation in Friend cells. *Nature* 1980; 287: 160-161.
37. Ikezaki K, Black KL. Stimulation of cell growth and DNA synthesis by peripheral benzodiazepine. *Cancer Lett.* 1990; 49: 115-120.
38. Tanimoto Y, Onishi Y, Sato Y, Kizaki H. Benzodiazepine receptor agonists modulate thymocyte apoptosis through reduction of the mitochondrial transmembrane potential. *Jpn. J. Pharmacol.* 1999; 79: 177-183.
39. Fischer R, Schmitt M, Bode JG and Haussinger D. Expression of the peripheral-type benzodiazepine receptor and apoptosis induction in hepatic stellate cells. *Gastroenterology* 2001; 120: 1212-1216.
40. Hipkind RA, Bilbe G. MAP kinase signaling cascades and gene expression in osteoblasts. *Front. Biosci.* 1998; 3: D804-D816.
41. Angel P, Karin M. The role of Jun, Fos and the AP-1 complex in cell proliferation and transformation. *Biochim. Biophys. Acta* 1991; 1072: 129-157.
42. Gottlicher M, Ramsdorf HJ, Herrlich P. The AP-1 family of transcription factors: Multi-level control of activity. In: Papavassiliou AG, editor. *Transcription factors in eukaryotes*. Heidelberg: Springer-Verlag. pp. 67-93.

43. Karin M. The regulation of AP-1 activity by mitogen-activated protein kinases. *J. Biol. Chem.* 1995; 270: 16483-16486.
44. Papavassiliou AG, Treier M, Bohmann D. Intramolecular signal transduction in c-Jun. *EMBO J.* 1995; 14: 2014-2019.
45. Whitmarsh AJ, Davis RJ. Transcription factor AP-1 regulation by mitogen-activated protein kinase signal transduction pathways. *J. Mol. Med.* 1996; 74: 589-607.
46. Karin M, Liu ZG, Zandi E. AP-1 function and regulation. *Curr. Opin. Cell Biol.* 1997; 9: 240-246.
47. Cox LS. Multiple pathways control cell growth and transformation: Overlapping and independent activities of p53 and p21^{Cip1/WAF1/Sdi1}. *J. Pathol.* 1997; 183: 134-140.
48. Taft WC, De Lorenzo RJ. Micromolar-affinity benzodiazepine receptors regulate voltage-sensitive calcium channels in nerve terminal preparations. *Proc. Natl. Acad. Sci. USA* 1984; 81: 3118-3122.
49. Kelly-Herskovitz E, Weizman R, Spannier H, Leschinen S, Lahav M, Weisinger G, and Gavish M. Effects of peripheral-type benzodiazepine receptor antisense knockout on MA-10 Leydig cell proliferation and steroidogenesis. *J. Biol. Chem.* 1998; 273: 5478-5483.
50. Benton L, Shah LX, Hardy MP. Differentiation of adult Leydig cells. *J. Steroid Biochem Mol Biol.* 1995; 53: 61-68.

51. Cantor EH, Kenessey A, Semenuk G, Spector S. Interaction of calcium channels blockers with non-neuronal benzodiazepine binding sites. *Proc. Natl. Acad. Sci. USA* 1984; 81: 1549-1552.
52. Python CP, Rossier MF, Vallotton MB, Capponi AM. Peripheral-type benzodiazepines inhibit calcium channels and aldosterone production in adrenal glomerulosa cells. *Endocrinology* 1993; 132: 1489-1495.
53. Kunert-Radek J, Stepień H and Pawlikowski M. Inhibition of rat pituitary tumor cell proliferation by benzodiazepines in vitro. *Neuroendocrinol.* 1994; 59: 92-96.
54. Liu J, Cavalli LR, Haddad BR, Papadopoulos V. Molecular cloning, genomic organization, chromosomal mapping and subcellular localization of mouse PAP7: a PBR and PKA-R1a associated protein. *Gene* 2003, 308:1-10.

Table 1

	Cell Cycle Phase (%)		
	G0/G1	S	G2/M
HFFF2			
Control	70.9	12.37	16.73
PK 11195	89.71	5.79	4.49
Ro5-4864	81.21	9.51	9.28
HT-1080			
Control	59.41	21.86	18.73
PK 11195	68.14	8.91	22.94
Ro5-4864	75.14	8.54	16.32

LEGENDS

Figure 1. Expression of PBR mRNA in human fibroblasts and fibrosarcoma cells. Total RNA was extracted from growing HT-1080, HFFF2 cells (cycling, as well as arrested by confluency and serum-starvation) and from MDA-MB-231 human breast cancer epithelial cells, and was subjected to Q-PCR analysis, as described in Materials and Methods. PBR mRNA levels were expressed in relative level to endogenous reference 18S rRNA.

Figure 2. PBR and mitochondrial localization in HFFF2 (A) and HT-1080 (B) cells. The cells were incubated with the fluorescent high-affinity PBR ligand compound 4 and with MitoTracker Red and were observed under a laser scanning confocal microscope. The green color indicates the presence of PBR and the red color that of mitochondria. Co-localization of both fluorescent images after superposition results in a yellow color. Bar = 20 μ m.

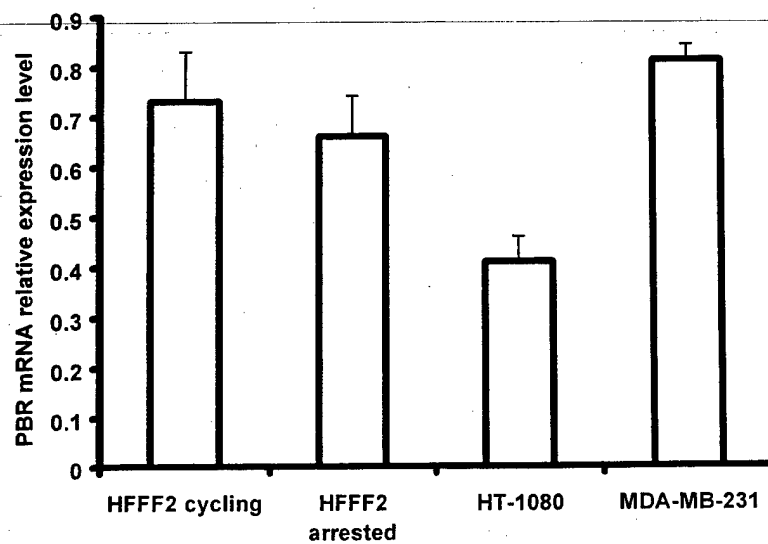
Figure 3. Dose-dependent effect of PBR ligands PK 11195 and Ro5-4864 on the proliferation of HFFF2 (A) and HT-1080 (B) cells. The cells were grown in 96-well plates and treated with the indicated concentrations of PK 11195 and Ro5-4864. 24-h later BrdU incorporation was measured as described under Materials and Methods. In (C) arrested HFFF2 cells were treated with PK 11195 and Ro5-4864, both at 10^{-4} M, and BrdU incorporation was also measured 24-h later. One representative experiment is present here, performed in quadruplicates. Qualitatively similar results were obtained in two other independent experiments.

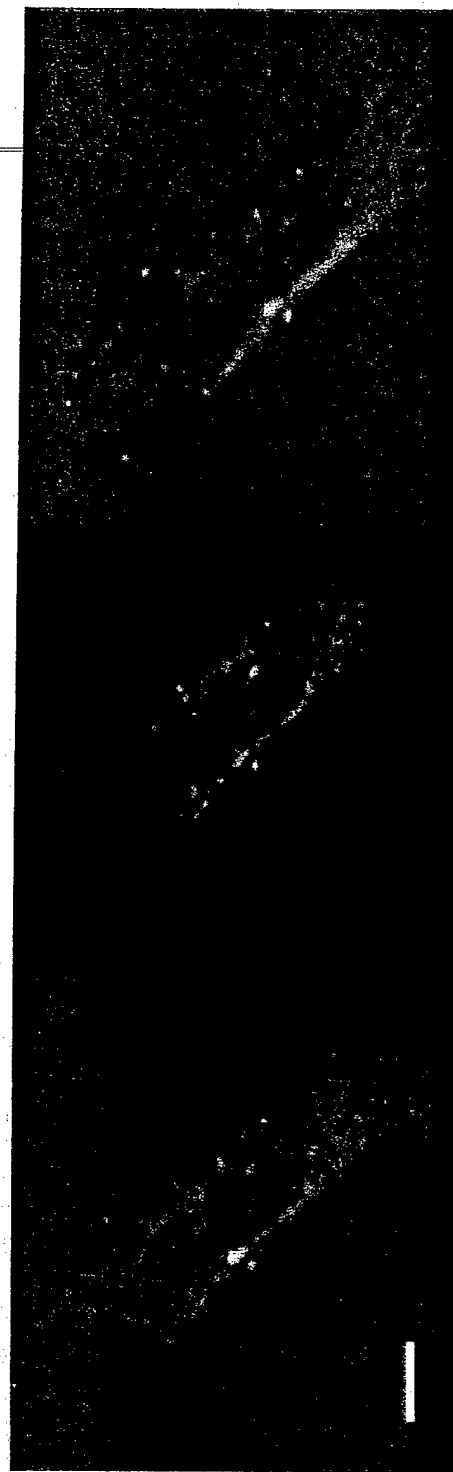
Figure 7. PBR siRNA does not affect the proliferation of human fibroblast and fibrosarcoma cells. One day after plating, HFFF2 and HT-1080 cells were transfected with the 548 and the scrambled (Scr) dsRNA. Subsequently, cell counting was performed and the proliferation occurred between day 2 and day 6 after transfection was estimated.

Values represent the mean of three individual experiments, each one performed in quadruplicates

Figure 8. The inhibitory effect of PBR ligands on the proliferation of HFFF2 and HT-1080 cells is not affected by the presence of high calcium concentrations. The cells were treated with PK 11195 and Ro5-4864, both at 10^{-4} M, in the presence or absence of CaCl_2 (5×10^{-3} M). DNA synthesis was measured by BrdU incorporation as described in Figure 3. One representative experiment is present here, performed in quadruplicates.

Kletsas et al.
Figure 1

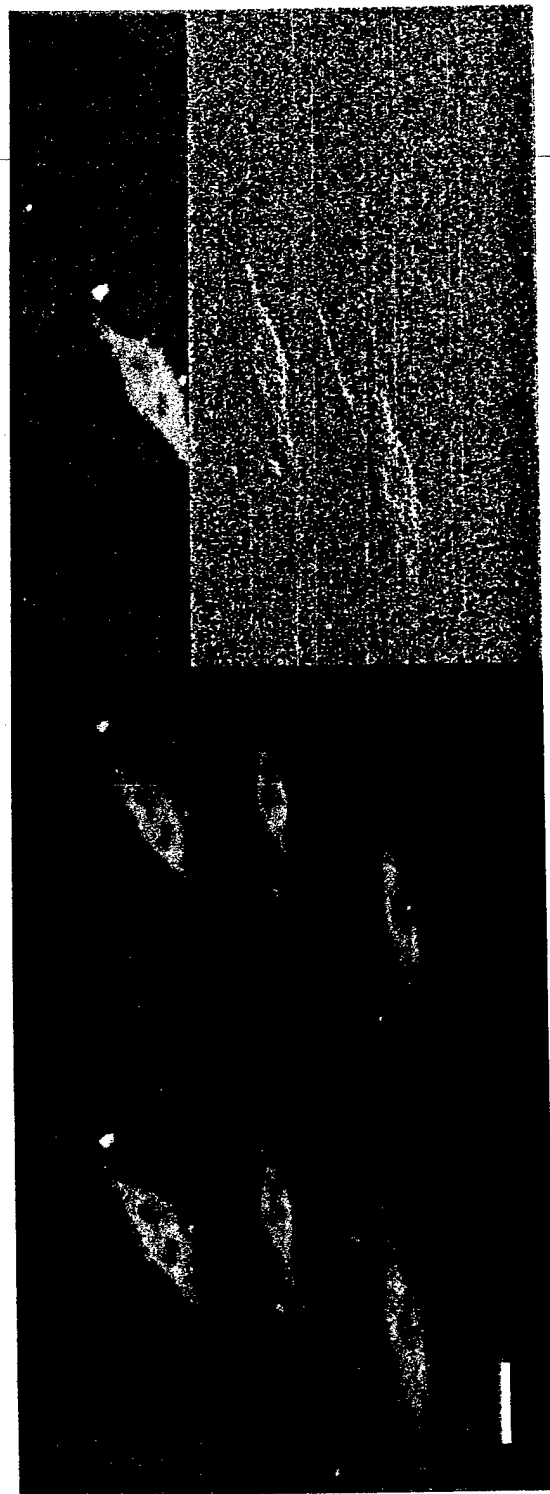




C4

Mitotracker

Merge

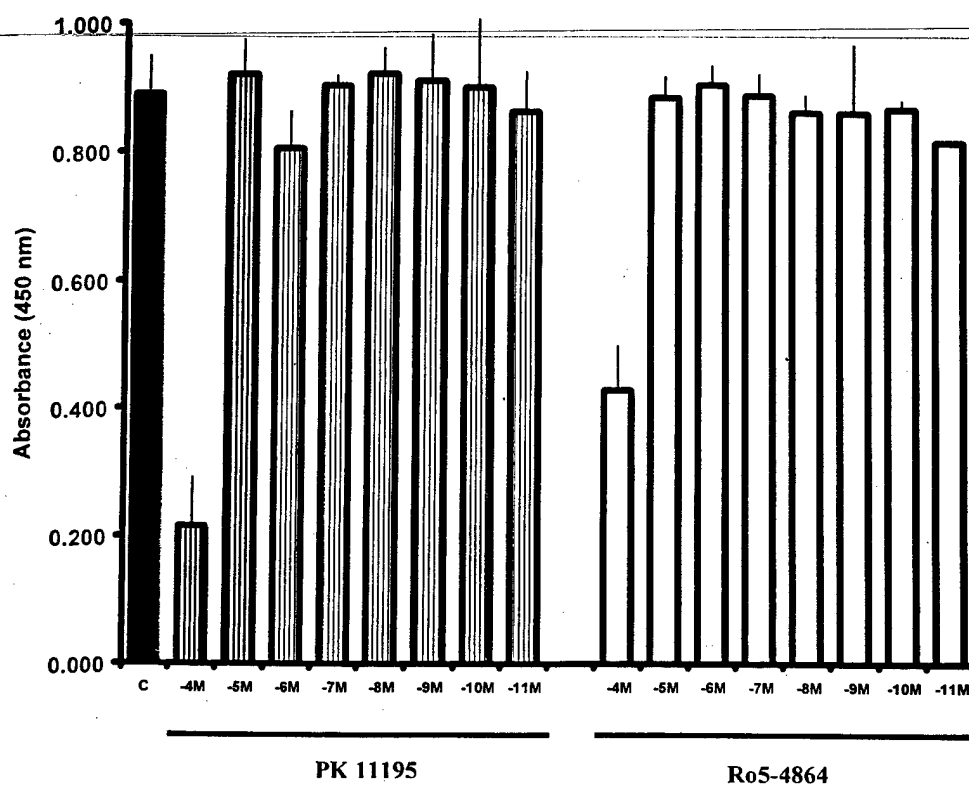


C4

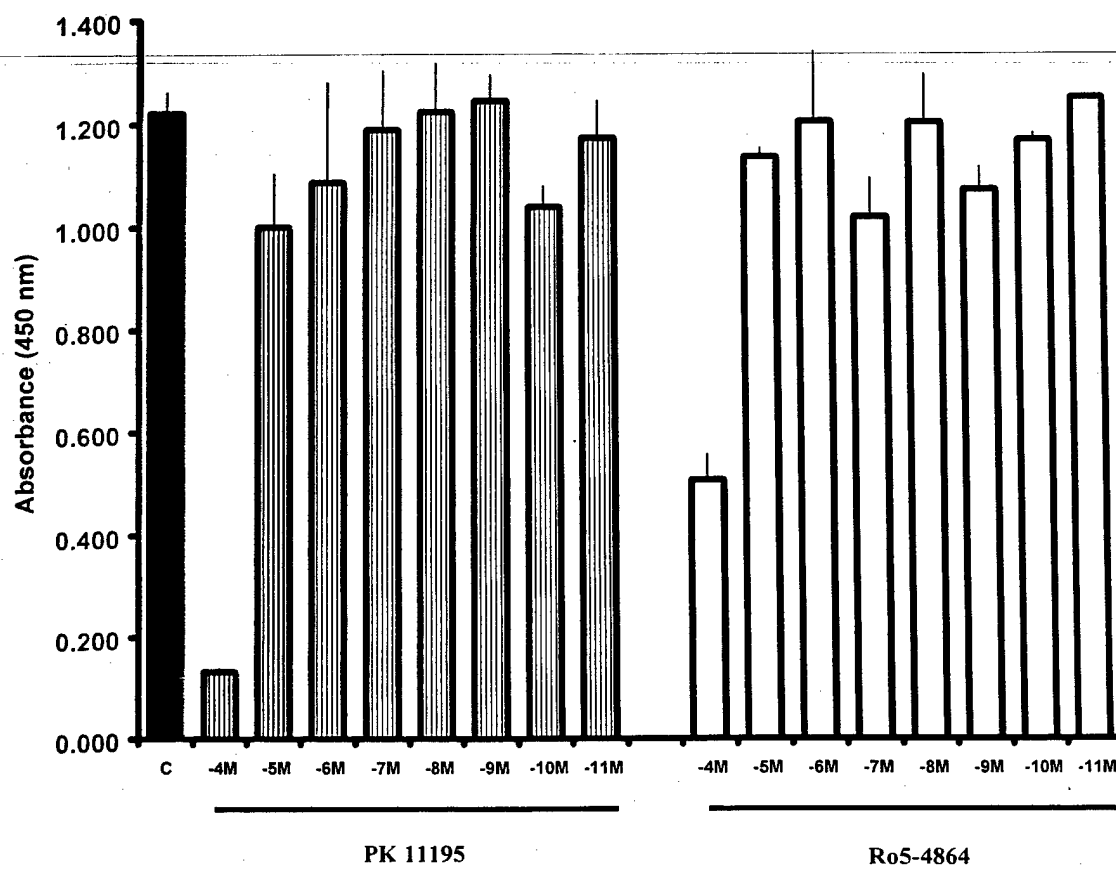
Mitotracker

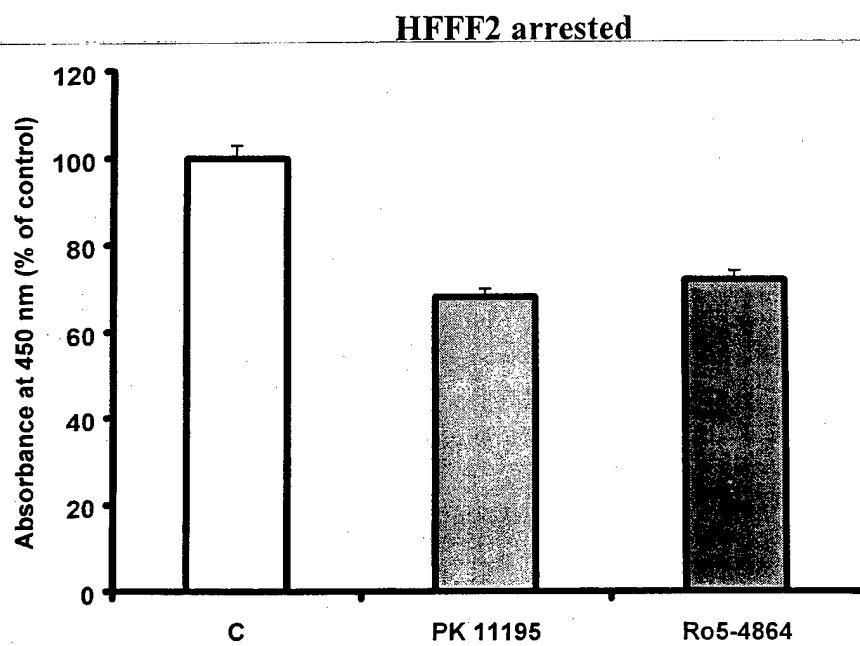
Merge

HFFF2 cycling

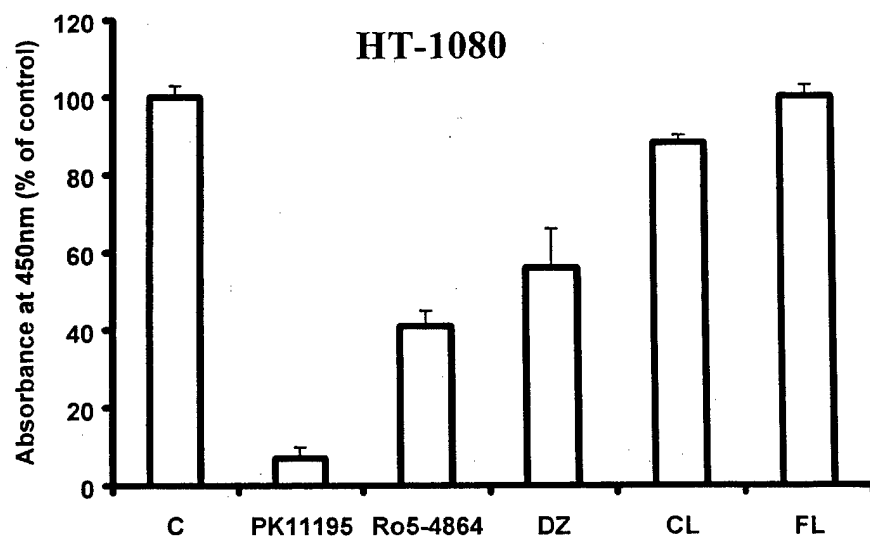
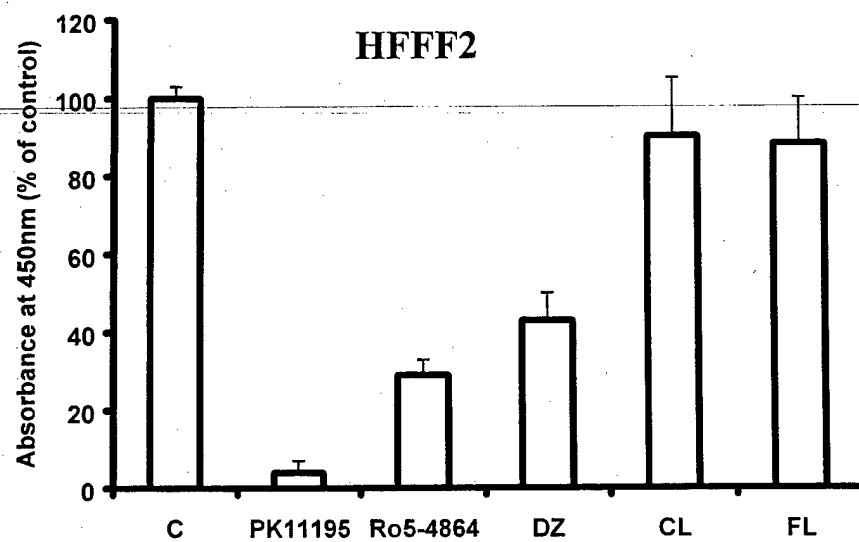


HT-1080





Kletsas et al.
Figure 4



PK 11195
Control

pERK



p-c-Jun



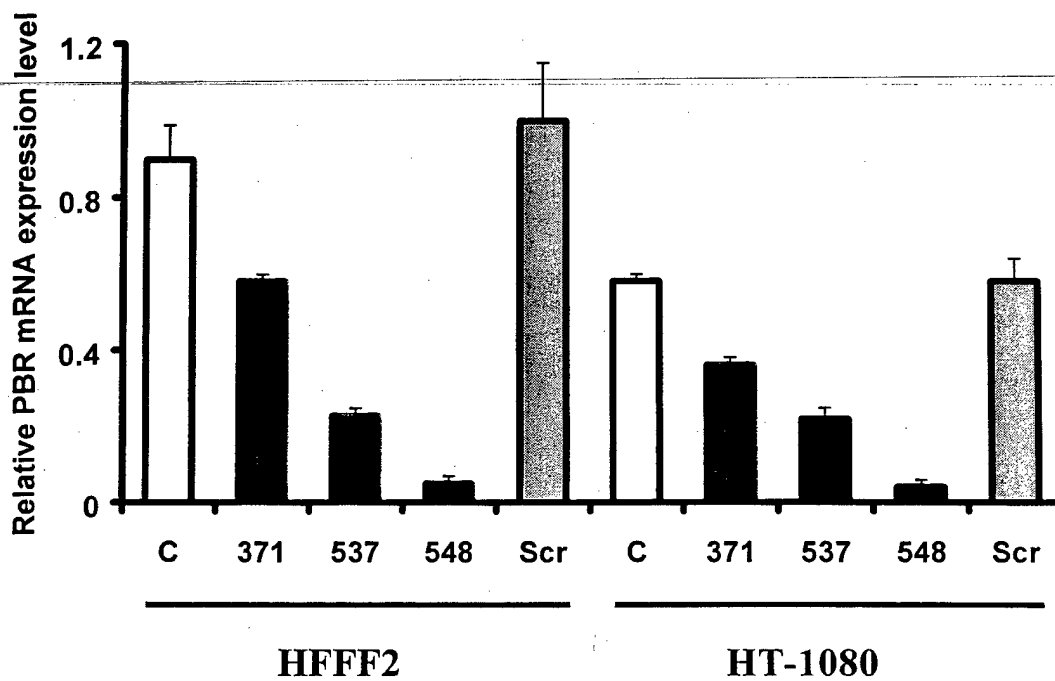
p21^{WAF1}



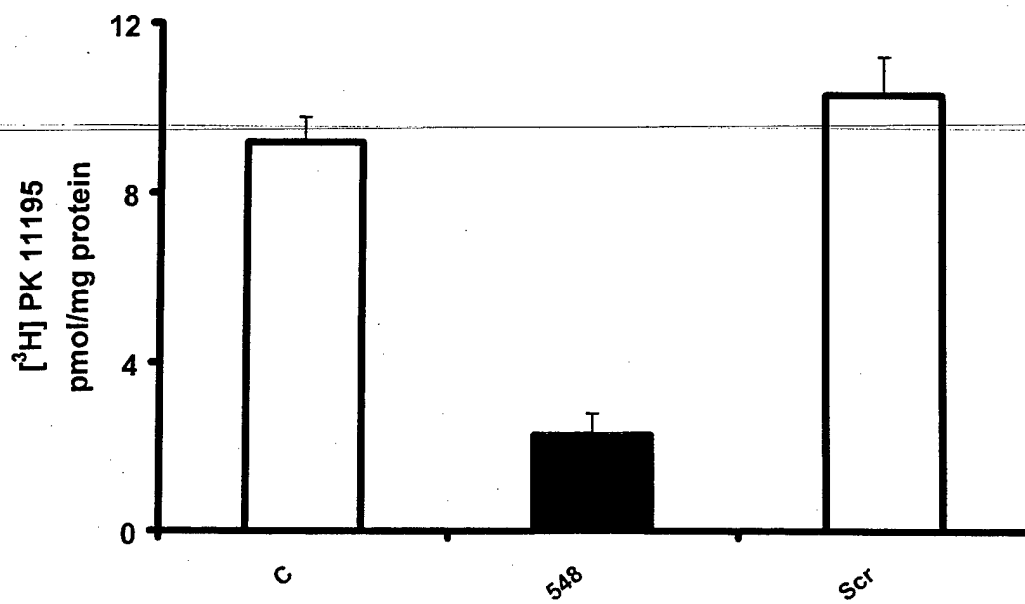
Actin



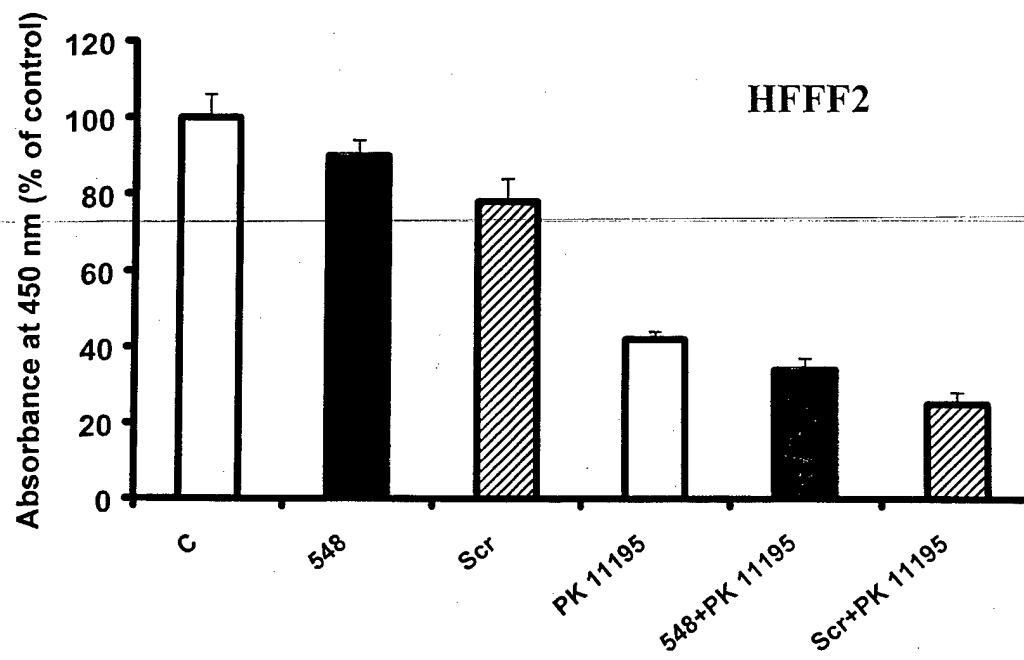
Kletsas et al.
Figure 6A



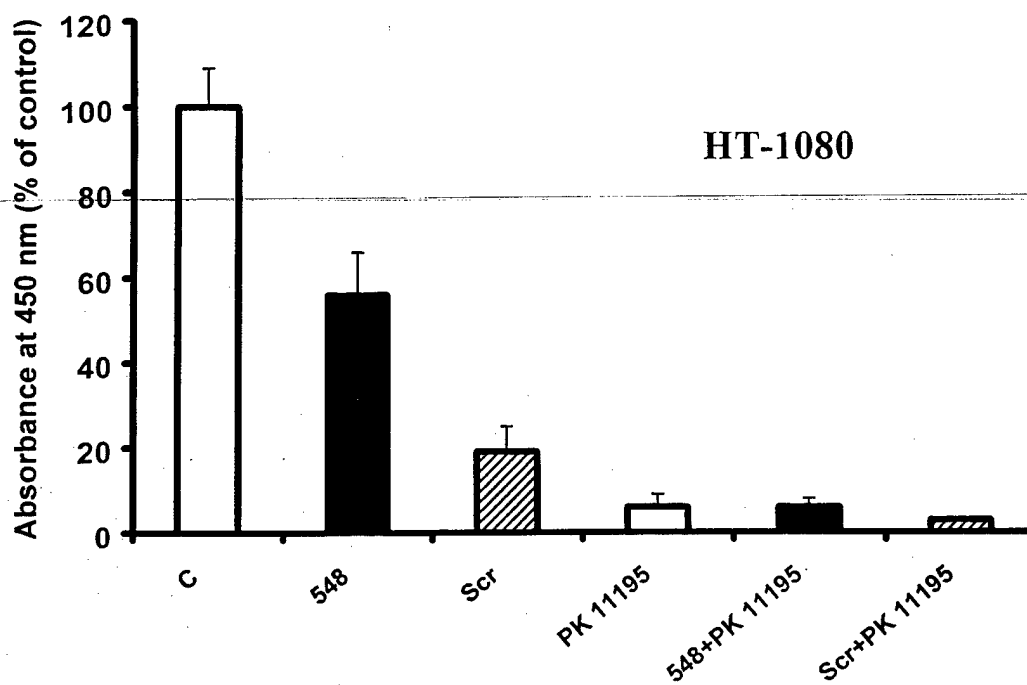
Kletsas et al.
Figure 6B



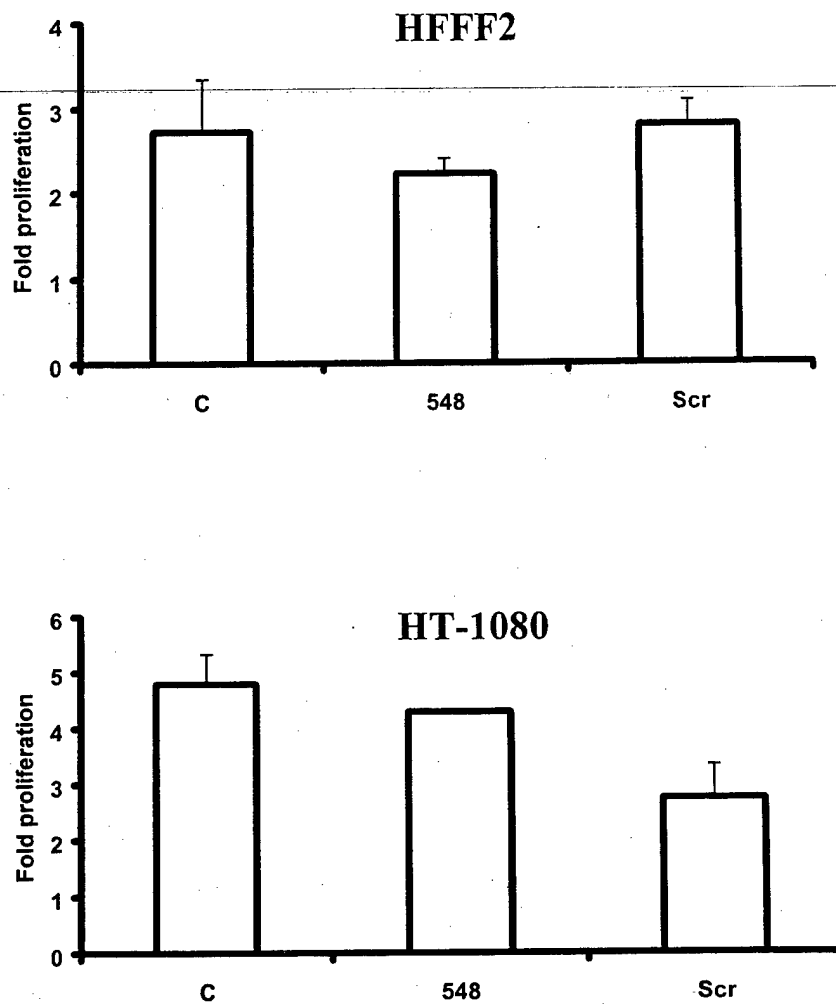
Kletsas et al.
Figure 6C



Kletsas et al.
Figure 6D



Kletsas et al.
Figure 7



Kletsas et al.
Figure 8

